Max-Planck-Institut für Meteorologie

EXAMENSARBEIT Nr. 69

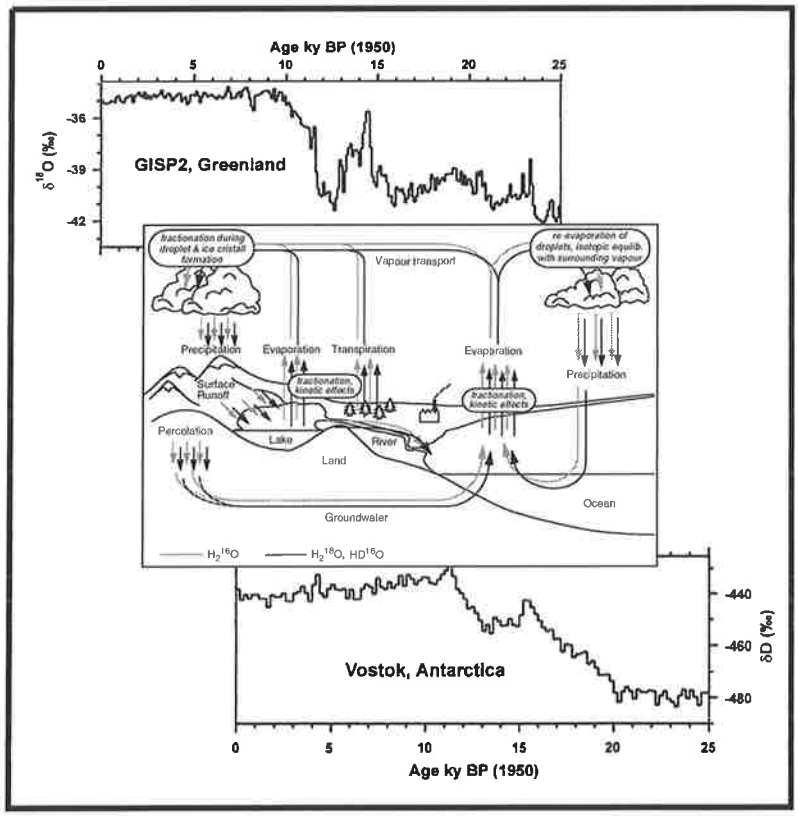

RÄUMLICHE UND ZEITLICHE VARIABILITÄT VON WASSERISOTOPEN IM POLAREN NIEDERSCHLAG

(Spatial and Temporal Variability of Water Isotopes in Polar Precipitation)

von

Martin Werner

HAMBURG, Februar 2000

Dissertation zur Erlangung des Doktorgrades

Autor:

Martin Werner

Max-Planck-Institut
für Meteorologie

MAX-PLANCK-INSTITUT
FÜR METEOROLOGIE
BUNDESSTRASSE 55
D - 20146 HAMBURG
GERMANY

Tel.: +49-(0)40-4 11 73-0
Telefax: +49-(0)40-4 11 73-298
E-Mail: <name> @ dkrz.de

Räumliche und zeitliche Variabilität von Wasserisotopen im polaren Niederschlag

(Spatial and Temporal Variability of Water Isotopes in Polar Precipitation)

Dissertation

zur Erlangung des Doktorgrades

der Naturwissenschaften im Fachbereich

Geowissenschaften

der Universität Hamburg

vorgelegt von

Martin Werner

aus

Köln

Hamburg

2000

ISSN 0938-5177

Als Dissertation angenommen vom Fachbereich Geowissenschaften

der Universität Hamburg

auf Grund der Gutachten von Prof. Dr. Martin Heimann

und Prof. Dr. Hartmut Graßl

Hamburg, den 25. Januar 2000

Prof. Dr. U. Bismayer

Dekan

des Fachbereich Geowissenschaften

Vorwort

Auch die Erstellung dieser Doktorarbeit wäre - wie wohl jede Dissertation - ohne die zahlreiche Hilfe von Kollegen und Freunden nicht möglich gewesen.

Zwei Personen sollen nicht ohne Grund am Anfang genannt werden: Zum einen ist es Martin Heimann, Leiter der Arbeitsgruppe „Biogeochemische Modellierung und Tracer im Klimasystem", der mich während der letzten 3½ Jahre mit seinen zahlreichen Ratschlägen und seinem wissenschaftlichen Überblick hervorragend betreute und motivierte. Zum anderen gilt mein Dank Georg Hoffmann. Er baute als erster Wasserisotope in das Hamburger Zirkulationsmodell ECHAM ein und schuf damit die Grundlage für diese Arbeit. Außerdem ist er mit Leib und Seele ein „Isotopist" und hat meine Forschung mit seinen Ideen und Kommentaren sehr bereichert.

Ich danke auch dem Institutsdirektor Klaus Hasselmann, der mir die Promotion am Max-Planck-Institut ermöglichte. Nicht nur die perfekte technische und finanzielle Unterstützung, sondern vor allem das wissenschaftliche und kollegiale Umfeld an diesem Institut habe ich genossen. Dadurch hat diese Arbeit von zahlreichen Diskussionen mit vielen Kollegen profitiert, wobei ich an dieser Stelle Uwe Mikolajewicz gesondert erwähnen möchte. Alle anderen werden es mir hoffentlich verzeihen, daß ich sie hier aus Platzmangel nicht einzeln mit Namen aufliste, mein Dank ist dafür nicht weniger herzlich. Genannt werden soll an dieser Stelle auch Frau Radmann für ihre persönlichen und aufmunternden Einladungen zur täglichen Teerunde. Meinen beiden „Institutsmitbewohnerinnen" Christine Weber und Sigrid Schöttle danke ich insbesondere für die nette Arbeitsatmosphäre, ein stets offenes Ohr, und auch für ihre Bereitschaft, mich in manchen Phasen dieser Arbeit einfach 'mal ungestört in meiner Ecke arbeiten zu lassen.

Die vielen Diskussionen mit meinen zwei alten Studienfreunden Stephan Venzke und Nils Scheithauer über Sinn und Zweck der Klimaforschung haben mir gerade gegen Ende der Doktorarbeit immer wieder geholfen, die richtige Einstellung und Perspektive zur Arbeit zu finden.

„Schuld" an dieser Dissertation sind aber eigentlich Dietmar Wagenbach und Hubertus Fischer, die mir die Grundlagen über Eisbohrkerne und Polarregionen während meiner Diplomarbeit am Institut für Umweltphysik in Heidelberg beibrachten. Meine Zeit dort war für diese Doktorarbeit äußerst hilfreich, und ich bin meinen beiden ehemaligen Betreuern dafür sehr dankbar.

Aber mein größter Dank gilt meinen Eltern und Tina.

Hamburg, im November 1999.

Summary

As with "normal" $^{1}H_2{}^{16}O$ water molecules, the two stable water isotopes $^{1}H_2{}^{18}O$ and $^{1}H^{2}H^{16}O$ (^{2}H=D=Deuterium) are passed through every part of the water cycle in the atmosphere: water evaporates from ocean and land surfaces, is transported by atmospheric circulation, condenses in clouds and finally forms precipitation falling back to the earth's surface. But since HDO and $H_2{}^{18}O$ have a different vapour saturation pressure and molecular diffusivity than $H_2{}^{16}O$, fractionation processes occur during every phase transition of any water sample. The heavier isotopes $H_2{}^{18}O$ and HDO become enriched in the liquid or solid phase while the vapour phase becomes more depleted in them. The strength of the fractionation processes highly depends on particular physical parameters, such as temperature and humidity. Numerous geophysical studies have used this dependency to infer information about past climates from measurements of the isotopic composition of precipitation stored in paleowater archives, e.g. in ice cores.

In the last several years, atmosphere general circulation models (AGCMs) have been used as a helpful tool for studying water isotopes. Incorporating both $H_2{}^{18}O$ and HDO explicitly into the water cycle of the AGCM enables analysing the relationship between the isotopic composition of precipitation and climate variables, such as surface temperatures. Different boundary conditions can be prescribed for the model simulations to gain a better understanding of isotope anomalies caused by different states of the climate.

This thesis focuses on the variability of $H_2{}^{18}O$ and HDO in precipitation falling on Greenland and Antarctica. Over the last two decades, isotope measurements on several ice cores from both polar regions have revealed new insight in the alternating occurrence of stable climate periods, like the Holocene or the last glacial stage, and fast climatic transition phases between, such as the Younger Dryas. The Hamburg AGCM ECHAM-4 was used to investigate several topics related to these isotope records from Greenland and Antarctica.

Simulations for both the present climate and the Last Glacial Maximum (LGM, ~21,000 years ago) were performed to test the reliability of $H_2{}^{18}O$ (or HDO) as a proxy for past surface temperatures on Greenland or Antarctica. The model results indicate that a strong change in the seasonal timing of precipitation occurred on Greenland during the LGM and that this change has a significant influence on the mean isotopic composition of ice core samples from this period. Further analyses of the major source regions of water vapour transported to the ice sheets explain some additional changes between the present and LGM climate.

So far, little is known about the timing and mechanisms of the transition phase between two stable climate stages. The performed ECHAM-4 sensitivity experiments concentrated on the effects of an meltwater event in the North Atlantic, similar to what might have happened during the Younger Dryas period (~ 16,000 years ago). The simulations revealed that several mechanisms influence the isotopic composition of precipitation during such a meltwater event. A simple interpretation of the isotope signal as a proxy for changed surface temperatures would lead to erroneous estimates of climate changes in many regions of the Northern Hemisphere.

Finally, the variability of the isotopic composition of polar precipitation for the climate of the last century is investigated: In an ECHAM-4 simulation of the period 1950-1994, only one-third of the modelled interannual variance is related to simultaneous changes in surface temperatures on Greenland or Antarctica. Several other climate variables, e.g. ocean temperatures of the evaporation areas and/or variability in the water vapour transport to the ice sheets, contribute together a non-negligible part of the fluctuations in the isotope signal in polar precipitation. The imprint of the North Atlantic Oscillation and the El Niño / Southern Oscillation phenomenon is detected in the isotopic composition of precipitation falling in Greenland and Antarctica, respectively.

As a summary we conclude from our AGCM isotope experiments, that the isotopic composition of polar precipitation can certainly be used as a proxy for paleoclimatic conditions, but that the interpretation of the isotope signal is neither simple nor straightforward. Especially the strong (spatial) correlation between the isotope signal and surface temperatures on the ice sheets, as it is observed for the present climate, might have been different for past climates.

Contents

Chapter 1

Introduction

1.1 Motivation

The instability of the earth's climate over the past hundred-thousand years is one of the most puzzling questions in climate research. The magnitude of the climatic shifts observed in many paleorecords is far greater than expected from any possible forcing, e.g. fluctuations in the solar output. Some of the global climatic shifts might be linked to variations in the earth's orbital parameters (Milankovitch 1930). Other modulations, like the Dansgaard-Oeschger-events or the El Niño / Southern Oscillation phenomenon, appear to be bound to certain regions of the earth and happen on a variety of shorter, suborbital time scales (e.g. Dansgaard et al. 1993, Philander 1990). Numerous research studies have focussed on the detection of climatic shifts in different paleorecords, the synchronicity between records from various archives, and on the interpretation of the proxy records in terms of climate change.

One of the key components for studying the climate system is water. For example, oceans cover ~70% of the earth's surface, and the radiation effect of water vapour in the atmosphere is responsible for a mean surface temperature increase of about 20°C (Kondratyev 1984). This increase does not include the net effect of clouds which is still under discussion since clouds simultaneously shield the surface from the incoming solar radiation (cooling effect) and back-scatter part of the thermal radiation from the earth's surface (warming effect). The uptake and release of latent heat during evaporation and condensation, respectively, is another important aspect for explaining many details of the atmospheric circulation. Thus, an extended knowledge of the hydrological cycle and its related processes is a fundamental requirement for a better understanding of our climate.

To study the processes of the water cycle, one can use the fact that both constituents of a water molecule, hydrogen and oxygen, exist in more than one stable isotopic form[1], namely

[1] Isotopes are defined as nuclides with the same atomic number (number of protons) but different mass number (number of protons and neutrons). The mass number is given in superscript and left of the chemical symbol of an element, e.g. ^{12}C.

^{1}H, ^{2}H and ^{16}O, ^{17}O, ^{18}O. A single water molecule can be built of any combinations of these isotopes, e.g. $^{1}H^{1}H^{16}O$, $^{1}H^{1}H^{17}O$, $^{1}H^{1}H^{18}O$, $^{1}H^{2}H^{16}O$, $^{1}H^{2}H^{17}O$ etc. Except "normal" water $^{1}H_{2}{}^{16}O$, so far only the two stable isotopes $^{1}H_{2}{}^{18}O$ and $^{1}H^{2}H^{16}O$=HDO have been of relevance in geophysical research since modern mass spectroscopy techniques enabled measurements of needed accuracy for these two isotopes. The ratio of natural occurrence of $H_{2}{}^{16}O$:$H_{2}{}^{18}O$:HDO is about $1 : \frac{1}{498.7} : \frac{1}{6420}$. But this isotope ratio is not identical for every water sample taken. Due to their different nuclear masses the water isotopes have different saturation pressures and also a different molecular diffusivity. This means, for example, that during an evaporation process involving water, the liquid phase becomes enriched in heavy isotopes while the vapour phase becomes depleted in them. Such fractionation processes between the different water isotopes will occur during every phase transition of any amount of water in the atmospheric water cycle (Fig. 1). The physical description of the fractionation processes was achieved by Friedmann (1953), Dansgaard (1953), Merlivat and Jouzel (1979) and others.

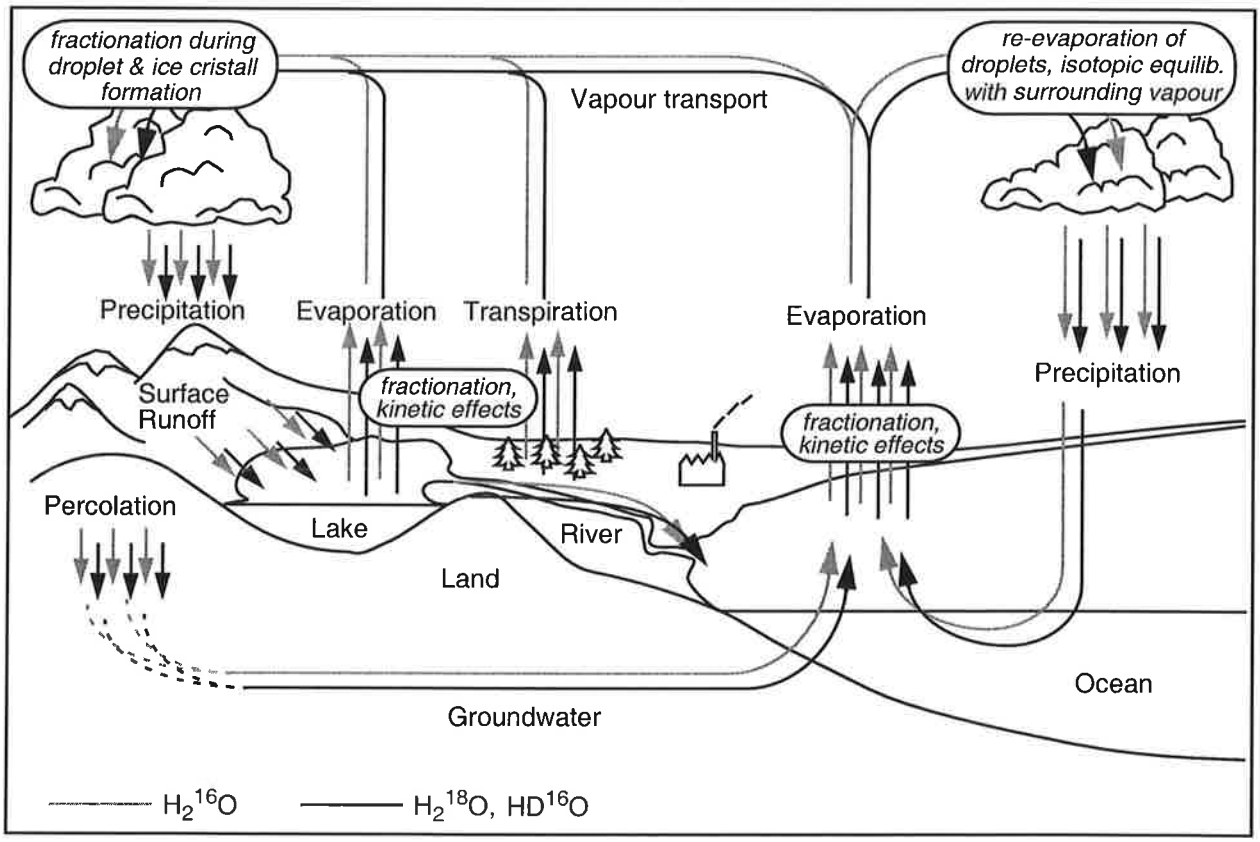

Figure 1: A schematic plot of the atmospheric water cycle in the climate system and the processes, at which fractionation of stable water isotopes occurs.

In 1961 the International Atomic Energy Agency (IAEA) together with the World Meteorological Organisation (WMO) started a global monitoring network of isotopes in precipitation (GNIP). Over the last 35 years monthly samples of precipitation from more than 550 stations from 93 countries were analysed for their isotopic composition (IAEA 1992). In 1966 the IAEA also defined a common isotopic reference standard which was proposed by Craig (1961): About 98% of all water is stored in the oceans and the defined standard V-SMOW[2] represents the mean isotopic composition of this water mass. The isotopic composition of any other water sample is now expressed as the deviation (δ-value) from this standard:

$$\delta_{Sample} = R_{Sample}/R_{SMOW} - 1$$

with $R_{Sample} = [^{18}O]:[^{16}O]$ as the isotope ratio of the water sample. The δ-values are in general expressed in permill and a mean sample of ocean water has by this definition a δ-value of 0‰. The exact absolute values of R_{SMOW} are:

^{18}O: $R_{SMOW} = (2005.2 \pm 0.45)\cdot 10^{-6}$ (Baertschi 1976)

D: $R_{SMOW} = (155.76 \pm 0.05)\cdot 10^{-6}$ (Hagemann et al. 1970)

Only three years after the start of the IAEA network, it was the pioneering work of Dansgaard (1964) which set the base for a widely use of stable water isotopes in geophysical research. By analysing numerous IAEA station data Dansgaard observed and explained a high correlation of the measured δ-values with surface temperatures ("temperature effect"), the amount of falling precipitation ("amount effect") and/or the geographical location of the sampling station ("continental effect", "altitude effect"). These observed close relationships between the isotopic composition of precipitation and other physical parameters are most relevant for the use of stable water isotopes in climate research. Measurements of the isotopic composition of different paleowater archives like marine sediment cores, ice cores, old groundwater reservoirs, lake sediments or speleothems enable the reconstruction of the climatic conditions which led to the specific isotope signal in the archives.

Among those paleorecords, ice cores certainly belong to the most important group for measurements of isotopic compositions of past precipitation. Compared to other archives the interpretation of the δ-values in the ice is more straightforward as no additional transfer function between the isotopic composition of precipitation and the δ-signal in the archive has to be known. Additionally, ice cores might have a much better temporal resolution than, for example, groundwater, if a significant re-layering of snow after the deposition can be excluded. At present, there exist several ice core records from Greenland, Antarctica and from some low-latitudinal alpine regions like the Andes or the Tibetan Plateau which have archived

[2] V-SMOW = Vienna Standard Mean Ocean Water

climatic information of the last glacial cycle and the transition to the present climate[3] (Fig. 2). The measured isotopic composition of most of these different ice core records all show a decrease of $\Delta\delta^{18}O$ = 5-8‰ during the last glacial maximum (LGM, ~21,000 years BP), a transition phase with varying $\delta^{18}O$ values between 21,000 years and 10,000 years BP and a rather smooth and stable $\delta^{18}O$-curve during the Holocene (10,000 years BP to present).

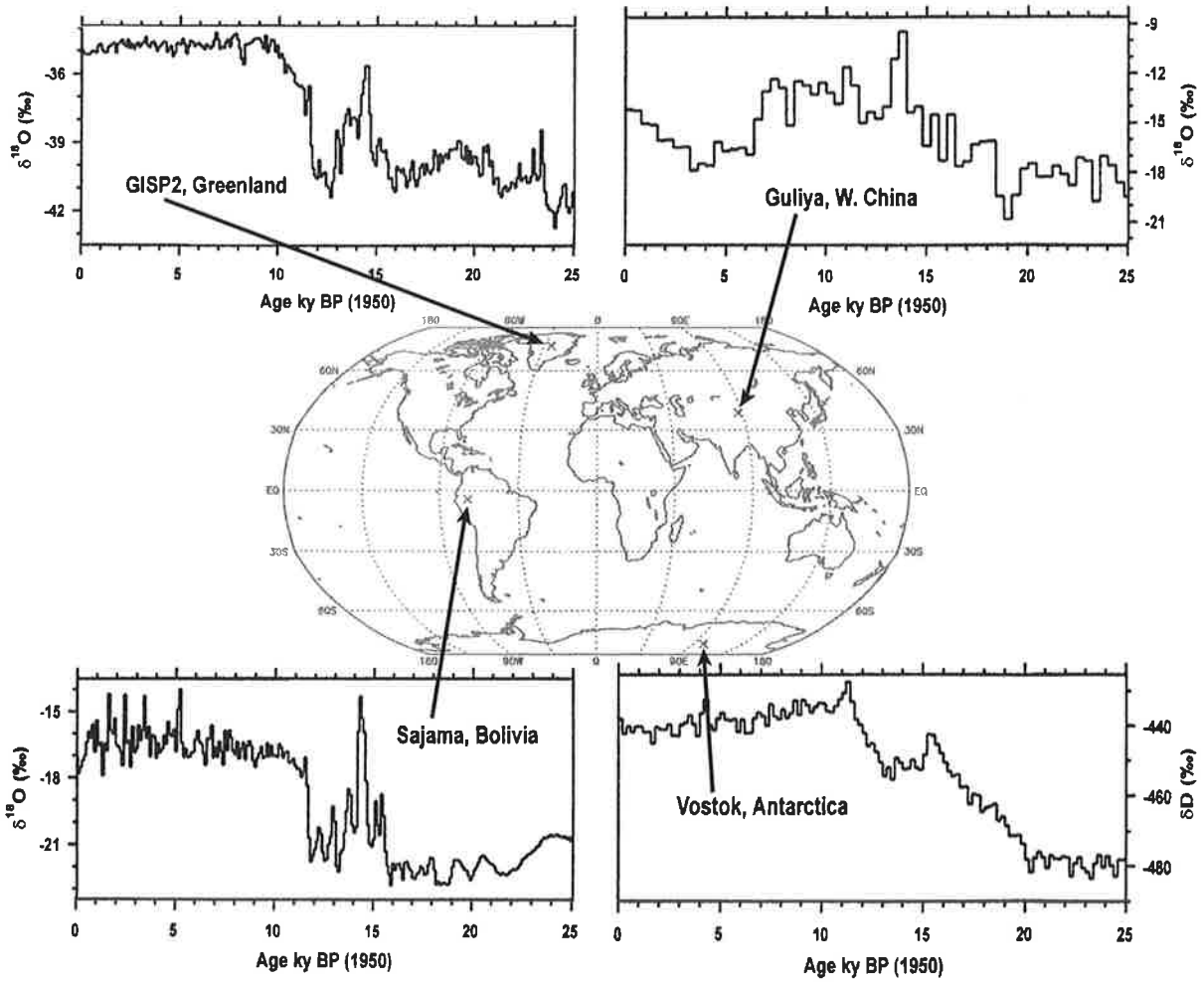

Figure 2: Four examples of $\delta^{18}O$ and δD records measured on ice cores from different geographical locations. A clear minimum during the LGM, varying values during the transition phase and a rather smooth isotope record during the Holocene can be seen in the GISP2, Vostok and Sajama record. For a more detailed discussion of the anomalous Guliya $\delta^{18}O$ curve, see Thompson et al. (1997).

To interpret the measured $\delta^{18}O$ changes as changes of related physical parameters (e.g. surface temperature) one must assume that the observed present-day relationship between isotope values and those parameters has remained constant through time. This assumption has to be made *a priori* and can not be validated by the isotopic data itself. One possibility for

[3] At present, the oldest ice core record available was drilled at Vostok Station, Antarctica. The record spans a period of 420,000 years and includes the last 4 climatic cycles (Petit et al. 1999).

checking the constancy of the considered relationship is performing other, isotope-independent measurements of the relevant physical parameters. Another possibility is using three-dimensional atmospheric general circulation models (AGCMs) with stable water isotopes explicitly built into the simulated water cycle. Incorporating water isotopes into an AGCM requires only that one prescribes the basic physical laws of fractionation during any water phase transition in the model. Thereby, the isotope values in precipitation and other quantities, like surface temperatures, are independent variables in the numerical simulations, and the constancy of their relation can be tested in model experiments under different climatic boundary conditions. Joussaume et al. (1984) and Koster et al. (1988) were among the first who implemented $H_2{}^{18}O$ and HDO into AGCMs. Georg Hoffmann added the "isotope module" to the Hamburg AGCM, ECHAM-3 (Hoffmann 1995) and the quality of various ECHAM-3 isotope simulations is discussed in several articles (Hoffmann and Heimann 1993, Hoffmann and Heimann 1997, Hoffmann et al. 1998).

The modelling of both $H_2{}^{18}O$ and HDO in AGCM simulations also enables detailed studies of the deuterium excess *d*, first defined by Dansgaard (1964). While two different fractionation processes occur during the evaporation of a water sample (equilibrium fractionation caused by the different vapour saturation pressure of the isotopes, plus kinetic fractionation due to the different molecular diffusivities), only equilibrium fractionation occurs during the condensation process (Merlivat and Jouzel 1979). Kinetic fractionation is stronger for $H_2{}^{18}O$ than for HDO, and the strength of this process is expressed by the deuterium excess $d = \delta D - 8\delta^{18}O$. Thus the deuterium excess signal in precipitation is related to the climate at the evaporation site only, while the $\delta^{18}O$ and δD signal in precipitation are influenced by climatic conditions during both evaporation and condensation (Fig. 3).

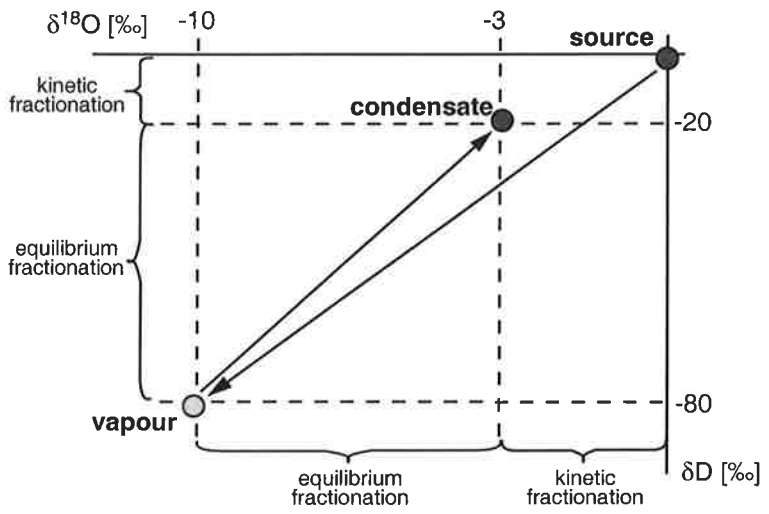

Figure 3: Schematic plot of the kinetic and equilibrium fractionation processes occurring during evaporation and condensation, respectively. As indicated in the plot, the effect of kinetic fractionation of $H_2{}^{18}O$ is stronger than of HDO. Additional effects might complicate this scheme (see text).

However this simple scheme of Fig. 3 does not include several other processes, e.g. re-evaporation of cloud droplets or mixing of water vapour from different source regions, which could also alter the deuterium excess signal. For the polar regions the interpretation is further complicated by an additional kinetic fractionation effect during the phase transition from vapour to ice at very low condensation temperatures (Jouzel and Merlivat 1984). But it is doubtless that the variations of the observed deuterium excess on various time scales (e.g. Johnsen et al. 1989, Vimeux et al. 1999) archive some information about past climates. AGCM simulations with both $H_2{}^{18}O$ and HDO included in the water cycle might be a helpful tool for an improved understanding of these variations.

1.2 Research Topics

The aim of this Ph.D. thesis is a better understanding of the temporal and spatial variations of the isotopic composition of precipitation found in ice cores from both polar regions. Using the improved Hamburg AGCM, ECHAM-4, the performed isotope simulations and extensive comparisons to ice core data from Greenland and Antarctica will focus on the following questions:

1. How good are isotope ECHAM-4 AGCM simulation results for both polar regions for the present-day climate? Are the main characteristics of present isotope data measured in ice cores (e.g. geographical distribution, seasonal cycle, temperature dependency) well reproduced in a numerical simulation?
2. Is $\delta^{18}O$ a reliable temperature proxy for different climate stages like the last glacial maximum (LGM)? Can AGCM simulations help to explain some observed deviations between isotope-based and other (isotope-independent) temperature estimates for this climate period?
3. Which mechanisms might effect the isotopic composition of precipitation during a transition between two different climate stages, e.g. during the transition from the LGM to the Holocene?
4. Are the observed present-day $\delta^{18}O$ variations on interannual to decadal time scales also temperature driven or are they more dominated by (other) atmospheric circulation changes? Is it possible to identify regions in Greenland or Antarctica where climate oscillations like the NAO[4] or ENSO[5] are imprinted in the $\delta^{18}O$ variations of precipitation?

[4] NAO: North Atlantic Oscillation
[5] ENSO: El Niño / Southern Oscillation

1.3 CONTENTS OF THE PH.D. THESIS

To answer the questions listed above, the content of this thesis is arranged as following:

Chapter 2 deals with the first topic, the comparison of model results to present-day ice core data from Greenland. Several extensive traverses across the Greenland ice shield have been performed during the last decade. The available ice core data offers a unique possibility to compare the observations to model results, and analyses of an ECHAM-4 simulation in T42 mode demonstrate the good agreement between observed and simulated isotope values for the present climate.

In Chapter 3 we present first ECHAM-4 isotope results of climate simulations under last glacial maximum (LGM) boundary conditions. Recent isotope-independent LGM temperature estimates by borehole thermometry on Greenland challenge the use of the isotopic paleo-thermometer for this climate stage. The ECHAM-4 simulations confirm the glacial surface temperatures on Greenland determined by borehole thermometry. The disagreement between $\delta^{18}O$ based temperatures and the borehole temperatures of the LGM is not only reproduced by the model, but the simulation results enable a rigorous test of several hypothesis proposed for explaining the different temperature estimates.

To extend the study of differences between the LGM and the present climate, the ECHAM-4 isotope module was expanded by the capability to identify the source regions of water vapour transported to both Greenland and Antarctica. Simulation results with this new model version are presented in Chapter 4 and they show that precipitation falling on both Greenland and Antarctica is a mixture of water masses from several different source regions with a wide range of isotopic signatures. In addition, the model results are analysed with respect to the unresolved question whether the glacial $\delta^{18}O$ signal of Antarctic ice cores is a more reliable surface temperature proxy than LGM isotope data from Greenland.

Chapter 5 deals with the transition phase between a cold climate stage, e.g. the LGM, and a warm climate stage, e.g. the Holocene. A highly idealised sensitivity study was performed to explore how a massive meltwater event in the North Atlantic might affect the isotopic composition of precipitation in the Northern Hemisphere, but also in the tropical Atlantic region. Moreover the effect of a changed isotopic composition of evaporating ocean surface waters (caused by a massive meltwater input into the North Atlantic) is discussed.

In Chapter 6 results of an simulation experiment covering the period 1950-1994 provide a more detailed insight in the variability of the $\delta^{18}O$ signal of precipitation falling in Greenland and Antarctica on interannual to decadal time scales. The temporal relation of the $\delta^{18}O$ values and surface temperatures is compared to the simulated spatial relations for the present climate. A multilinear regression technique is used to identify other climate variables, which contribute to the variability of $\delta^{18}O$ in polar precipitation for the present climate.

1.4 PUBLICATIONS

Chapter 2 to Chapter 5 are all based on manuscripts, which are either published or submitted for publication:

Chapter 2: Werner, M., G. Hoffmann and M. Heimann (1997). "Stable Water Isotopes in Greenland Ice Cores: ECHAM-4 Model Simulation versus Field Measurements." International Symposium on Isotope Techniques in the Study of Past and Current Environmental Changes in the Hydrosphere and the Atmosphere, Vienna, I.A.E.A.

Chapter 3: Werner, M., U. Mikolajewicz, M. Heimann and G. Hoffmann (1999). "Borehole Versus Isotope Temperatures on Greenland: Seasonality Does Matter." Geophysical Research Letters, in press (also: Max-Planck-Institut für Meteorologie, Report 295).

Chapter 4: Werner, M., M. Heimann and G. Hoffmann (1999). "Isotopic Composition and Origin of Polar Precipitation in Present and Glacial Climate Simulations." Tellus A, submitted.

Chapter 5: Werner, M., U. Mikolajewicz, G. Hoffmann and M. Heimann (1999). "Possible Changes of $\delta^{18}O$ in Precipitation Caused by a Meltwater Event in the North Atlantic." Journal of Geophysical Research, in press (also: Max-Planck-Institut für Meteorologie, Report 294).

Chapter 6 ("Modelling Interannual Variability of Water Isotopes in Greenland and Antarctica") is based on a draft of another article, which will be submitted to a peer-reviewed journal, soon.

REFERENCES

Baertschi, P. (1976). "Absolute ^{18}O content of Standard Mean Ocean Water." *Sci.Letters* **31**: 341.

Craig, H. (1961). "Standard for reporting concentrations of deuterium and oxygen-18 in natural waters." *Science* **133**: 1833-1834.

Dansgaard, W. (1953). "The abundance of ^{18}O in meteoric water and water vapour." *Tellus* **5**: 461-469.

Dansgaard, W. (1964). "Stable isotopes in precipitation." *Tellus* **16**(4): 436-468.

Dansgaard, W., S. J. Johnsen, H. B. Clausen, D. Dahl-Jensen, N. S. Gundestrup, C. U. Hammer, C. S. Hvidberg, J. P. Steffensen, A. E. Sveinbjörnsdottir, J. Jouzel and G. Bond (1993). "Evidence for general instability of past climate from a 250-kyr ice-core record." *Nature* **364**: 218-220.

Friedmann, I. (1953). "Deuterium content of natural water and other substances." *Cosmochim. Acta* **4**: 89-103.

Hagemann, R., G. Hief and E. Roth (1970). "Absolute isotopic scale for deuterium analysis of natural waters. Absolute D/H ratio for SMOW." *Tellus* **22**: 712.

Hoffmann, G. (1995). "Stabile Wasserisotope im Allgemeinen Zirkulationsmodell ECHAM." *Examensarbeit Nr.27*, Max-Planck-Institut für Meteorologie, Hamburg.

Hoffmann, G. and M. Heimann (1993). "Water Tracers in the ECHAM General Circulation Model." *Isotope Techniques in the Study of Past and Current Environmental Changes in the Hydrosphere and the Atmosphere*, International Atomic Energy Agency, Vienna.

Hoffmann, G. and M. Heimann (1997). "Water isotope modeling in the Asian monsoon region." *Quaternary International* **37**: 115-128.

Hoffmann, G., M. Werner and M. Heimann (1998). "The water isotope module of the ECHAM atmospheric general circulation model - a study on time scales from days to several years." *Journal of Geophysical Research* **103**(D14): 16871-16896.

IAEA (1992). "Statistical treatment of data on environmental isotopes in precipitation." *Technical Report,* I.A.E.A., Vienna.

Johnsen, S. J., W. Dansgaard and J. W. C. White (1989). "The origin of Arctic precipitation under present and glacial conditions." *Tellus* **41B**: 452-468.

Joussaume, J., R. Sadourny and J. Jouzel (1984). "A general circulation model of water isotope cycles in the atmosphere." *Nature* **311**: 24-29.

Jouzel, J. and L. Merlivat (1984). "Deuterium and Oxygen 18 in precipitation: Modeling of the isotopic effects during snow formation." *Journal of Geophysical Research* **89**(D7): 11749-11575.

Kondratyev, K. Y. and N. I. Moskalenko (1984). "The role of carbon dioxid and other minor gaseous components and aerosols in the radiation budget." *Cambridge University Press*, Cambridge.

Koster, R. D., P. S. Eagleson and W. S. Broecker (1988). "Tracer water transport and subgrid precipitation variation within atmospheric general circulation models." Dept. of Civ. Eng., M.I.T., Cambridge.

Merlivat, L. and J. Jouzel (1979). "Global climatic interpretation of the deuterium-oxygen 18 relationship for precipitation." *Journal of Geophysical Research* **84**(C8): 5029-5033.

Milankovitch, M. (1930). "Mathematische Klimalehre und Astronomische Theorie der Klimaschwankungen." in: *Handbuch der Klimatologie,* (ed. by W. Köppen and R. Geiger), Gebrüder Borntraeger, Berlin.

Petit, J. R., J. Jouzel, D. Raynaud, N. I. Barkov, J. M. Barnola, I. Basile, M. Bender, J. Chappellaz, M. Davis, G. Delaygue, M. Delmotte, V. M. Kotlyakov, M. Legrand, V. Y. Lipenkov, C. Lorius, L. Pepin, C. Ritz, E. Saltzman and M. Stievenard (1999). "Climate and atmospheric history of the past 420,000 years from the Vostok ice core, Antarctica." *Nature* **399**: 429-436.

Philander, S. G. H. (1990). "El Niño, La Niña, and the Southern Oscillation." *Academic Press,* San Diego.

Thompson, L. G., T. Yao, M. E. Davis, K. A. Henderson, E. Mosley-Thompson, P.-N. Lin, J. Beer, H.-A. Synal, J. Cole-Dai and J. F. Bolzan (1997). "Tropical climate instability: The last glacial cycle from a Qinghai-Tibetan ice core." *Science* **276**: 1821-1825.

Vimeux, F., V. Masson, J. Jouzel, M. Stievenard and J. R. Petit (1999). "Glacial-interglacial changes in ocean surface conditions in the southern hemisphere." *Nature* **398**: 410-413.

Chapter 2

Stable Water Isotopes in Greenland Ice Cores: ECHAM-4 Model Simulation versus Field Measurements

ABSTRACT. The stable water isotopes HDO and $H_2{}^{18}O$ have been built into the latest version of the Hamburg atmospheric general circulation model ECHAM-4. First results of a 10 years control experiment (T42 resolution) are discussed, focussing on modelling the isotopic composition of precipitation over the Greenland ice sheet. The spatial distributions of $\delta^{18}O$ and its two most related climatic parameters, surface temperature and precipitation, are in good agreement with observations over the inner ice sheet (mean $\delta^{18}O$ at Summit: -34.6‰ observed, -35.1‰ modelled). Significant deviations between model results and measurements are only observed for coastal stations and around Dye3 (-27.8‰ observed, -23.9‰ modelled). These deviations can partly be explained by the coarse model resolution. The spatial linear relationship between surface temperature and mean ^{18}O concentration ("Dansgaard slope") is well reproduced by the model. A detailed comparison of the seasonal cycle of the isotopic composition in precipitation and ice core measurements shows a good agreement not only for the seasonal phase of $\delta^{18}O$ and δD but also for the deuterium excess. The absolute amplitudes of the modelled isotope signal are overestimated, though. Peak-to-peak variations in the seasonal cycle of the isotopes are higher in the model than in ice core analyses (seasonal $\delta^{18}O$ variations at Summit: 8-10‰ observed, 20-25‰ modelled). Post-depositional processes in the snow might explain this deviation between the model results and observations.

2.1 INTRODUCTION

Over the last 30 years stable water isotopes have been used as a very valuable tool to get a better understanding of the global water cycle. Dansgaard (1964) showed that the global distribution pattern of the stable water isotopes HDO and $H_2{}^{18}O$ reveals important information about climatic conditions during formation and transportation of precipitation. Since then there have been numerous studies on the global and regional distribution of $H_2{}^{18}O$ in precipitation (e.g. Jouzel and Merlivat 1984, Johnsen et al. 1989, Fisher 1992). Nowadays, stable water isotopes are not only used to investigate different aspects of recent climate conditions but are also some of the key tracers in paleoclimatological studies.

During the last decade stable water isotopes have been built into the hydrological cycle of several atmospheric general circulation models (AGCMs) (Joussaume et al. 1984). These models have enhanced our understanding of the basic physical processes of isotope fractionation and helped to understand observed isotope signals at various locations. One of these

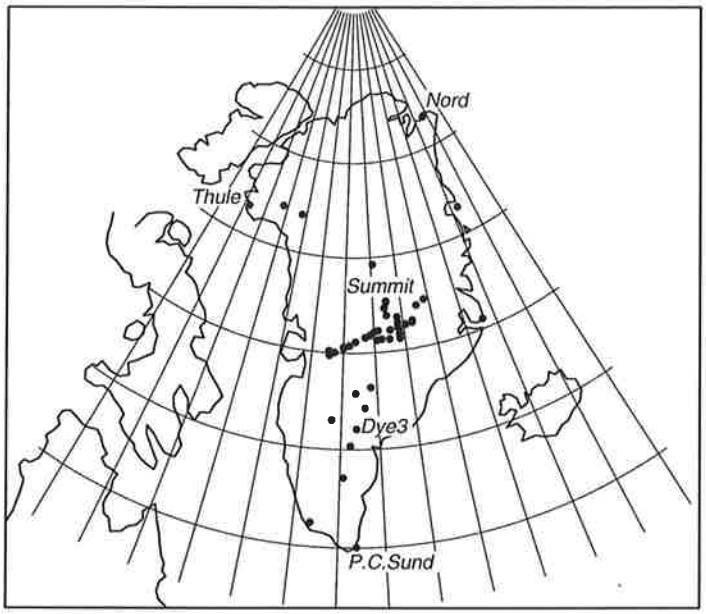

Figure 1: Location of coastal IAEA stations and of ice/firn core studies on the Greenland ice sheet (published in Clausen et al. 1988, Johnsen et al. 1989, IAEA 1992, Dansgaard et al. 1993, Fischer et al. 1995).

AGCMs is the ECHAM model developed at the Max-Planck-Institute for Meteorology, Hamburg. First the isotopes were built into the model version ECHAM-3 and the results and quality of this model have been discussed in several publications (Hoffmann and Heimann 1993, Hoffmann and Heimann 1997, Hoffmann et al. 1998). In this article we show first results of isotope modelling using the next version of the Hamburg AGCM, ECHAM-4, focussing our interest on the modelled isotope signal in precipitation over Greenland. A detailed analysis of the model results and an extended comparison with observation data from both coastal stations and ice core records are performed to reveal the quality of isotope modelling for this northern polar region.

2.2 Model Experiment

We have performed a 10 years control experiment with ECHAM-4 in T42 mode (horizontal resolution: 2.8° x 2.8°, time step: 24 min, 19 vertical levels). The experiment started at January 1st of year 3, after a spin-up time of two years. Initialisation and transportation of the water tracers were identical to an ECHAM-3 experiment described by Hoffmann (1993). Compared to the older model a number of substantial changes have been built into ECHAM-4. These include a new radiation scheme with modifications concerning the water

vapour continuum, a new formulation of the vertical diffusion coefficients, a new closure for deep convection and minor changes concerning the parameterisation of horizontal diffusion, stratiform clouds and land surface processes. For a detailed discussion of these changes, see Roeckner and Arpe (1995). Additional modifications affecting especially the physics and numerics of the stable water isotope module (as described in Hoffmann and Heimann 1993) have not been introduced to the model.

2.3 OBSERVATIONS

Greenland's inner ice sheet offers a unique possibility to study major aspects of the Northern Hemisphere climate under present and past climate conditions. Over the last three decades strong efforts have been made to recover deep ice cores to provide long time records of isotopic composition and chemical tracers. Several additional traverses over the Greenland ice sheet were performed to get a more detailed insight into the geographical distribution of these species and to help interpret long-time records. In this article we compare our model experiment with the field work of several authors (Clausen et al. 1988, Johnsen et al. 1989, Dansgaard et al. 1993, Fischer et al. 1995). Since direct measurements of stable water isotopes in precipitation over a period of several years are only available from coastal IAEA-stations (IAEA 1992) we included them in our database. Fig. 1 gives an overview of the geographical distribution of all observations used. The reader should notice that these observations are not distributed uniformly and that there is a lack of observations in the north-east region of the inner Greenland ice sheet.

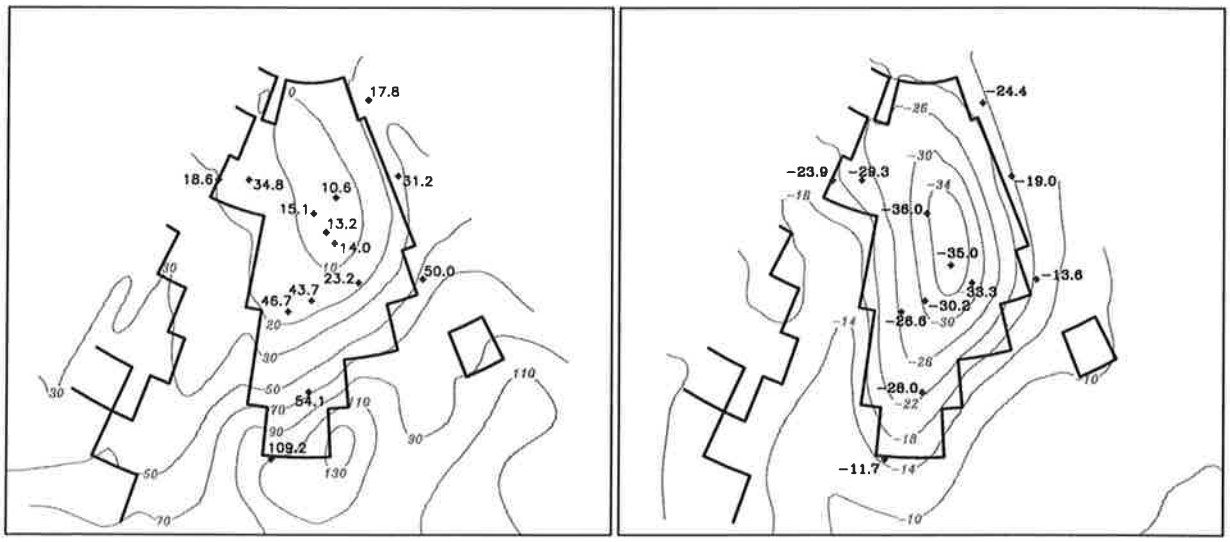

Figure 2: Left: Spatial distribution of mean precipitation amount (in cmy^{-1}); Right: mean $\delta^{18}O$ in precipitation (in ‰) over Greenland. Additional to the isolines of the model (grey lines) several observations at various locations of Greenland are shown (black numbers).

2.4 Simulation Results

2.4.1 Spatial Distribution of Mean Isotope Values

In Fig. 2 (left) the spatial distribution of the modelled mean precipitation amount is shown. Additionally to the isolines of the modelled distribution, observations at several locations on Greenland are plotted. The low accumulation area in northern Greenland (≤ 10 cm water equivalent per year) is well represented in the model although this area seems to be overestimated in north-west direction compared to recent accumulation maps of Ohmura (1991). Modelled precipitation values in the southern part of Greenland are too high (about 20-40% around Dye3) while data from coastal IAEA stations agree well with the model results. Fig. 2 (right) shows the mean values of $\delta^{18}O$ in precipitation and the pattern is similar to the temperature distribution (not shown).

Modelled $\delta^{18}O$ values of the central Greenland ice sheet agree well with measurements of ice cores (e.g. Summit: modelled: -34.6 ‰, observed: -35.1‰) while there is a stronger discrepancy between model results and ice core data around Dye3 (-23.9‰ modelled, -27.8‰ observed). The coastal IAEA stations show some difference between modelled $\delta^{18}O$ values and observations. This can be explained by the steep orographic gradient at the coast of Greenland, which is not represented very well in the used model resolution. For a linear regression analysis between measured $\delta^{18}O$ data and model values we therefore excluded data points from coastal areas and from locations around Dye3. Using only the remaining data values of the inner Greenland ice sheet we obtain a linear relation of m=0.91±0.09 between measured and modelled values with a small offset of b=-2.49±2.72 (Fig. 3). The correlation coefficient of this analysis was r=0.95. Similar results can be obtained for surface temperature and precipitation.

2.4.2 The $\delta^{18}O$-T_S-Relation

The spatial linear relationship between surface temperature T_S and mean $\delta^{18}O$-signal has been described first by Dansgaard (1964) and is well established for central Greenland. Johnsen gives in his work a linear relation of $\delta^{18}O=(0.67\pm0.02)T_S-(13.7\pm0.5)$‰ for observations in south and west Greenland (Johnsen et al. 1989). Fischer showed that the $\delta^{18}O$-T_S-gradients west and east of the main Greenland ice divide differ slightly (Fischer et al. 1995). Neglecting this effect we plotted in Fig. 4 (left) the $\delta^{18}O$ data of all observation points on the ice sheet versus the mean surface temperatures. A linear regression analysis results in $\delta^{18}O=(0.68\pm0.02)T_S - (13.7\pm0.5)$‰. This relation is almost identical to the one of Johnsen mentioned above. In Fig. 4 we also show the modelled $\delta^{18}O$ values versus modelled surface temperatures (right plot). The resulting relation $\delta^{18}O=(0.69\pm0.03)T_S -(11.8\pm0.8)$‰ is in perfect agreement with the observations.

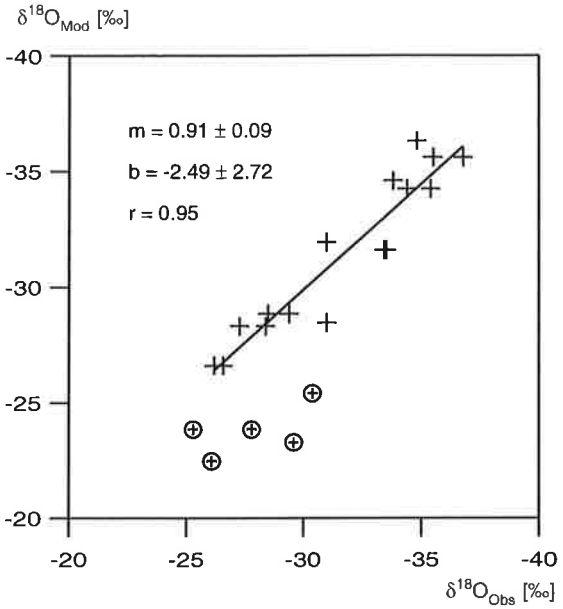

Figure 3: Linear relation between measured and modelled $\delta^{18}O$ values. Only observations of the inner Greenland ice sheet (+) were used for the computation of the regression line whereas observations from coastal stations and the Dye3 area (⊕) were excluded.

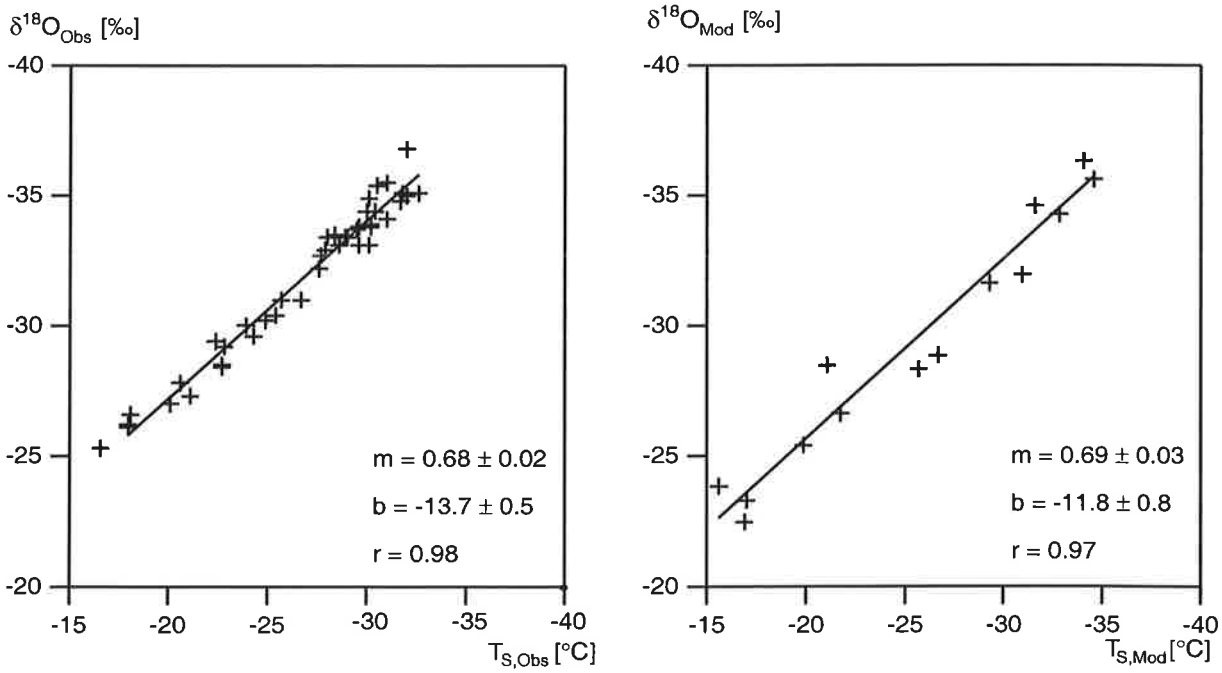

Figure 4: The spatial linear relation between mean $\delta^{18}O$ values and surface temperatures T_S on the Greenland ice sheet. Left: observations, right: model results.

2.4.3 The Seasonal Cycle

Besides of the yearly mean values of temperature, precipitation and isotopic composition we have analysed the seasonal cycle of these parameters. Fig. 5 shows the modelled monthly variations at the grid point 71.2°N, 39.4°W near Summit, central Greenland, for the simulation period of 10 years. The strong annual cycle of the surface temperature (Fig. 5a) is caused primarily by increased solar radiation during polar summer versus polar winter. The cycle agrees well with a recently published record of an automatic weather station located at 72.28°N, 38.82°W (Shuman et al. 1996). The temporal variations of precipitation (Fig. 5b) do not show any clear seasonal cycle in the model. This result is difficult to verify by observations since, to our knowledge, there does not exist any multi-year record of directly observed monthly precipitation anywhere on the Greenland ice sheet. In Fig. 5c and Fig. 5d the modelled seasonal cycles of $H_2{}^{18}O$ and HDO are shown. Like the temperature record clear maxima of the δ-values during summer and minima during winter period can be observed. These cycles agree well with many isotope studies performed on firn and ice cores (e.g. Johnsen et al. 1989, Fischer et al. 1995) although peak-to-peak $\delta^{18}O$ variations observed in ice cores are smaller than the peak-to-peak variations seen in Fig. 5c (observed: 8-10‰, modelled: 20-25‰). This higher seasonal variability of modelled δ-values might be explained by post-depositional processes in snow and firn, which are not included in the model. These processes will probably smooth out peak-to-peak variations observed in several years old firn cores. For example Shuman reported $\delta^{18}O$ peak-to-peak variations of about 20‰ observed in a "fresh" snow pit (Shuman et al. 1995). Despite of the clear seasonal cycle the mean δD value of Fig. 5d is significantly lower than firn core measurements done at the nearby position T99 published by Fischer (1995). While the model yields a mean δD value of -290.5‰, Fischer reports a mean δD value of -266.3‰. At this point we do not have a reasonable explanation for this shortcoming of the model simulation. In Fig. 5e we plot a second order quantity, the so-called deuterium excess $d=\delta D-8\delta^{18}O$. This parameter represents an indicator of kinetic effects occurred during evaporation and, in high polar regions, during sublimation in snowflake formation. It contains therefore additional information about sources and transport pathways of the precipitation over Greenland (Jouzel and Merlivat 1984, Fisher 1992). The seasonal cycle of the deuterium excess *d* in Fig. 5e agrees well with measurements of Johnsen (1989) or Fischer (1995) but two differences between observations and model results should be noticed: (1) Both authors report a clear shift between the $\delta^{18}O$ maxima and the *d* maxima of about 2-3 month leading to maximum *d* values in autumn (and minimum *d* values in spring). This shift can not be clearly seen in the modelled *d* cycle, which is almost in phase with the $\delta^{18}O$ cycle. (2) The modelled mean *d* value is significantly lower compared to the observations (-13.7‰ modelled, +13.6 ‰ observed). This shift is caused by the too low mean δD value mentioned above.

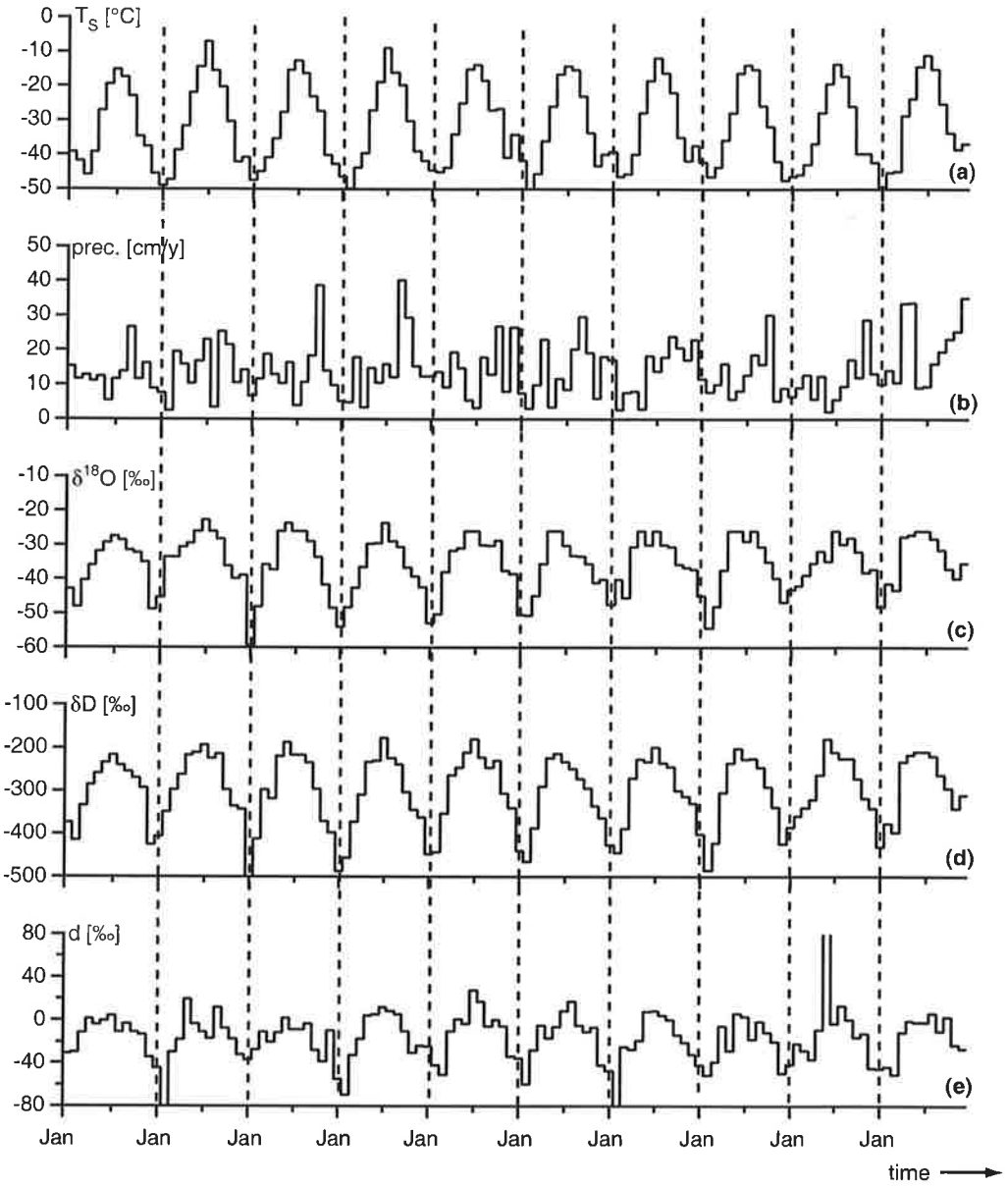

Figure 5: Seasonal cycle of (a) surface temperature T_S, (b) precipitation, (c) $\delta^{18}O$, (d) δD and (e) deuterium excess *d*. The time series present modelled monthly values for the total simulation period of 10 years.

2.5 Conclusions and Outlook

This detailed study of modelling the stable water isotopes HDO and $H_2{}^{18}O$ over the Greenland ice sheet clearly shows the potential of the global circulation model ECHAM-4 for isotope studies. The spatial distributions of $\delta^{18}O$ and its two most related climate parameters, surface temperature and precipitation, are in very good agreement with observations over the inner ice sheet. This agreement leads to a modelled $\delta^{18}O$-T-relationship almost identical to the observed one. The modelling of the annual cycle of the stable water isotopes is also quite satisfying, not

only for the isotopic compositions but also for the deuterium excess. Especially the clear annual cycles of $\delta^{18}O$, δD and d over the Greenland ice sheet are one of the major improvements of the ECHAM-4 experiment with respect to simulations made with older versions of the model.

In a next step we are interested in long time variations of the isotopic composition of precipitation. Model experiments over several decades or even centuries will give information about model variability on those time scales. Detailed comparisons with long duration ice core records might extend our knowledge about the natural variability of the stable water isotope signal. We will also try to identify the major source regions and transport pathways for the precipitation of the polar regions. Doing this for model experiments run under different paleoclimatic boundary conditions might also help to interpret long time isotope records.

ERRATUM

In the preceding article we report problems to model the correct mean values of δD and the deuterium excess d in precipitation falling on Greenland. Further sensitivity studies after the publication of the article revealed that a software coding error in the isotope module of ECHAM-4 caused the erroneous δ-values. After correcting this error a new 5-years simulation in T42 resolution was performed. Not only the modelled $\delta^{18}O$ value (-31.7‰) but also the deuterium excess (+10.9‰) of the grid box enclosing Summit is now in good agreement with a new measurement (d = 8.8 - 9.3‰) from the GRIP ice core (Hoffmann et al. 1997). The same is true for the seasonal amplitude of the deuterium excess (modelled: ~10‰, observed: 5-12‰). We also observe a clear shift between the seasonal cycles of $\delta^{18}O$ and d in this simulation. However, the simulated phase lag of the deuterium excess seems to be overestimated by 1-2 months compared to ice core data.

REFERENCES:

Clausen, H. B., N. S. Gundestrup, S. J. Johnsen, R. A. Bindschadler and J. Zwally (1988). "Glaciological investigations in the Crête area, central Greenland: a search for a new deep-drilling site." *Annals of Glaciology* **10**: 10-15.

Dansgaard, W. (1964). "Stable isotopes in precipitation." *Tellus* **16**(4): 436-468.

Dansgaard, W., S. J. Johnsen, H. B. Clausen, D. Dahl-Jensen, N. S. Gundestrup, C. U. Hammer, C. S. Hvidberg, J. P. Steffensen, A. E. Sveinbjörnsdottir, J. Jouzel and G. Bond (1993). "Evidence for general instability of past climate from a 250-kyr ice-core record." *Nature* **364**: 218-220.

Fischer, H., D. Wagenbach, M. Laternser and W. Haeberli (1995). "Glacio-meteorological and isotopic studies along the EGIG line, central Greenland." *Journal of Glaciology* **41**: 515-527.

Fisher, D. A. (1992). "Stable isotope simulations using a regional stable isotope model coupled to a zonally averaged global model." *Cold Regions Science and Technology* **21**: 61-77.

Hoffmann, G. and M. Heimann (1993). "Water Tracers in the ECHAM General Circulation Model." *Isotope Techniques in the Study of Past and Current Environmental Changes in the Hydrosphere and the Atmosphere*, International Atomic Energy Agency, Vienna.

Hoffmann, G. and M. Heimann (1997). "Water isotope modeling in the Asian monsoon region." *Quaternary International* **37**: 115-128.

Hoffmann, G., M. Stievenard, J. Jouzel, J. W. C. White and S. J. Johnsen (1997). "Deuterium excess record from central Greenland (modelling and observations)." *International Symposium on Isotope Techniques in the Study of Past and Current Environmental Changes in the Hydrosphere and the Atmosphere*, I.A.E.A, Vienna.

Hoffmann, G., M. Werner and M. Heimann (1998). "The water isotope module of the ECHAM atmospheric general circulation model - a study on time scales from days to several years." *Journal of Geophysical Research* **103**(D14): 16871-16896.

IAEA (1992). "Statistical treatment of data on environmental isotopes in precipitation." *Technical Report,* I.A.E.A., Vienna.

Johnsen, S. J., W. Dansgaard and J. W. C. White (1989). "The origin of Arctic precipitation under present and glacial conditions." *Tellus* **41B**: 452-468.

Joussaume, J., R. Sadourny and J. Jouzel (1984). "A general circulation model of water isotope cycles in the atmosphere." *Nature* **311**: 24-29.

Jouzel, J. and L. Merlivat (1984). "Deuterium and Oxygen 18 in precipitation: Modeling of the isotopic effects during snow formation." *Journal of Geophysical Research* **89**(D7): 11749-11575.

Ohmura, A. and N. Reeh (1991). "New precipitation and accumulation maps for Greenland." *Journal of Glaciology* **37**: 140-148.

Roeckner, E. and K. Arpe (1995). "AMIP experiments with the new Max Planck Institute for Meteorology Model ECHAM4." *AMIP Scientific Conference*, WMO, Monterey, USA.

Shuman, C. A., R. B. Alley, S. Anandakrishnan, J. W. C. White, P. M. Grootes and C. R. Stearns (1995). "Temperature and accumulation at the Greenland Summit: Comparison of high resolution isotope profiles and satellite passive microwave brightness temperature trends." *Journal of Geophysical Research* **100**(D5): 9165-9177.

Shuman, C. A., M. A. Fahnestock, R. A. Bindschadler, R. B. Alley and C. R. Stearns (1996). "Composite temperature record from the Greenland Summit, 1987-1994: Synthesis of multiple automatic weather station records and SSM/I brightness temperatures." *Journal of Climate* **9**: 1421-1428.

Chapter 3

Borehole versus Isotope Temperatures on Greenland: Seasonality Does Matter

ABSTRACT. New simulation results of the Hamburg atmosphere general circulation model ECHAM-4 under maximum glacial boundary (LGM) conditions confirm the paleotemperatures on Greenland determined by borehole thermometry. The disagreement between $\delta^{18}O$ isotope based temperatures and the borehole temperatures of the LGM is not only reproduced by the model but the simulation results provide a plausible explanation: Paleotemperatures inferred from $\delta^{18}O$ measurements in ice cores are biased by a substantially increased seasonality of precipitation over Greenland during the LGM. During the glacial winter a much more zonal circulation prevents the effective transport of moisture to the Greenland ice sheet and therefore reduces the contribution of isotopically strongly depleted winter snow to the annual mean isotope signal.

3.1 INTRODUCTION

Since several decades stable water isotopes ($H_2{}^{18}O$, HDO) have been shown to provide a valuable tool for paleoclimate studies (e.g. Dansgaard 1964, Jouzel et al. 1987). To determine past surface temperatures it has been generally assumed that the observed present-day spatial relationship between surface temperature (T_S) and the isotopic composition of precipitation (usually given as $\delta^{18}O$ or δD) can be used as an analogue of the temporal T_S-$\delta^{18}O$-relation. However, recent isotope-independent measurements of paleotemperatures on Greenland by borehole thermometry (Cuffey et al. 1995, Johnsen et al. 1995, Dahl-Jensen et al. 1998) indicate that the temperature difference at Summit, central Greenland, between the last glacial maximum (LGM) and the present-day was in the range of -23 ± 2 K, twice as large as estimated from $\delta^{18}O$ data using the classical approach. Several hypotheses have been proposed to reconcile this discrepancy: (1) a different origin of precipitation under LGM climate (Charles et al. 1994), (2) changes in the seasonality of precipitation (Steig et al. 1994, Krinner et al. 1997), (3) cool tropical sea surface temperatures (Boyle 1997), (4) a change in the cloud vs. surface temperature relation (Krinner et al. 1997), and (5) changes of microphysical and atmospheric processes (Fisher 1991). A more detailed overview of these hypotheses has been provided by Jouzel (1997). Here, we report the results of a new study,

where we have tested all but one of these hypotheses using an atmospheric general circulation model (AGCM) which explicitly models two stable water isotopes ($H_2{}^{18}O$, HDO) in the hydrological cycle. Such an AGCM allows an independent simulation of both quantities $\delta^{18}O$ and T_S. Hence possible changes of the isotope-temperature-relation in time and space can be explored by using different boundary conditions for AGCM model experiments.

3.2 MODEL EXPERIMENTS

Our results are based on isotope modelling using the Hamburg AGCM, ECHAM-4 (Roeckner et al. 1996). The model is capable to simulate many aspects of the isotope signal in precipitation found in modern observations (Hoffmann et al. 1998). All experiments reported here were performed in 3.75° x 3.75° model resolution (T30), each of them running for 10 years with seasonally varying constant boundary conditions. The model includes diagnostic code to tag water vapour from different source regions.

The control experiment was integrated under present-day climate boundary conditions. For the LGM simulation CLIMAP (1981) boundary conditions (sea surface temperatures, solar insulation, glacial atmospheric CO_2) were prescribed except for the Greenland topography. In agreement with new results of Cuffey and Clow (1997) the glacial Greenland topography change proposed by Peltier (1994) was lowered by three-quarters, yielding an absolute glacial rise at Summit of +200 m compared to present. Additionally, we assumed a slight glacial enrichment ($\delta^{18}O$: +1.5‰, δD: +12‰) of the heavy water isotopes in the oceans to correct for the isotopically lighter water locked up in glacial ice sheets (Duplessy et al. 1980).

Fourteen different evaporation areas of the water vapour were defined for tagging. Over land, each continent was selected as a distinct source region. For the ocean, yearly mean sea surface temperatures (SSTs) were chosen to define different evaporation regions of the polar seas ($SST \leq 10°C$), the northern Atlantic and northern Pacific ($10°C < SST \leq 25°C$) and the tropical Atlantic and tropical Pacific ($SST > 25°C$), respectively. Thus, the ocean source regions of the control experiment and the LGM simulation differed in their geographical position but had the same mean SST range.

Besides of the control experiment and the LGM simulation we performed two additional LGM sensitivity experiments: In the first one we used the Peltier (1994) topography change to evaluate the influence of a higher Greenland ice shield. In the second sensitivity experiment we investigated the influence of cooler tropical SSTs during the LGM. Several authors have claimed the CLIMAP SST reconstruction as too warm for tropical regions (e.g. Broecker 1996). Thus, for the second sensitivity study, we assumed between 30°S and 30°N at least 5° cooler SSTs compared to present, but kept the CLIMAP SST if they prescribed an even

stronger cooling. Northwards (southwards) of 45°N (45°S) the standard CLIMAP SSTs were prescribed with a linear transition zone between 30° and 45°.

3.3 Results & Discussion

3.3.1 Mean State for Present-day and LGM Climate

Modelled 10-year-mean values of T_S (-29.4°C), precipitation (22.6cm/y) and $\delta^{18}O$ (-29.5‰) of the grid box enclosing the Summit area are close to in-situ observations and measurements on ice cores (Table 1). In order to compare mean model values in a consistent way with field data, the modelled T_S and precipitation values are calculated as standard arithmetic means while the modelled mean $\delta^{18}O$ value is a precipitation-weighted mean based on monthly isotope values $\delta^{18}O_i$ and precipitation pr_i:

$$\delta^{18}O = \Sigma_i (\delta^{18}O_i \cdot pr_i) / \Sigma_i pr_i$$

The slightly lower model values of T_S and $\delta^{18}O$ as compared to the observations can be explained by model resolution: the grid box enclosing the Summit area is 500 m lower than the true Summit location. In the LGM experiment T_S (-53°C) and precipitation (4.5cm/y) are also close to the estimates derived from borehole thermometry and ice core data, although the precipitation amount is slightly underestimated. But the mean $\delta^{18}O$ value (-33.2‰) is significantly higher than the ice core data (-41‰ to -43‰) which can partly be explained again by model resolution. However, the modelled difference, $\Delta\delta^{18}O$, between LGM and present climate is about 3‰ less than observed, too. This shortcoming in the LGM experiment is not fully understood. It is also obvious from Table 1 that the higher glacial elevation of the Greenland ice sheet proposed by Peltier (1994) results in even lower model values of T_S and precipitation which deviate from the ice core data.

Climate	Data	T_S (°C)	Prec. (cm/y)	$\delta^{18}O$ (‰)
present	Measurements	-32	23	-34.8
	Control Experiment	-29.4 ± 1.2	22.6 ± 4.3	-29.5 ± 0.7
LGM	GRIP/GISP Estimates	-50 to -55	5.5 to 7	-41 to -43
	LGM Experiment	-52.9 ± 1.3	4.5 ± 0.9	-33.2 ± 1.9
	Sensitivity Study 1 (Peltier topography)	-59.2 ± 1.0	2.9 ± 0.7	-36.7 ± 2.0
Δ(LGM-present)	GRIP/GISP Estimates	-18 to -23	-16 to -17.5	-6.2 to -8.2
	LGM Exp. - Control Exp.	-23.5 ± 2.7	-18.6 ± 5.2	-3.7 ± 2.6

Table 1: Comparison of in-situ measurements or GRIB/GISP ice core data, respectively, (Johnsen et al. 1992, Grootes et al. 1993, Cuffey and Clow 1997) and ECHAM-4 simulation values for the present-day climate and the last glacial maximum (LGM). The additional LGM sensitivity experiment varies in the prescribed glacial topography (see text).

3.3.2 The Seasonal Cycle

In the control experiment, T_S shows a clear seasonal cycle with a minimum of -41±3°C in January and a maximum of -14±2°C in July (Fig. 1) which agrees well with observations (Shuman et al. 1996). Parallel to T_S, there is also a strong seasonal cycle of the modelled $\delta^{18}O$ signal (amplitude: ~10±5‰) which is confirmed by many studies on ice cores (e.g. Johnsen et al. 1989). In contrast to T_S and $\delta^{18}O$, the modelled precipitation under a present-day climate does not show such a strong seasonal cycle. However the simulated higher values in late summer/early autumn and the small minimum in late winter/early spring have also been reported before (Bromwich et al. 1993). Under LGM boundary conditions the shape of the

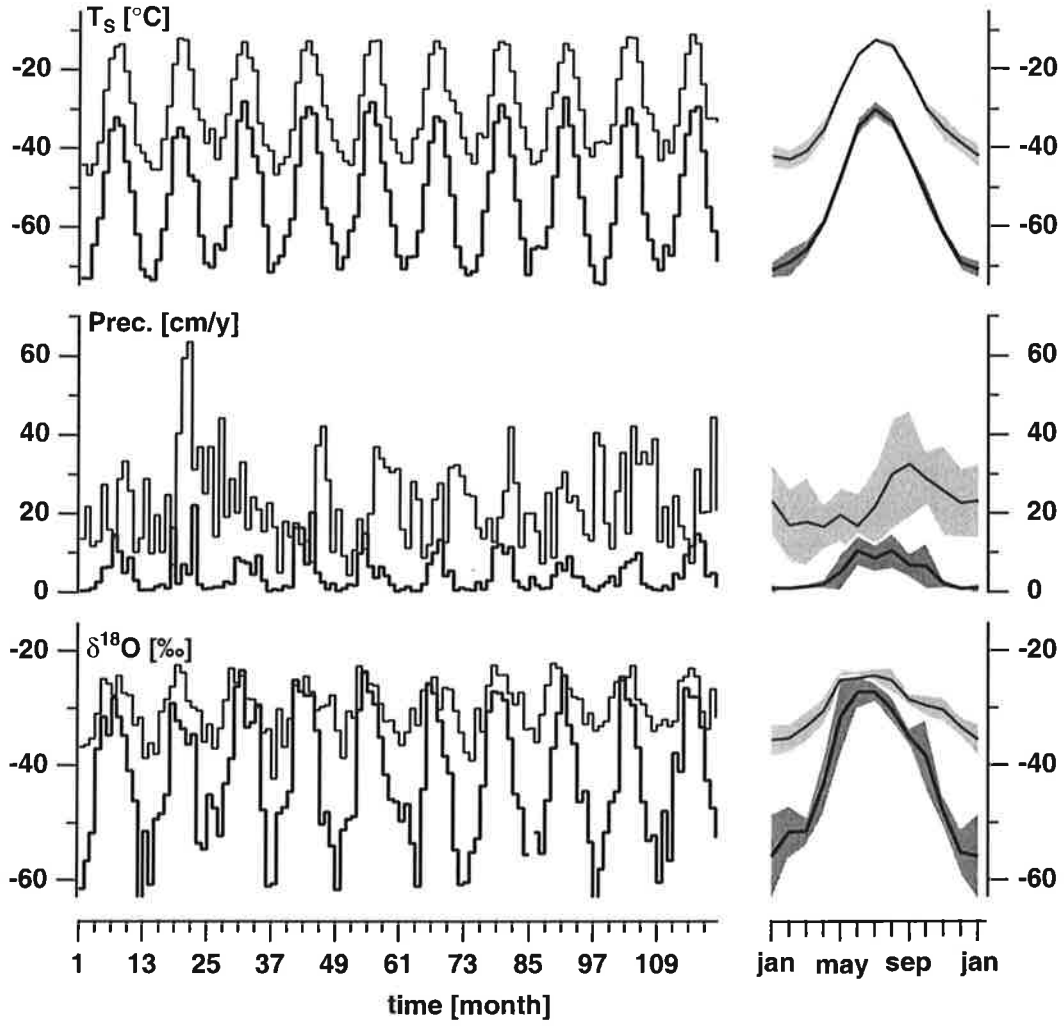

Figure 1: Modelled seasonality of T_S, precipitation and $\delta^{18}O$ in the grid box enclosing Summit. Left: monthly mean values over the simulation period of 10 years (control simulation: thin line, LGM simulation: bold line). Right: The averaged seasonal cycle (thin or bold line) and its standard deviation 1σ (light or dark grey area). For clarity reasons, the January values are drawn twice in the right plot.

seasonal cycle of T_S and $\delta^{18}O$ is almost unchanged. In contrast, the seasonal cycle of precipitation is considerably affected: Modelled LGM winters are very dry with monthly precipitation values of less than 1mm/month. Analyses of the geopotential height at 500hPa show that such extreme dry glacial winters are caused by strong changes in the general circulation pattern. While in the glacial summer the mean flow of air mass is comparable to the present-day climate, a flow from more northerly directions is seen in the glacial winter. The advected air masses are substantially colder and dryer, and thus responsible for the aridity and stronger cooling over central Greenland in glacial winter compared to glacial summer.

3.3.3 Modelled Isotope-Temperature-Relations

As seen in Fig. 2a, the simulated modern spatial isotope-temperature-slope is close to the observations (0.67±0.02‰/°C) (Johnsen et al. 1989). For the LGM simulation the spatial slope (0.38±0.10‰/°C) is significantly lower and its variance larger than for the control experiment. To determine the temporal $\delta^{18}O$-T_S-relationship for the Summit area we correct the LGM $\delta^{18}O$ values for the changed isotope values of the ocean source and then calculate for each combination of the ten control and ten LGM simulation years the temporal slope as $m = \Delta\delta^{18}O(\text{LGM-present}) / \Delta T_S(\text{LGM-present})$. The mean value of the grid box enclosing Summit (0.23±0.08‰/°C) is about 60% smaller than the modelled modern spatial slope, similar to the relationship based on the borehole thermometry measurements.

Thus, the observed discrepancy between borehole and isotope temperatures is clearly reproduced in our simulations. Based on the model simulation we now investigate the different hypotheses that have been proposed to explain the discrepancy:

3.3.4 Origin of Precipitation

Modelled precipitation on Summit, Greenland, originates mainly from 6 different source regions (Table 2). The mean isotopic signatures of these different source regions show variations in the range of -20‰ to -48‰. An extreme moisture source change could therefore result in an isotopic signal, which is independent of local temperature changes on Greenland (Charles et al. 1994). But as seen in Table 2, a major change of the heterogeneous collection of moisture sources does not occur in the LGM simulation. Therefore the small temporal isotope-temperature gradient can not be explained by this effect. Our findings agree with older tagging experiments performed with the GISS AGCM (Charles et al. 1994).

	Present		LGM	
Region	Prec. (%)	$\delta^{18}O$ (‰)	Prec. (%)	$\delta^{18}O$ (‰)
polar seas	15.2	-19.8	12.4	-20.2
northern Pacific	7.9	-41.1	9.2	-41.0
northern Atlantic	27.8	-26.7	26.1	-25.6
tropical Pacific	9.6	-46.6	12.2	-48.4
tropical Atlantic	13.9	-31.6	6.4	-30.8
North America	15.3	-24.9	18.0	-26.5
Eurasia	6.1	-31.5	11.0	-32.3
rest	4.9	-	4.7	-

Table 2: Contribution (in %) and mean $\delta^{18}O$ value (in ‰) of different vapour source regions to the modelled precipitation at Summit, Greenland. Annual mean SST were chosen to define several ocean evaporation regions (see text).

3.3.5 Changes in Seasonality

Since the $\delta^{18}O$ signal is temperature dependent but only archived during precipitation events, the isotopic composition is more closely related to a precipitation-weighted temperature $T_{S,pr}$

$$T_{S,pr} = \Sigma_i (T_{S,i} \cdot prec_i) / \Sigma_i prec_i$$

where $T_{S,i}$ and pr_i are the temperature and precipitation amount, respectively, at time i (Steig et al. 1994). For a yearly uniform distribution of precipitation events the $\delta^{18}O$-temperature-relation will be quite similar for T_S and $T_{S,pr}$. On the opposite, a strong seasonal cycle of precipitation with less snow fall during winter than during summer will shift $T_{S,pr}$ to warmer temperatures than T_S and thus alter the $\delta^{18}O$-temperature-relation. To quantify this effect for our model results we re-calculate the simulated spatial and temporal slopes for $T_{S,pr}$ using monthly mean values of $T_{S,i}$ and pr_i. The spatial $\delta^{18}O$-T-slope for the control experiment is similar for T_S and $T_{S,pr}$ (Fig. 2b). The spatial LGM slope (0.55±0.06‰/°C) computed with $T_{S,pr}$ is now close to the modern value (0.53±0.08‰/°C), despite significant lower mean temperatures during the LGM climate. Because of the warmer LGM $T_{S,pr}$ values the temporal slope (0.41±0.11‰/°C) is now close to both spatial relations, too. Thus, we see in our model results a strong influence of the changed glacial precipitation cycle on the simulated isotope-temperature-relations.

3.3.6 Cool Tropical SSTs

Boyle (1997) proposed that cooler glacial tropical SSTs might explain the borehole versus isotope temperature discrepancy. Cooling of the initial source of water vapour transported to Greenland shifts the spatial isotope-temperature-relation towards colder temperatures and

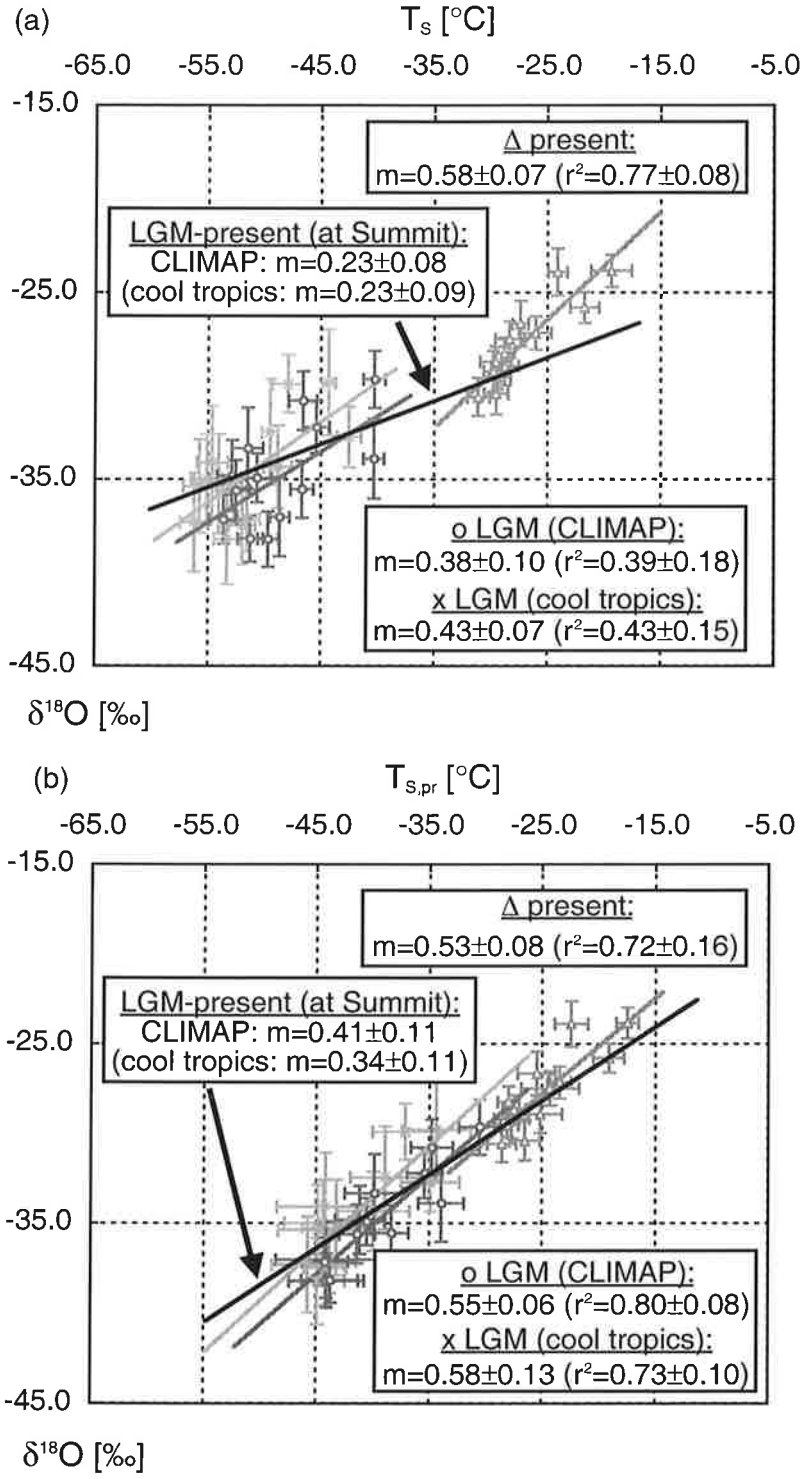

Figure 2: a: Modelled mean values of T_S and $\delta^{18}O$ for all grid boxes of the inner Greenland ice sheet for a present-day climate (Δ) and for a LGM climate with CLIMAP SSTs (o) or cooler tropical SSTs (x). Modelled 1σ-values are given as error bars. Present-day and LGM spatial $\delta^{18}O$-T_S-relations are drawn as grey lines, the temporal relation (LGM-present) for Summit as a black line. Calculated slopes are given in the text boxes. b: Same as Fig. 2a, but for the precipitation-weighted temperature $T_{S,pr}$.

would thereby also change the temporal relation. To test this hypothesis, we calculated the spatial and temporal temperature-isotope-relations on Summit for our second LGM sensitivity experiment, in which we applied cooler tropical SSTs. As clearly seen in Fig. 2a, the hypothesis of Boyle (1997) is correct: Cooler tropical SSTs shift the glacial temperature-isotope-relation on Greenland but this shift is small. The seasonality of precipitation is similar to the CLIMAP LGM simulation and the effect of the changed seasonality is dominating the temperature-isotope-slopes (Fig. 2b).

3.3.7 Difference in Cloud versus Surface Temperatures

The temperature directly imprinted in the isotope signal is not the surface temperature but the temperature during formation of precipitation, i.e. the cloud temperature. A shift in the relation between cloud and surface temperatures under a glacial climate could explain the difference between modern spatial and temporal $\delta^{18}O$-T_S-relation (Krinner et al. 1997). We assume as a first guess that most of the precipitation is formed near the warmest tropospheric layer (Krinner et al. 1997) and define the inversion temperature T_{inv} as the temperature of the warmest model layer in the troposphere. The mean inversion strength T_S-T_{inv} over Greenland in the LGM simulation is 6.3° larger than in the control experiment. However, the strongest changes are found during the winter season when no precipitation is formed in the LGM simulation. The precipitation-weighted inversion strength $T_{S,pr}$-$T_{inv,pr}$ changes only by 4.2° between present and LGM climate. If we use the estimated inversion temperatures, the temporal slopes become slightly steeper (for T_{inv}: 0.32±0.11‰/°C, for $T_{inv,pr}$: 0.61±0.16‰/°C) but this inversion effect is much smaller than the seasonality effect. These findings agree with previous results performed with the LMDz model (Krinner et al. 1997).

3.4 Conclusions

To our knowledge, the present ECHAM-4 results are the first isotope AGCM simulations, which clearly reproduce the borehole versus isotope temperature discrepancy. They also suggest that a change in the seasonal cycle of precipitation is the most plausible explanation for the disagreement: The extremely dry winters during the LGM lead to a systematic bias of isotope estimated annual mean surface temperatures towards summer values. A change in the inversion strength and/or cooler tropical SSTs might have altered the temporal isotope-temperature relation, too, but the impact of these effects is much smaller.

How reliable are these new model results? Older isotope AGCM simulations under full LGM conditions did not show a notable change in the seasonality of precipitation (Charles et al. 1995). But neither were those simulations able to clearly reproduce the discrepancy between borehole and isotope temperatures (Jouzel et al. 1997). To the contrary, a majority of the

AGCMs participating in the PMIP project (8 out of 13) strongly support our findings of a changed seasonality of precipitation under LGM conditions (Krinner 1997). Similar results are found in two further AGCM studies (Fawcett et al. 1997, Krinner et al. 1997).

Clearly, there might also be other regions and past climate stages where isotope temperatures are biased by a change in the seasonality of precipitation. There is no a priori guarantee that any modern spatial isotope-temperature-relation is appropriate to calculate past temporal temperature variations. Isotope modelling with AGCMs clearly has shown being a helpful tool to infer the changes of such isotope-temperature-relations under different paleoclimates.

REFERENCES

Boyle, E. A. (1997). "Cool tropical temperatures shift the global δ^{18}O-T relationship: An explanation for the ice core δ^{18}O - borehole thermometry conflict?" *Geophysical Research Letters* **24**(3): 273-276.

Broecker, W. S. (1996). "Glacial climate in the tropics." *Science* **272**(5270): 1902-1904.

Bromwich, D. H., F. M. Robasky, R. A. Keen and J. F. Bolzan (1993). "Modeled variations of precipitation over Greenland ice sheet." *Journal of Climate* **6**: 1253-1268.

Charles, C. D., D. H. Rind, J. Jouzel, R. D. Koster and R. G. Fairbanks (1994). "Glacial-interglacial changes in moisture sources for Greenland: Influences on the ice core record of climate." *Science* **263**: 508-511.

Charles, C. D., D. H. Rind, J. Jouzel, R. D. Koster and R. G. Fairbanks (1995). "Seasonal precipitation timing and ice core records." *Science* **269**: 247-248.

CLIMAP Project Members, (1981). "Seasonal reconstruction of the Earth surface at the last glacial maximum." Map. Chart. Ser., MC-36, Geol. Soc. of Am., Boulder, Colorado.

Cuffey, K. M. and G. D. Clow (1997). "Temperature, accumulation, and ice sheet elevation in central Greenland through the last deglacial transition." *Journal of Geophysical Research* **102**(C12): 26383-26396.

Cuffey, K. M., G. D. Clow, R. B. Alley, M. Stuiver, E. D. Waddington and R. W. Saltus (1995). "Large arctic temperature change at the Wisconsin-Holocene glacial transition." *Science* **270**: 455-458.

Dahl-Jensen, D., K. Mosegaard, N. S. Gundestrup, G. D. Clow, S. J. Johnsen, A. W. Hansen and N. Balling (1998). "Past temperatures directly from the Greenland ice sheet." *Science* **282**: 268-271.

Dansgaard, W. (1964). "Stable isotopes in precipitation." *Tellus* **16**(4): 436-468.

Duplessy, J., J. Moyes and C. Pajol (1980). "Deep water formation in the North Atlantic ocean during the last ice age." *Nature* **286**: 479-482.

Fawcett, P. J., A. M. Agustsdottir, R. B. Alley and C. A. Shuman (1997). "The Younger Dryas termination and North Atlantic Deep Water formation - insights from climate model simulations and Greenland ice cores." *Paleoceanography* **12**: 23-38.

Fisher, D. A. (1991). "Remarks on the deuterium excess in precipitation in cold regions." *Tellus* **43B**: 401-407.

Grootes, P. M., M. Stuiver, J. W. C. White, S. J. Johnsen and J. Jouzel (1993). "Comparison of oxygen isotope records from the GISP2 and GRIP Greenland ice cores." *Nature* **366**: 552-554.

Hoffmann, G., M. Werner and M. Heimann (1998). "The water isotope module of the ECHAM atmospheric general circulation model - a study on time scales from days to several years." *Journal of Geophysical Research* **103**(D14): 16871-16896.

Johnsen, S. J., H. B. Clausen, W. Dansgaard, K. Fuhrer, N. S. Gundestrup, C. U. Hammer, P. Iversen, J. Jouzel, B. Stauffer and J. P. Steffensen (1992). "Irregular glacial interstadials recorded in a new Greenland ice core." *Nature* **359**: 311-313.

Johnsen, S. J., D. Dahl-Jensen, W. Dansgaard and N. S. Gundestrup (1995). "Greenland paleotemperatures derived from GRIP bore hole temperature and ice core isotope profiles." *Tellus* **47B**: 624-629.

Johnsen, S. J., W. Dansgaard and J. W. C. White (1989). "The origin of Arctic precipitation under present and glacial conditions." *Tellus* **41B**: 452-468.

Jouzel, J., R. B. Alley, K. M. Cuffey, W. Dansgaard, P. M. Grootes, G. Hoffmann, S. J. Johnsen, R. D. Koster, D. Peel, C. A. Shuman, M. Stievenard, M. Stuiver and J. W. C. White (1997). "Validity of the temperature reconstruction from water isotopes in ice cores." *Journal of Geophysical Research* **102**(C12): 26471.

Jouzel, J., C. Lorius, J. R. Petit, C. Genthon, N. I. Barkov, V. M. Kotlyakov and M. Petrov (1987). "Vostok ice core: a continuous isotope temperature record over the last climatic cycle (160,000 years)." *Nature* **329**: 403-408.

Krinner, G. (1997). "Simulations du Climat des Calottes de Glace." Université Joseph Fourrier, Grenoble.

Krinner, G., C. Genthon and J. Jouzel (1997). "GCM analysis of local influences on ice core delta signals." *Geophysical Research Letters* **24**(22): 2825-2828.

Peltier, W. R. (1994). "Ice age paleotopography." *Science* **265**: 195-201.

Roeckner, E., K. Arpe, L. Bengtsson, M. Christoph, M. Claussen, L. Dümenil, M. Esch, M. Giorgetta, U. Schlese and U. Schulzweida (1996). "The atmospheric general circulation model Echam-4: Model description and simulation of present-day climate." *MPI-Report 218*. Max-Planck-Institute for Meteorology, Hamburg.

Shuman, C. A., M. A. Fahnestock, R. A. Bindschadler, R. B. Alley and C. R. Stearns (1996). "Composite temperature record from the Greenland Summit, 1987-1994: Synthesis of multiple automatic weather station records and SSM/I brightness temperatures." *Journal of Climate* **9**: 1421-1428.

Steig, E. J., P. M. Grootes and M. Stuiver (1994). "Seasonal precipitation timing and ice core records." *Science* **266**: 1885-1886.

Chapter 4

Isotopic Composition and Origin of Polar Precipitation in Present and Glacial Climate Simulations

ABSTRACT. The Hamburg atmospheric general circulation model (AGCM) ECHAM-4 is used to identify the main source regions of precipitation falling on Greenland and Antarctica. Both water isotopes $H_2{}^{18}O$ and HDO are explicitly built into the water cycle of the AGCM, and in addition the capability to trace water from different source regions was added to the model. Present and LGM climate simulations show that water from the most important source regions has an isotopic signature similar to the mean isotope values of the total precipitation amount. However, water from other source regions (with very different isotopic signatures) contributes an additional, non-negligible part to the total precipitation amount on both Greenland and Antarctica. Analyses of the temperature-isotope-relations for both polar regions reveal a solely bias of the glacial isotope signal on Greenland, which is caused by a strong change in the seasonal deposition of precipitation originating from nearby polar seas and the northern Atlantic. Although the performed simulations under LGM boundary conditions show a decrease of the $\delta^{18}O$ values in precipitation in agreement with ice core measurements, the AGCM fails to reproduce the observed simultaneous decrease of the deuterium excess signal.

4.1. INTRODUCTION

Ice cores from polar regions certainly belong to the most intriguing paleoarchives of climate. Measurements of isotopes, radio-nuclides and chemical impurities in deep ice cores from Greenland and Antarctica have revealed many new details of past climate changes, especially of the last glacial stage and its transition to the Holocene (e.g. Jouzel et al. 1987, Beer et al. 1988, Dansgaard et al. 1993, Yang et al. 1997). For a correct interpretation of the variations of such tracers in the ice, the origin of precipitation and the climatic conditions during the formation of precipitation are important information to know.

Measurements of stable water isotopes $H_2{}^{18}O$ and HDO in ice cores (expressed as $\delta^{18}O$ and δD) have been used to derive such essential information. On its way, typically from low latitudes to high latitudes, an air parcel undergoes successive condensation processes continuously depleting isotopically the remaining water vapour. In various theoretical studies it has been shown that the isotopic composition of precipitation is mainly controlled by the temperature difference between the evaporation site and the condensation site (Dansgaard

1964, Aristarain et al. 1986, Jouzel et al. 1997). Given the oceanic source region has not significantly changed the $\delta^{18}O$ (δD) signal of polar ice cores therefore reflects local temperature variations. The observed present-day (spatial) relation between $\delta^{18}O$, δD and surface temperatures of polar sampling sites (Dansgaard 1964, Lorius et al. 1979, Johnsen et al. 1989, Dahe et al. 1994) are taken as transfer functions to interpret temporal changes of the δ-values as changes of surface temperatures at the drill site. Additional information is gained by analysis of the deuterium excess d (defined as $d = \delta D - 8\delta^{18}O$). The strength of the deuterium excess signal is in general related to kinetic fractionation effects during evaporation, and can therefore be used as an indicator of changes in temperature and/or humidity at the evaporation site (Merlivat and Jouzel 1979). But new, isotope-independent estimates of past temperatures on the Greenland ice sheet (Cuffey et al. 1995, Johnsen et al. 1995, Dahl-Jensen et al. 1998, Severinghaus et al. 1998) raise doubt about the temporal constancy of the used transfer functions, at least for Greenland.

In this study, the Hamburg atmospheric general circulation model (AGCM) ECHAM-4 is used to investigate the coherency between isotopes, temperatures and source regions of precipitation falling on Greenland and Antarctica under the present and glacial climate. Both isotopes $H_2{}^{18}O$ and HDO are explicitly simulated in the water cycle of the AGCM, and in addition the capability to trace water from different source regions was added to ECHAM-4. The independent simulation of isotope values and other physical parameters (e.g. surface temperatures) plus the simultaneous "tagging" of water vapour from different evaporation areas enables us to focus on the following questions: (1) What are the major source regions of the precipitation in Greenland and Antarctica for the present and the glacial climate? (2) Can the major source areas contributing to the polar precipitation be identified by the mean isotopic signature (^{18}O and deuterium excess d) of the precipitation? (3) Are water isotopes still a reliable proxy for glacial surface temperatures on the Greenland and the Antarctic ice sheet?

4.2. Model Description & Prescribed Boundary Conditions

All results reported here are based on the Hamburg AGCM ECHAM-4 (Roeckner et al. 1996). Experiments were performed in T30 resolution (3.75° x 3.75° on the physical grid, 19 vertical levels) running for 10 years with seasonally varying constant boundary conditions. The stable water isotopes $H_2{}^{18}O$ and HDO are both explicitly cycled through the water cycle of the model (Hoffmann et al. 1998). The capability to trace water evaporating from different source regions was implemented by adapting the approach described by Joussaume (1984): Water masses from different source regions get a tag from their origin and can be identified as long as they are in the atmosphere. The tag is removed if the water reaches the surface as

precipitation, dew and exchanged vapour. In total, we defined 14 different tagging areas (Fig. 1). For land surfaces, each continent was defined as a different evaporation source. For ocean surfaces, the yearly mean SST of each grid box was chosen to define several evaporation areas of the Atlantic and the Indopacific, respectively. Therefore, the ocean evaporation regions for different prescribed ocean states can vary in their spatial extent but always have the same mean SST. The first tagging experiment was performed under present-day boundary conditions. For the second simulation we assumed glacial boundary conditions according to the outline of the Paleo Modelling Intercomparison Project (PMIP): SST and sea ice extent according to CLIMAP (1981), solar insulation according to the astronomical theory (Berger 1978), a glacial CO_2 value of 200 ppmv (Barnola et al. 1987), land surface and glacier distribution as reconstructed by Peltier (1994). In agreement with a new estimation of the glacial Greenland ice sheet elevation by Cuffey and Clow (1997) the Peltier reconstruction of the Greenland ice sheet elevation change was reduced by three-quarters. No changes of the Peltier reconstruction were made for Antarctica.

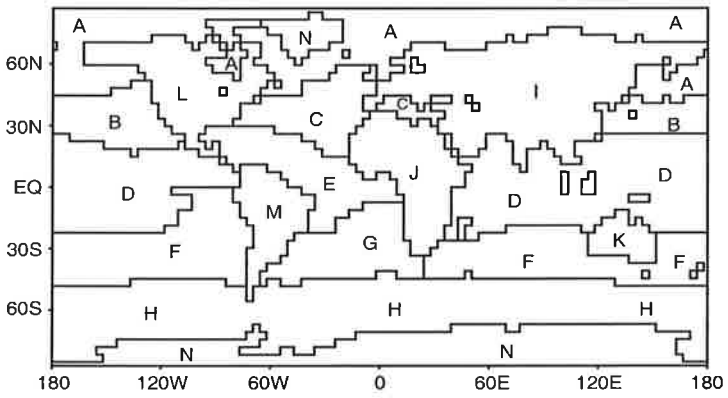

Figure 1: The definition of 14 different source regions of water vapour under the present-day climate. Evaporation from ocean surfaces is divided into 8 different areas (A-H) while each continent is separated as a unique source of water vapour (I-N).

There is a still ongoing discussion about the CLIMAP reconstruction of tropical glacial SSTs. Several authors claim the tropical CLIMAP SSTs as too warm (e.g. in Broecker 1996). New measurements also indicate a partly ice-free North Atlantic during glacial summer periods (Weinelt et al. 1996). To account for these critics on CLIMAP SSTs we have performed an additional glacial sensitivity experiment with cooler tropical SST and a partly warmer North Atlantic. We used SSTs published by Webb et al (1997) which are based on an AGCM simulation with the NASA-GISS model (8°x10°). Instead of fixed glacial SSTs, ocean heat convergence and associated transports close to present-day values were prescribed for the LGM climate. This different boundary condition leads to an enhanced cooling, particularly in the tropics, which is in agreement with recent geochemical evidence (Guilderson et al. 1994,

Stute et al. 1995). The monthly mean SSTs are in the range of 1° to 7° cooler than CLIMAP SSTs (between 40°S and 40°N) and also partly warmer in the North Atlantic. Monthly ocean surface temperature fields of this LGM simulation by Webb et al. (1997) were interpolated to the finer spatial ECHAM grid and used as a boundary condition for our sensitivity study. All other glacial boundary conditions were set like in the LGM simulation with CLIMAP SSTs.

4.3 Results and Discussion

4.3.1 Source Areas of Present Precipitation

GREENLAND: In Fig. 2a the modelled spatial pattern of mean annual precipitation on Greenland is shown. Using a coarse model resolution of 3.75°x3.75° does not allow reproducing many small-scale features of the actual precipitation pattern observed on Greenland (Ohmura and Reeh 1991). But the large scale trend of high precipitation amounts in the south (at Dye 3: observed: 54.1 cm/a, modelled: 90.4 ± 14.6 cm/a), decreased values in the Summit region, central Greenland, (observed: 24.0, modelled: 22.5 ± 3.2 cm/a) and a very dry region in the north is reproduced by the model. However, the extent of this dry region is over-estimated in western direction by our simulation. For example, precipitation values near Camp Century (14.8 ± 4.1 cm/a) are more than twice lower than observed (34.8 cm/a). Overall, there seems to be a too large latitudinal gradient in precipitation over the Greenland ice sheet and the high accumulation belt on the west coast is missing, probably due to an under-representation of circulation on a synoptical scale in connection with topography. In the simulation, precipitation stems from 7 different source regions. Water from the Polar Seas surrounding Greenland (source region A, annual mean SST ≤ 10°C) is mainly transported to coastal regions with a slightly lower gradient of decreasing precipitation amounts at the western coast of Greenland than at the eastern coast (Fig. 2b). Besides the Polar Seas, we find two major, far-distanced source regions of water transported to Greenland: the mid-latitudinal and sub-tropical Atlantic regions (source region C, annual mean SST between 10°C and 25°C) and the North American continent (source region L). While the main transport direction for the Atlantic water masses is from the east (Fig. 2c) and can be associated with the Icelandic Low, water from the North American continent reaches Greenland from a south-westerly direction (Fig. 2f). Smaller oceanic water contribution to Greenland's precipitation stem from the tropical Atlantic (source region E, annual mean SST ≥ 25°C, Fig. 2d) and from the Pacific (not shown). Besides North America, the Eurasian land surface (source I) is another continental water source. Water from Eurasia reaches Greenland not from the east, but from the very north, following the circumpolar circulation (Fig. 2e). Simulated year-by-year variations of the contribution of different ocean or land source regions are in the range of 5% to 20% of the annual mean (1σ standard deviation).

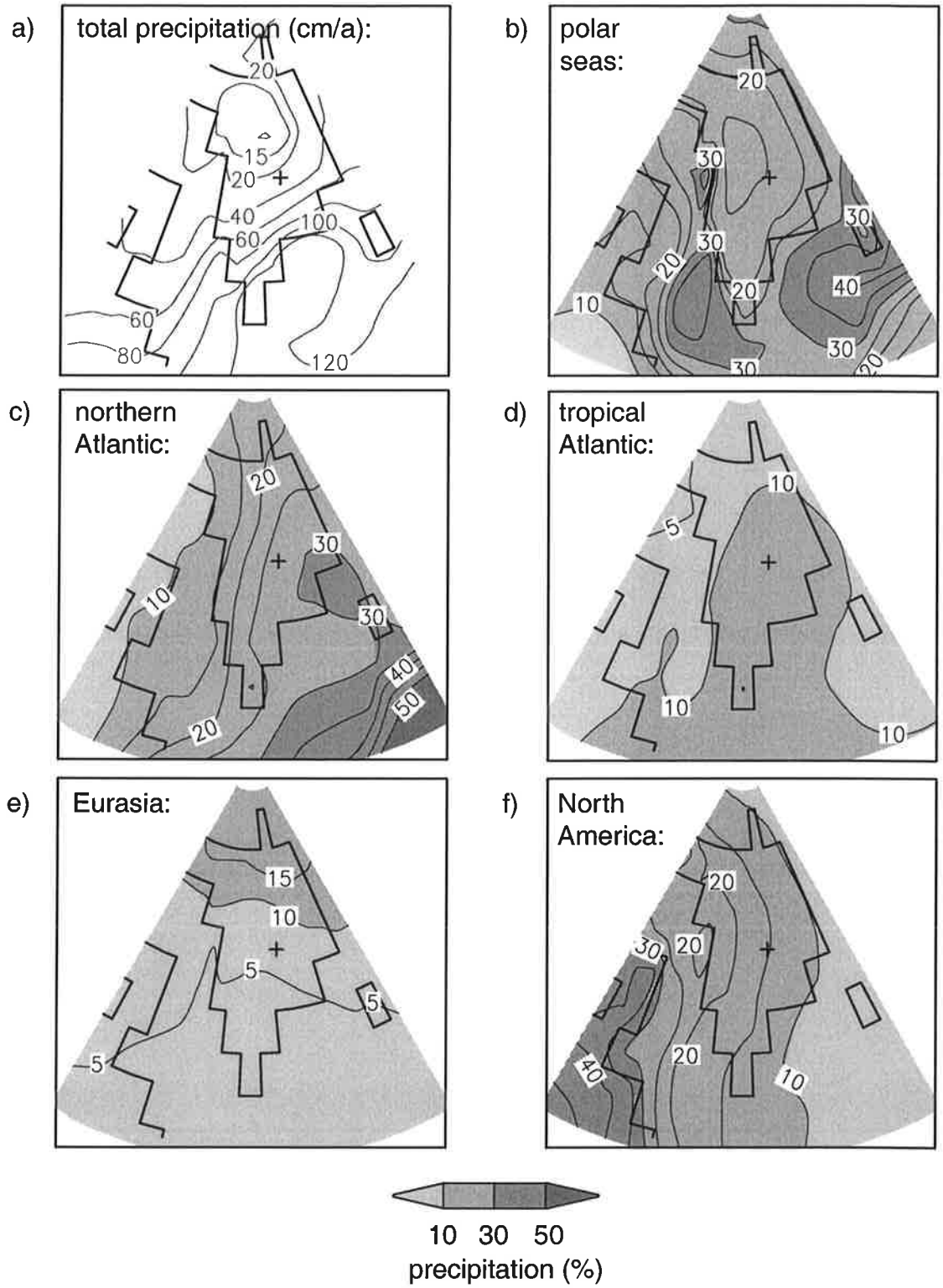

Figure 2: a: Modelled long-time mean precipitation values of Greenland for the present-day climate (contour lines at 10, 15, 20, 40, 60, 80, 100, 120 cm/a); Fig. 2 b-f: the relative contribution of different source areas (expressed as percent of the modelled mean precipitation values, contour lines at every 5%). The cross marks the Summit drill site.

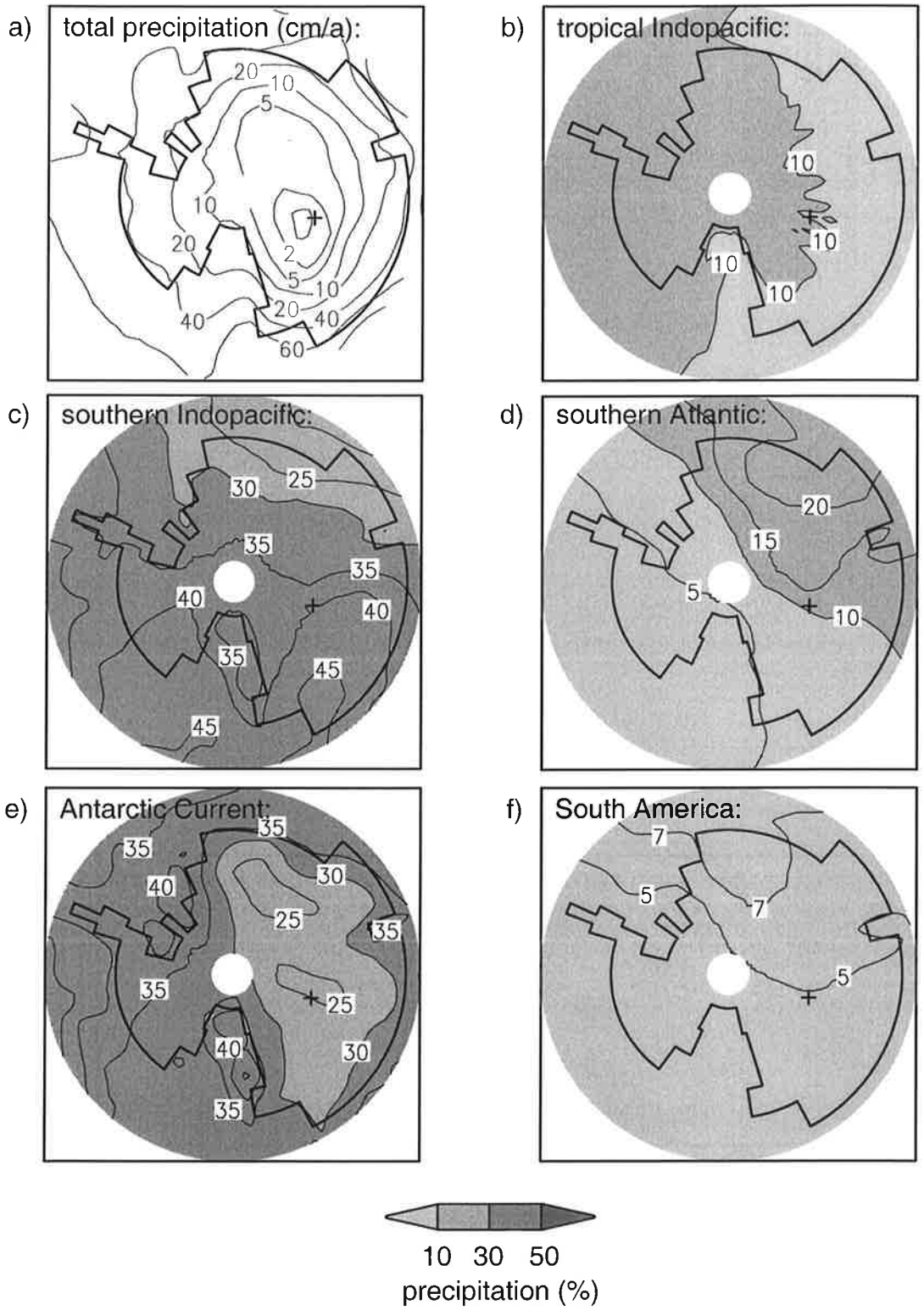

Figure 3: a: Modelled long-time mean precipitation values of Antarctica for the present-day climate (contour lines at 1, 2, 5, 10, 20, 30, 40, 50, 60, 70 cm/a); b-f: the relative contribution of different source areas (expressed as percent of the modelled mean precipitation values, contour lines at every 5%, extra contour line at 7% in Fig. 3f). The cross marks the Vostok drill site.

ANTARCTICA: The simulated precipitation amounts of our present-day simulation (Fig. 3a) are similar to ECMWF reanalyses results (Cullather et al. 1998). Like for the Greenland ice sheet, many small-scale features are not represented by the coarse model resolution. But the very dry inner region of East Antarctica around the Vostok drill site (precipitation values as low as 1 cm/a) is fairly well represented in the simulation. The major simulated water sources contributing to the present-day precipitation of Antarctica are the southern Indopacific (source region F, annual mean SST between 10°C and 25°C), the southern Atlantic (source region G, annual mean SST between 10°C and 25°C) and the Antarctic Current ACC (source H, annual mean SST ≤ 10°C). Water from the southern Atlantic is mainly transported to a wedge-shaped sector between 0° and 90°E (Fig. 3d), and the strongest contribution of southern Indopacific water can be found west and east of the Ross ice-shelf between 100°E and 120°W (Fig. 3c). The relative water contribution of the ACC is 10-15% higher in West Antarctica than in East Antarctica (Fig. 3e). An additional small amount of tropical Indopacific water (source region D, annual mean SST ≥ 25°C) is transported to West Antarctica in the simulation (Fig. 3b). In Queen Maud Land, up to 10% of the precipitation amount stems from the South American continent (source M, Fig. 3f). The year-by-year variations (1σ) of different water vapour sources contributing to the Antarctic precipitation are in the range of 10-20% of the annual mean.

4.3.2 The Isotopic Signature of Present Precipitation

GREENLAND: Previous studies with simpler transport models have concluded from the observed isotopic composition of the precipitation that the dominating water masses found in central Greenland stem from the subtropical part of the North Atlantic ocean (Johnsen et al. 1989, Hoffmann et al. 1997). In Table 1 we have listed $\delta^{18}O$ and d values of all source regions with a significant contribution (i.e. >5% of the total precipitation) to the precipitation falling in the model grid box enclosing the Summit region. The simulated annual mean $\delta^{18}O$ value (-30.1±0.7‰) is somewhat lower than the ice core data (-34.8±0.1‰, Grootes et al. 1993) but this deviation is mainly caused by the coarse model resolution (the grid box enclosing the Summit area is 500m lower than the true Summit location). The modelled mean excess d = 9.6±0.6‰ is close to the GRIP ice core data (d = 8.8-9.3‰, Hoffmann et al. 1997). The analysis of the δ-values of different source regions shows that the results of our AGCM simulation are in good agreement with the earlier findings. Water which stems from subtropical Atlantic regions (= transition region between sources C and E) has presumably an isotopic signature similar to the one of the total precipitation amount. The additive contribution of these regions represents about 42% of the precipitation in the Summit area. The sub-tropical and tropical Atlantic is therefore the most important source region for central Greenland. But two other important aspects can also be seen from Table 1: (1) Other sources of water vapour with a different isotopic composition than measured in the ice cores (more

enriched in heavy isotopes: polar seas, more depleted: Pacific sources) contribute also a non-negligible part to the total precipitation amount falling in the Summit region. (2) Water from the North American continent has a very similar isotopic composition as water from the northern Atlantic. Thus, the isotopic signature of the total precipitation amount falling at Summit is a reliable indicator for the major source area (source regions C and E) but it does not reveal information about precipitation from other source regions with counterbalancing isotopic compositions. Similar to this ECHAM-4 simulation, two studies to identify the major source regions of Greenland's precipitation with the GISS AGCM (Charles et al. 1994, Armengaud et al. 1998) report also a significant contribution of continental water and a minor contribution of far-distanced Pacific water transported to Greenland.

	Summit			Vostok		
	Prec. (cm/a)	$\delta^{18}O$ (‰)	*d* (‰)	Prec. (cm/a)	$\delta^{18}O$ (‰)	*d* (‰)
observed: total	23	-34.8	9	2.3	-57.2	16.3
modelled: total	22.6 (100%)	-30.1	9.6	0.9 (100%)	-49.3	21.0
polar seas	3.4 (15%)	-19.8	-3.5	-	-	-
northern Atlantic	6.3 (28%)	-26.7	4.2	-	-	-
tropical Atlantic	3.1 (14%)	-31.5	11.4	-	-	-
southern Atlantic	-	-	-	0.1 (11%)	-52.4	27.2
northern Pacific	1.8 (8%)	-41.1	19.0	-	-	-
tropical Indopacific	2.2 (10%)	-46.6	31.3	0.1 (11%)	-62.2	53.8
southern Indopacific	-	-	-	0.4 (44%)	-48.7	16.9
Antarctic Current	-	-	-	0.2 (22%)	-39.7	-1.2
Eurasia	1.4 (6%)	-31.5	15.3	-	-	-
North America	3.5 (15%)	-24.9	5.5	-	-	-
South America	-	-	-	0.05 (6%)	-51.0	16.5

Table 1: Modelled precipitation amounts and isotopic composition of water masses from different source regions transported to the Summit region, central Greenland, and the Vostok region, East Antarctica, respectively. The relative contributions (in %) of the different water sources to the total precipitation amount are given in brackets.

ANTARCTICA: In contrast to central Greenland, continental water sources can be neglected for most areas in Antarctica. For example, for the remote area of the Vostok drill site the modelled precipitation stems from the tropical Indopacific (11%), the southern Indopacific

(45%), the southern Atlantic (11%) and the Antarctic Current (22%). This is in agreement with previous studies of the deuterium excess from coastal and central Antarctica observations, which suggested a major subtropical source but could not exclude an additional coastal water contribution. Results are also similar to tagging experiments of Delaygue et al. (1999) using the GISS AGCM. Like for Summit, Greenland, the isotopic composition of water from the major source region (region F, the southern Indopacific) is very similar to the δ-values of the total precipitation. But water from other source regions (either more depleted or enriched in $H_2{}^{18}O$) contributes a non-negligible part to the precipitation at Vostok, too. The isotopic results for Antarctica, however, deviate stronger from the observations than in Greenland though the deviation is in the same direction, e.g. at Vostok: modelled $\delta^{18}O = -49.3‰$, observed $\delta^{18}O = -57.2‰$ (Dahe et al. 1994). One might argue that an overestimation of water transport from coastal regions causes the too positive $\delta^{18}O$ values in the model. But as seen in Table 1, an increased water contribution from distant sources would not only lead to lower $\delta^{18}O$ values, but also increase the simulated deuterium excess values ($d = 21.0‰$), which is in contrast to the observations ($d = 16.3‰$, Dahe et al. 1994). Thus, the reason for this model mismatch remains unclear.

In fact this problem can nicely be illustrated by Fig. 4, in which the ^{18}O composition for the different source regions of both Summit and Vostok is plotted against their respective deuterium excess value *d*. The GCM nicely reproduces what we would expect from a simple Rayleigh distillation model (Dansgaard 1964): as warmer and therefore more distant from the polar deposition site the vapour source is situated as lower is the corresponding δ value. This relation can be explained by the fact that the isotopic composition of polar precipitation is mainly controlled by the temperature difference between the evaporation and the condensation site. On the other hand, the deuterium excess is largely affected by the climatic condition prevailing at the evaporation site. Warmer sea surface temperatures provoke isotopic non-equilibrium conditions during evaporation and thus enhance the deuterium excess (Merlivat and Jouzel 1979). Since there is a kinetic (non-equilibrium) effect during snow formation, too, the deuterium excess is also influenced by condensation temperatures. However, since the condensation temperature is the same for all different vapour sources we see in Fig. 4 just the effect of the varying source temperatures. This explains why increasing evaporation temperatures produce both lower isotope values ($\delta^{18}O$ and δD) and higher deuterium excess values as it can be seen in Fig. 4. Thus, the dilemma for the isotopic composition in central Antarctica and to a lesser extent for Greenland reads like this: Any mixture of source regions deviating from the simulated one will not diminish the model versus observation difference ($\delta^{18}O$ and *d*) since the mean isotopic composition will just move along the fitted line in Fig. 4. This clearly points to parameterisation problems of the water isotopes, particularly of the deuterium excess which is as a second order quantity more sensitive to the description of kinetic processes in the model.

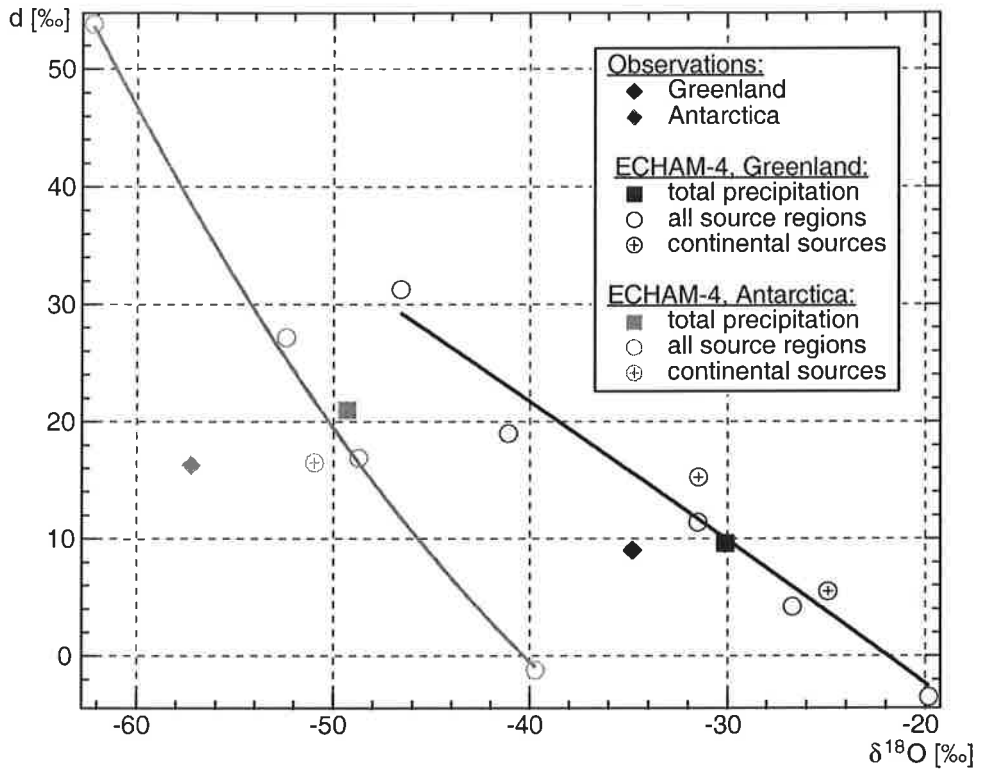

Figure 4: Relation between $\delta^{18}O$ and deuterium excess *d* in precipitation at the Summit drill site, Greenland, and the Vostok drill site, Antarctica (measurements: solid rhombi, simulation values: solid squares). In addition, simulated $\delta^{18}O$ and *d* values of water from different source areas are plotted (open circles). Model values were fitted by a cubic polynom function (solid lines).

4.3.3 Source Areas of Glacial Precipitation

GREENLAND: It has been proposed that changes in the circulation and water vapour transport pathways to Greenland might have occurred during the LGM (Kapsner et al. 1995). Our simulation under LGM climate boundary conditions with CLIMAP SSTs shows no major changes of the most important source regions of Greenland's precipitation (Fig. 5). While the total amount of precipitation on Greenland is reduced by a factor 3-4 during the glacial climate (Fig. 5a) the most important source regions are still the nearby polar seas, the northern Atlantic, the North American continent and Eurasia. The main transport directions of water from the northern Atlantic and North America have both shifted to a more southern flow compared to the present-day climate (Fig. 5c, 5f). The small contribution of the tropical Atlantic region is reduced by about 5-7% during the LGM (Fig. 5d). The circumpolar circulation seems increased in the LGM simulation. Consequently the contribution of the Eurasian water source is now larger, especially in North Greenland (Fig. 5e). There exists also a minor contribution of Pacific water comparable in relative size to the present climate (not

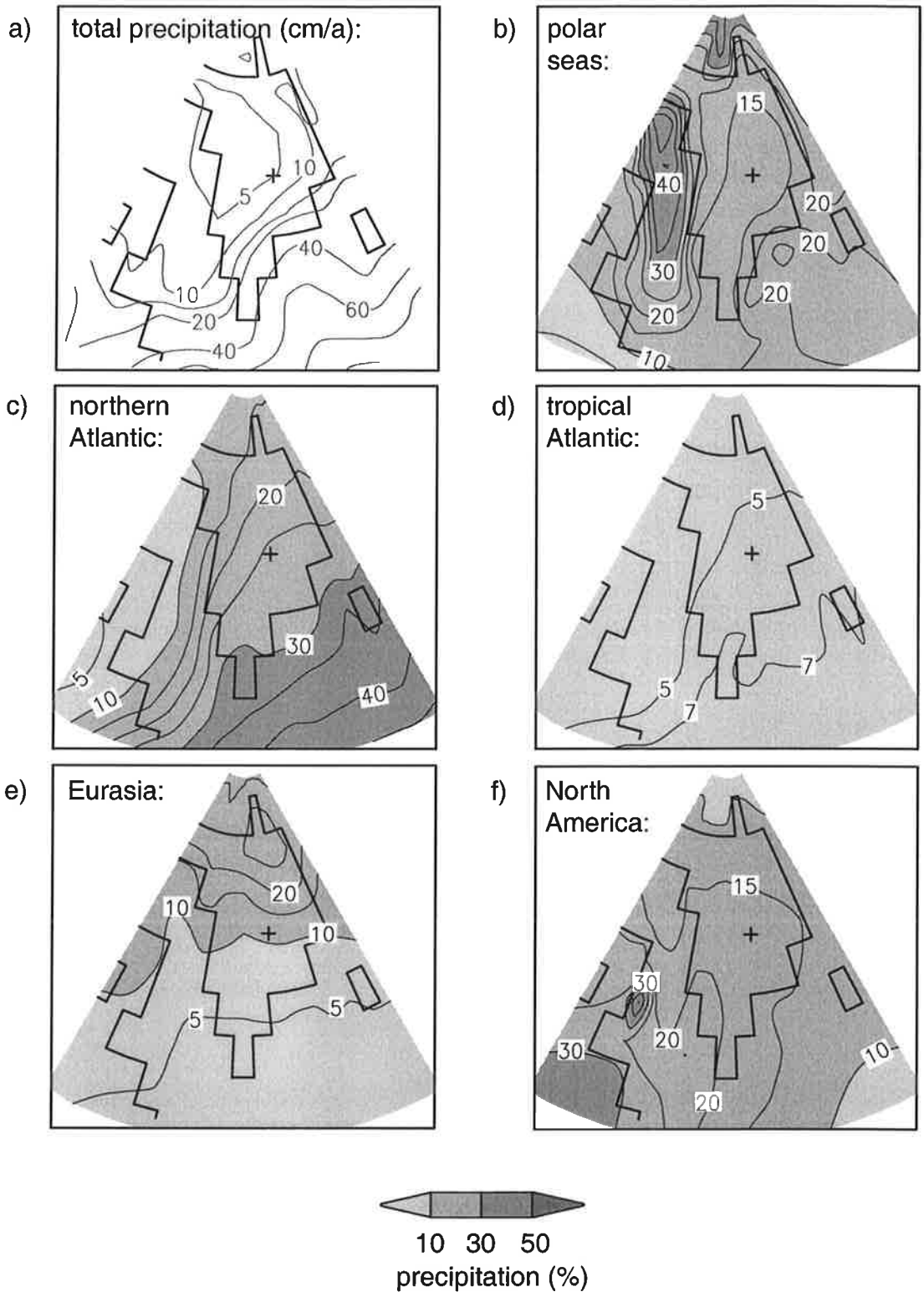

Figure 5: a: Modelled long-time mean precipitation values of Greenland for the LGM climate with prescribed CLIMAP SSTs (contour lines at 5, 10, 15, 20, 40, 60, 80 cm/a); b-f: the relative contribution of different source areas (expressed as percent of the modelled mean precipitation values, contour lines at every 5%, extra contour line at 7% in Fig. 5d). The cross marks the Summit drill site.

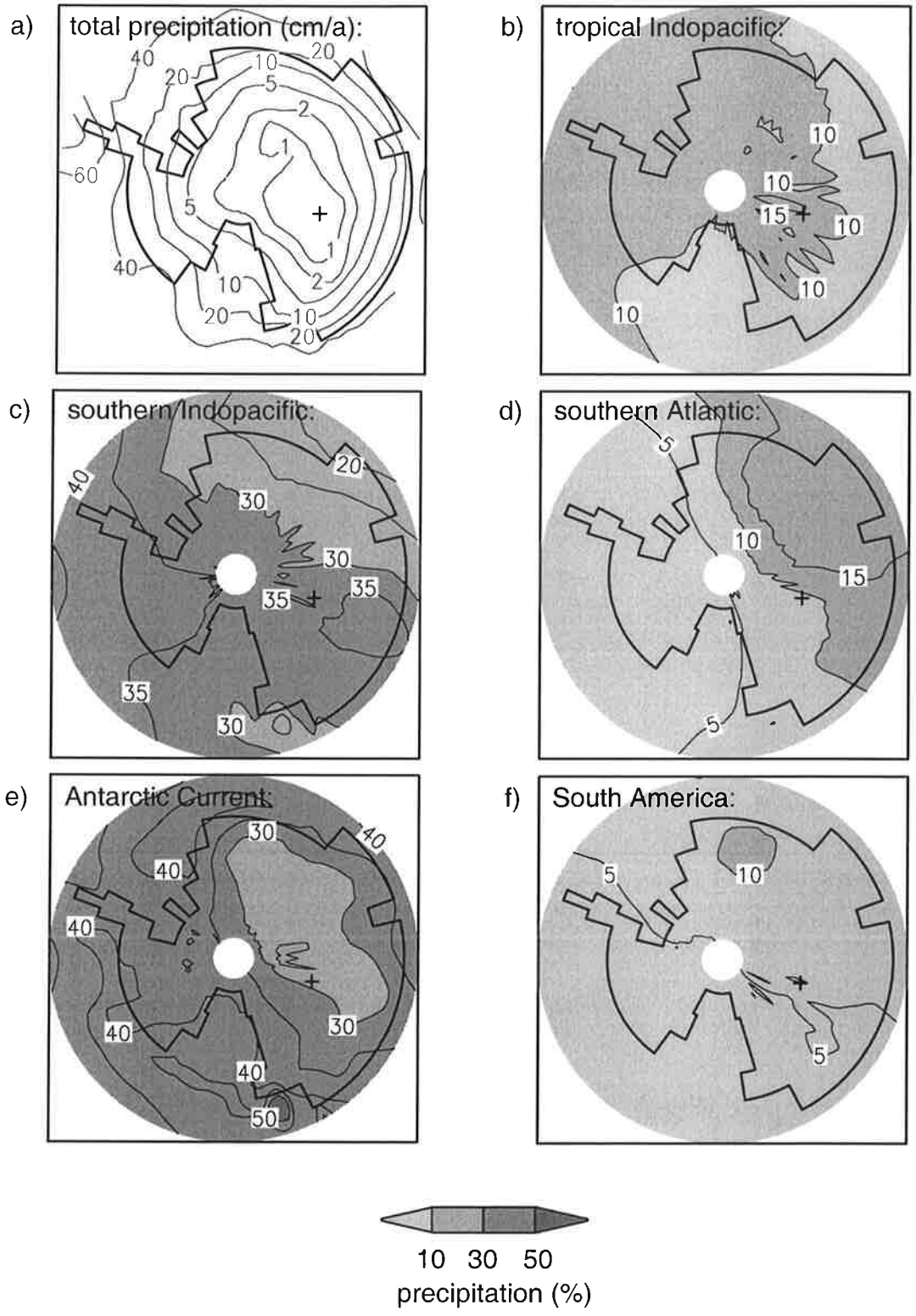

Figure 6: a: Modelled long-time mean precipitation values of Antarctica for the LGM climate with prescribed CLIMAP SSTs (contour lines at 1, 2, 5, 10, 20, 30, 40, 50 cm/a); b-f: the relative contribution of different source areas (expressed as percent of the modelled mean precipitation values, contour lines at every 5%). The cross marks the Vostok drill site.

shown). Our findings are comparable to results of Charles et al. (1994) but in contrast to their work, we do not find a relative increase of the small Pacific water contribution for the LGM climate. In our sensitivity study with much cooler tropical SSTs and a partly warmer North Atlantic we observe very similar results as for a glacial climate using CLIMAP SSTs: the major source regions are again the polar seas, the northern Atlantic and the North American continent. Due to the warmer, partly ice-free Norwegian Sea the relative contribution of water from the polar seas and the North Atlantic to Greenland increases by 15-20% compared to the CLIMAP LGM simulation.

ANTARCTICA: For the LGM simulation under CLIMAP boundary conditions we observe a reduction of precipitation, especially in the interior areas of both West and East Antarctica (Fig. 6a). The driest region is still the Vostok area with mean annual precipitation values as low as 0.6cm/a. Analysing the relative contribution of different source areas reveals a split of the Antarctic continent into two parts: Between 90°W and 90°E the different precipitation source regions (most important: southern Atlantic ocean) have not changed in their relative contribution to the total precipitation amount. But for the area between 90°E and 90°W the relative strength of the southern Pacific source is reduced by 5-15% under the glacial climate (Fig. 6c), while the contribution of water from the Antarctic Current region has increased by up to 10% (Fig. 6e). If cooler tropical SSTs are prescribed instead of the CLIMAP SST data, the relative contribution of water from the Atlantic or Indopacific is reduced by about 15-20%, and the amount of coastal waters transported to the Antarctic ice sheet is increased instead. In contrast to these ECHAM-4 results, Delaygue et al. (1999) reports an increased transport of water from subtropical regions and a decreased transport of coastal water to Antarctica for an LGM simulation with CLIMAP SSTs using the GISS AGCM. Similar to our sensitivity study, an additional GISS simulation with cooler tropical glacial SSTs results in a minor influence of subtropical water masses due to a decreased meridional ocean surface temperature gradient (Delaygue et al. 1999).

4.3.4 The Isotopic Signature of Glacial Precipitation

In Table 2 we have listed observed (or estimated) versus simulated glacial anomalies Δ of surface temperature T_S, precipitation amount, $\delta^{18}O$ and deuterium excess d for both Summit, Greenland, and Vostok, Antarctica. For Summit, simulated anomalies of ΔT_S, Δprecipitation amount and $\Delta\delta^{18}O$ agree well with the estimates, although the simulated glacial $\Delta\delta^{18}O$ anomaly is 2-4‰ less than observed. But the LGM simulation with CLIMAP SSTs clearly fails to model the observed glacial drop of -3‰ of the deuterium excess Δd (Jean Jouzel, personal comm.). Similar results are found for the Vostok region in the simulation: Although deviations of ΔT_S, Δprecipitation and $\Delta\delta^{18}O$ between ice core estimates and model values are larger than for central Greenland, the sign and magnitude of the modelled anomalies are correct. But like for Summit, an erroneous positive deuterium excess anomaly Δd is found in

the LGM simulation. Apparently, the ECHAM-4 model fails to simulate an observed glacial drop of the deuterium excess for both polar regions and neither cooler tropical SSTs (see Table 2) nor a changed mixture of moisture sources would resolve this mismatch: Any process resulting in a lower (higher) deuterium excess value also leads to higher (lower) $\delta^{18}O$ values, and vice versa, as demonstrated for the present climate in Fig. 4. Thus, from our LGM climate simulations it is not understood how a glacial decrease of both $\delta^{18}O$ and the deuterium excess *d* could be achieved. In this context it is interesting to mention that similar problems of modelling correct glacial isotope and deuterium excess anomalies are reported for the GISS AGCM (G. Delaygue, personal comm.).

		observed: LGM-present	modeled: LGM-present	modelled: cool tropics-CLIMAP
Summit:	ΔT_S (°C)	-18 to -23	-23.5±2.7	+7.0
	ΔPrec. (cm/a)	-16 to -17.5	-18.1±5.2	+2.2
	$\Delta\delta^{18}O$ (‰)	-6.2 to -8.2	-4.1±2.6	+1.2
	Δd (‰)	-3[1]	+0.3±1.5	-2.1
Vostok:	ΔT_S (°C)	-6	-10.0±1.4	-6.5
	ΔPrec. (cm/a)	-1 to -1.2	-0.4±0.3	-0.3
	$\Delta\delta^{18}O$ (‰)	-3 to -5	-7.7±5.4	-7.1
	Δd (‰)	-2	+5.2±11.7	+9.2

[1] Jean Jouzel, personal communication

Table 2: Observed (or estimated) versus simulated anomalies Δ of glacial minus present values of surface temperature T_S, precipitation amounts, isotopic composition $\delta^{18}O$ and deuterium excess *d*. In the right column the modelled anomalies for LGM simulations using cooler tropical SSTs minus CLIMAP SST are given. Observed data is compiled from Lorius et al. (1985), Lorius (1989), Grootes et al. (1993), Cuffey and Clow (1997).

4.3.5 The Temporal Isotope-Temperature Relations

Recently, paleotemperature estimates by borehole thermometry (Cuffey et al. 1995, Johnsen et al. 1995, Dahl-Jensen et al. 1998) and gas diffusion measurements (Severinghaus et al. 1998) have questioned the use of spatial $\delta^{18}O$-T_S-relations to calculate past temperature changes on Greenland and Antarctica. In this chapter we therefore focus on the modelled isotope-temperature-relations on both ice sheet under the present and glacial climate to compare our model results to those new findings.

GREENLAND: In a previous article (Werner et al. 1999)[1] we discussed in detail how the significant change of the seasonal distribution of precipitation seen in the LGM simulation on Greenland (Fig. 7) results in a disagreement between temporal and spatial $\delta^{18}O$-T_S-relations

[1] see Chapter 3

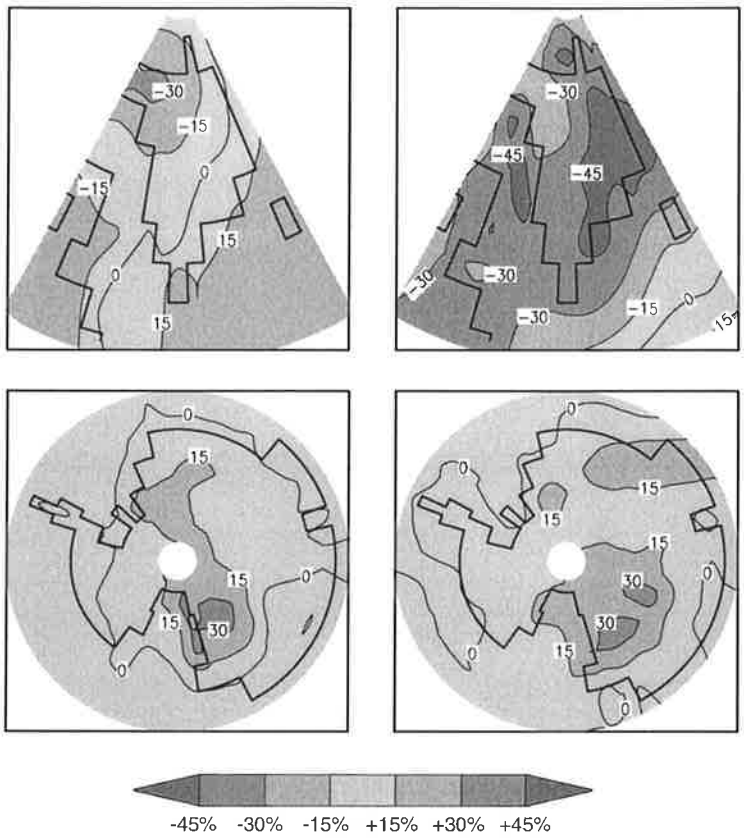

Figure 7: Difference between winter (DJF) minus summer (JJA) precipitation values on the Greenland (top) and Antarctic (bottom) ice sheet for the simulated present (left) and glacial (right) climate. The seasonal differences are expressed as percentage of the modelled mean precipitation values.

(Fig. 9). In the context of this article we extend our previous findings and analyse how the different source contributions of Greenland's precipitation are affected by this change in seasonality. In Fig. 8 the mean seasonal contributions of modelled precipitation values of the grid box enclosing Summit are plotted for the present and glacial climate. A clear seasonal signal in the amount of precipitation is not seen in our present-day simulation, but slightly higher values in late summer/early autumn and the small minimum in late winter/early spring have been reported before (Bromwich et al. 1993). The seasonal influence of different source regions can be grouped as follows: Water from both North America and Eurasia reaches Summit mainly in summer and can be neglected for winter precipitation. A summer maximum is also seen for the small water contribution, which stems from the tropical Pacific. Conversely, because of higher oceanic evaporation fluxes south of Greenland and in the GIN Sea in winter compared to summer, water from the nearby polar seas reaches Summit mostly in winter. The northern Atlantic and northern Pacific sources do not show a well-defined seasonality but larger values are seen in autumn / winter and smaller values in late spring /

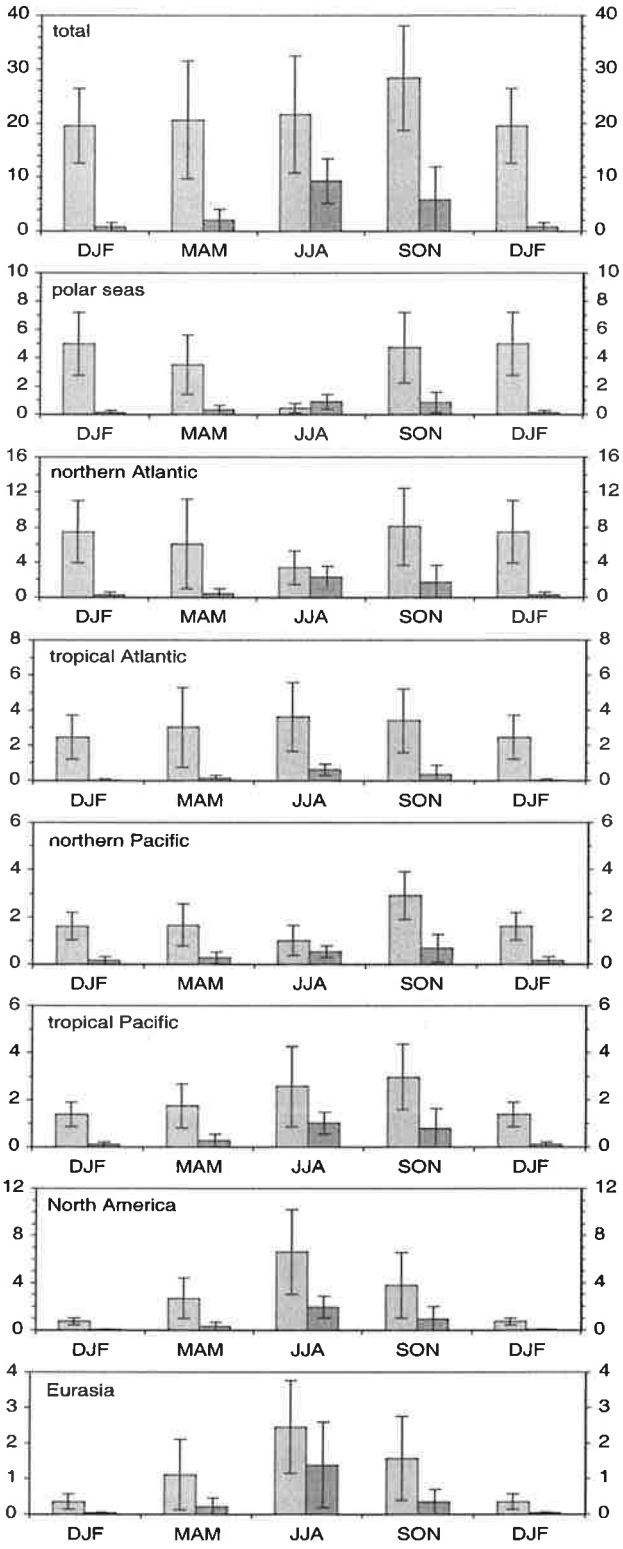

Figure 8: Simulated seasonal mean values of the total precipitation and of all major source areas contributing to the precipitation falling at Summit, Greenland, for the simulated present and glacial climate. All values are expressed in cm/a, the winter season DJF is shown twice for clarity reasons.

early summer. Water from the tropical Atlantic shows no pronounced seasonality at all. Hence, we find in our simulation that the weak seasonality of the modelled total precipitation for the present climate is based on several strong seasonal signals phase-shifted against each other. While in winter (DJF) about 77% of the Summit precipitation origins from the polar seas and the Atlantic, it is only 35% in summer (JJA). On the opposite, 42% of the summer precipitation stems from North America and Eurasia but only 6% of the winter precipitation. Very similar results of the seasonal variances of water from different source regions transported to Greenland were found in a tagging experiment with the GISS GCM (Armengaud et al. 1998). The analysis of simulated seasonal precipitation values for the LGM climate shows that the most significant changes are seen in the seasonal cycle of water from polar seas and the northern Atlantic. Under the LGM climate, water from these source regions is no longer transported to Greenland during autumn and winter, but during summer season. Analyses of the mean geopotential height at 500 hPa show that the shift in the seasonality of glacial precipitation can be attributed to an increased mean flow from northerly directions over central Greenland and more zonal flow over the North Atlantic and Europe. The advected air mass is substantially colder and dryer, and thus responsible for the very low precipitation in central Greenland in LGM winter.

ANTARCTICA: For most areas of Antarctica, a clear seasonal cycle in precipitation is not observed for the present-day climate simulation (Fig. 7). Only at the eastern border of the Ross Ice Shelf slightly more austral summer than winter precipitation is seen. Our model results are in good agreement with findings of van Lipzig (1999) using a high resolution regional climate model (RACMO) for the decade 1980-1989 with lateral boundary conditions relaxed to re-analyses from the European Center for Medium-Range Weather Forecasts (ECMWF). On the contrary, Cullather et al. (1998) report an unimodal seasonal cycle (with higher precipitation values in austral winter) for the coastal area and interior of West Antarctica. Observation data from South Pole and Vostok show also slightly higher precipitation values in austral winter (Bromwich 1988). Compared to the present climate, the ECHAM-4 LGM simulation shows an increased seasonal cycle of precipitation in the interior East Antarctica and in Queen Maud Land. The relative difference of austral summer (DJF) minus austral winter (JJA) snow is in the range of +10% to +25% of the annual mean values (Fig. 7). In contrast to Greenland, changes of the seasonal distribution of precipitation are much smaller for Antarctica in the LGM climate simulation. Therefore, spatial $\delta^{18}O$-T_S-relations for LGM and present climate have very similar slopes in West- or East Antarctica (Fig. 9), and the latter is in agreement with present-day observations (Giovinetto and Zwally 1997). Modelled temporal $\delta^{18}O$-T_S-relations on the Antarctic ice sheet have a slightly steeper slope than the spatial relations (e.g. mean temporal slope of all East Antarctica grid boxes: $m = 1.06 \pm 0.11$). But because of the general model deficit to simulate correct low $\delta^{18}O$-values

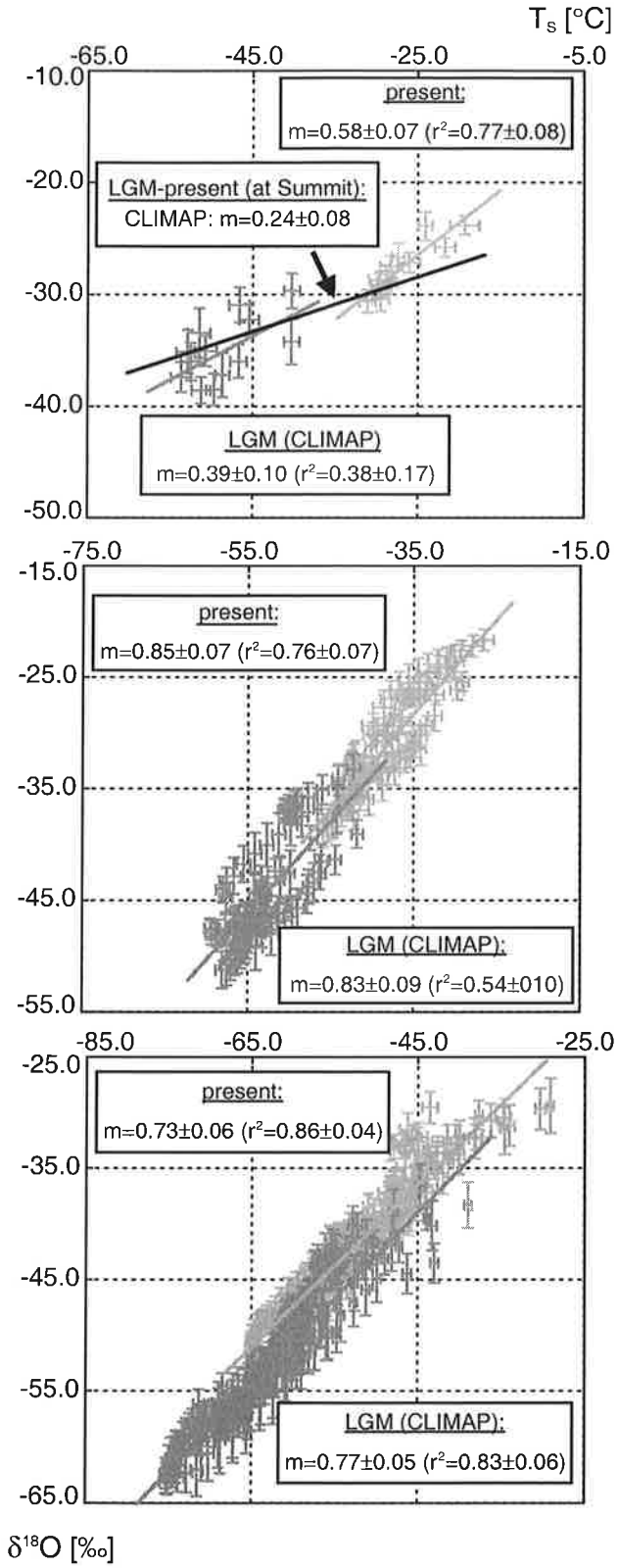

Figure 9: Modelled mean values of T_S and $\delta^{18}O$ for all grid boxes of the inner Greenland ice sheet (top), West Antarctica (middle) and East Antarctica (bottom) for the present-day climate (light grey) and for the LGM climate (dark grey). Both present-day and LGM spatial $\delta^{18}O$-T_S-relations are plotted (grey lines) and the calculated spatial slopes are given in the text boxes. The temporal $\delta^{18}O$-T_S-relation of the model grid box enclosing Summit, Greenland, between LGM and present-day values is also shown in the upper plot (black line).

in Antarctica, the significance of these small deviations between temporal and spatial slopes remains unclear. In general, the analysis of the seasonal cycle of precipitation indicates that glacial δ-values from Antarctica might be a more reliable proxy for mean LGM surface temperatures than the isotope data retrieved from Greenland ice cores. The use of cooler tropical SSTs instead of CLIMAP data does not change these findings.

4.4 Conclusions

In this article we used an AGCM which included both stable water isotopes and the possibility to identify different source regions of water vapour in precipitation to study the climate of Greenland and Antarctica for both the present and full glacial climate. Simulated precipitation values on Greenland agree quite well with present-day observations. Model results suggest that the tropical and subtropical Atlantic is the dominant source region of Greenland's precipitation but that water from several different ocean and continental areas contribute together about half of the total precipitation amount falling in the Summit region. Water from these additional sources has an isotopic signature, which differs significantly from the mean isotopic composition of the precipitation, and the relative strengths of these additional sources vary with season. For the present-day climate of Antarctica, the most dominant water vapour sources are the surrounding oceans, but no land surfaces. Like for Greenland, water transported to Antarctica stems not from a single source region but is a mixture of coastal and far-distanced evaporation regimes. The influence of the southern Atlantic is bound to a wedge-shaped region between 0°-100°E on the Antarctic ice sheet, while other regions are more influenced by the southern Indopacific. This is, for example, of some importance for the two new deep drilling sites of the European Project of Ice Coring in Antarctica (EPICA), one located in Dronning Maud Land (near 1°E) and one at Dome Concordia (124°E).

Simulations of the Last Glacial Maximum climate show decreased precipitation amounts in both polar regions but the relative contribution of different vapour sources is comparable to present values if CLIMAP SSTs are applied as a boundary condition for the LGM simulation. A sensitivity study with cooler tropical SSTs and a partly warmer North Atlantic results in an enhanced contribution of coastal waters transported to both Greenland and Antarctica. An increased seasonality in the annual precipitation cycle is observed for most regions of Greenland during the LGM, but not for Antarctica. As a direct consequence, the water isotope signal of Antarctic ice cores seems to be a surface temperature proxy less biased by seasonality of the precipitation than isotope data from Greenland ice cores.

But all performed ECHAM-4 simulations under LGM boundary conditions (either CLIMAP or cooler tropical SSTs) fail to reproduce the simultaneous decrease of both $\delta^{18}O$ and the deuterium excess d, as it is measured in the GRIP and Vostok ice cores. Analyses of the

isotopic signature of water from different source areas transported to the ice sheets reveal a relation between $\delta^{18}O$ and *d* similar to a simple Raleigh-type model. A decreased $\delta^{18}O$ signal in precipitation is always related to an increased deuterium excess signal, and vice versa. Thus, the reason for this mismatch between LGM model results and glacial ice core data remains unclear.

REFERENCES:

Aristarain, A. J., J. Jouzel and M. Pourchet (1986). "Past Antarctic Peninsula climate (1850-1980) from an ice isotope record." *Climatic Change* **8**: 69-86.

Armengaud, A., R. D. Koster, J. Jouzel and P. Ciais (1998). "Deuterium excess in Greenland snow - analysis with simple and complex models." *Journal of Geophysical Research* **103**(D8): 8947-8953.

Barnola, J. M., D. Raynaud, Y. S. Korotkevich and C. Lorius (1987). "Vostok ice core provides 160,000-year record of atmospheric CO_2." *Nature* **329**: 408-414.

Beer, J., U. Siegenthaler, G. Bonani, R. C. Finkel, H. Oeschger, M. Suter and W. Wölfli (1988). "Information on past solar activity and geomagnetism from ^{10}Be in the Camp Century ice core." *Nature* **331**: 675-679.

Berger, A. L. (1978). "Long-term variations of daily insolation and Quarternary climatic changes." *Journal of Atmosheric Science* **35**: 2362-2367.

Broecker, W. S. (1996). "Glacial climate in the tropics." *Science* **272**: 1902-1904.

Bromwich, D. H. (1988). "Snowfall in high southern latitudes." *Reviews of Geophysics* **26**: 149-168.

Bromwich, D. H., F. M. Robasky, R. A. Keen and J. F. Bolzan (1993). "Modeled variations of precipitation over Greenland ice sheet." *Journal of Climate* **6**: 1253-1268.

Charles, C. D., D. H. Rind, J. Jouzel, R. D. Koster and R. G. Fairbanks (1994). "Glacial-interglacial changes in moisture sources for Greenland: Influences on the ice core record of climate." *Science* **263**: 508-511.

CLIMAP Project Members, (1981). "Seasonal reconstruction of the Earth surface at the last glacial maximum." Map. Chart. Ser., MC-36, Geol. Soc. of Am., Boulder, Colorado.

Cuffey, K. M. and G. D. Clow (1997). "Temperature, accumulation, and ice sheet elevation in central Greenland through the last deglacial transition." *Journal of Geophysical Research* **102**(C12): 26383-26396.

Cuffey, K. M., G. D. Clow, R. B. Alley, M. Stuiver, E. D. Waddington and R. W. Saltus (1995). "Large Arctic temperature change at the Wisconsin-Holocene glacial transition." *Science* **270**: 455-458.

Cullather, R. I., D. H. Bromwich and M. L. Vanwoert (1998). "Spatial and temporal variability of Antarctic precipitation from atmospheric methods." *Journal of Climate* **11**: 334-367.

Dahe, Q., J. R. Petit, J. Jouzel and M. Stievenard (1994). "Distribution of stable isotopes in surface snow along the route of the 1990 International Trans-Antarctica Expedition." *Journal of Glaciology* **40**: 107-118.

Dahl-Jensen, D., K. Mosegaard, N. S. Gundestrup, G. D. Clow, S. J. Johnsen, A. W. Hansen and N. Balling (1998). "Past temperatures directly from the Greenland ice sheet." *Science* **282**: 268-271.

Dansgaard, W. (1964). "Stable isotopes in precipitation." *Tellus* **16**(4): 436-468.

Dansgaard, W., S. J. Johnsen, H. B. Clausen, D. Dahl-Jensen, N. S. Gundestrup, C. U. Hammer, C. S. Hvidberg, J. P. Steffensen, A. E. Sveinbjörnsdottir, J. Jouzel and G. Bond (1993). "Evidence for general instability of past climate from a 250-kyr ice-core record." *Nature* **364**: 218-220.

Delaygue, G., V. Masson and J. Jouzel (1999). "Climatic stability of the geographic origin of Antarctic precipitation simulated by an atmospheric general circulation model." *Annals of Glaciology* **29**: in press.

Giovinetto, M. B. and H. J. Zwally (1997). "Areal distribution of the oxygen-isotope ratio in Antarctica: an assessment based on multivariate models." *Annals of Glaciology* **25**: 153-158.

Grootes, P. M., M. Stuiver, J. W. C. White, S. J. Johnsen and J. Jouzel (1993). "Comparison of oxygen isotope records from the GISP2 and GRIP Greenland ice cores." *Nature* **366**: 552-554.

Guilderson, T. P., R. G. Fairbanks and J. L. Rubenstone (1994). "Tropical temperature variations since 20,000 years ago: Modulating interhemispheric climate change." *Science* **263**: 663-665.

Hoffmann, G., M. Stievenard, J. Jouzel, J. W. C. White and S. J. Johnsen (1997). "Deuterium excess record from central Greenland (modelling and observations)." *International Symposium on Isotope Techniques in the Study of Past and Current Environmental Changes in the Hydrosphere and the Atmosphere*, I.A.E.A, Vienna.

Hoffmann, G., M. Werner and M. Heimann (1998). "The water isotope module of the ECHAM atmospheric general circulation model - a study on time scales from days to several years." *Journal of Geophysical Research* **103**(D14): 16871-16896.

Johnsen, S. J., D. Dahl-Jensen, W. Dansgaard and N. S. Gundestrup (1995). "Greenland paleotemperatures derived from GRIP bore hole temperature and ice core isotope profiles." *Tellus* **47B**: 624-629.

Johnsen, S. J., W. Dansgaard and J. W. C. White (1989). "The origin of Arctic precipitation under present and glacial conditions." *Tellus* **41B**: 452-468.

Joussaume, J., R. Sadourny and J. Jouzel (1984). "A general circulation model of water isotope cycles in the atmosphere." *Nature* **311**: 24-29.

Jouzel, J., R. B. Alley, K. M. Cuffey, W. Dansgaard, P. M. Grootes, G. Hoffmann, S. J. Johnsen, R. D. Koster, D. Peel, C. A. Shuman, M. Stievenard, M. Stuiver and J. W. C. White (1997). "Validity of the temperature reconstruction from water isotopes in ice cores." *Journal of Geophysical Research* **102**(C12): 26471.

Jouzel, J., C. Lorius, J. R. Petit, C. Genthon, N. I. Barkov, V. M. Kotlyakov and M. Petrov (1987). "Vostok ice core: a continuous isotope temperature record over the last climatic cycle (160,000 years)." *Nature* **329**: 403-408.

Kapsner, W. R., R. B. Alley, C. A. Shuman, S. Anandakrishnan and P. M. Grootes (1995). "Dominant influence of atmospheric circulation on snow accumulation in Greenland over the past 18,000 years." *Nature* **373**: 52-54.

Lorius, C. (1989). "Polar ice cores and climate." *Climate and Geo-Sciences* (ed. by A. L. Berger), Kluwer Academic Publishers.

Lorius, C., J. Jouzel, C. Ritz, L. Merlivat, N. I. Barkov, Y. S. Korotkevich and V. M. Kotlyakov (1985). "A 150,000-year climatic record from Antarctic ice." *Nature* **316**: 591-596.

Lorius, C., L. Merlivat, J. Jouzel and M. Pourchet (1979). "A 30,000-yr isotope climatic record from Antarctic ice." *Nature* **280**: 644-648.

Merlivat, L. and J. Jouzel (1979). "Global climatic interpretation of the deuterium-oxygen 18 relationship for precipitation." *Journal of Geophysical Research* **84**(C8): 5029-5033.

Ohmura, A. and N. Reeh (1991). "New precipitation and accumulation maps for Greenland." *Journal of Glaciology* **37**: 140-148.

Peltier, W. R. (1994). "Ice age paleotopography." *Science* **265**: 195-201.

Roeckner, E., K. Arpe, L. Bengtsson, M. Christoph, M. Claussen, L. Dümenil, M. Esch, M. Giorgetta, U. Schlese and U. Schulzweida (1996). "The atmospheric general circulation model Echam-4: Model description and simulation of present-day climate." *MPI-Report 218*. Max-Planck-Institute for Meteorology, Hamburg.

Severinghaus, J. P., T. A. Sowers, E. J. Brook, R. B. Alley and M. L. Bender (1998). "Timing of abrupt climate change at the end of the Younger Dryas interval from thermally fractionated gases in polar ice." *Nature* **391**: 141-146.

Stute, M., M. Forster, H. Frischkorn, A. Serejo, J. F. Clark, P. Schlosser, W. S. Broecker and G. Bonani (1995). "Cooling of tropical Brazil (5-degrees-C) during the last glacial maximum." *Science* **269**: 379-383.

van Lipzig, N. P. M. (1999). "The surface mass balance of the Antarctic ice sheet: a study with a regional atmospheric model." *Ph.D. thesis*. Universiteit Utrecht, Utrecht.

Webb, R. S., D. H. Rind, S. J. Lehman, R. J. Healy and D. Sigman (1997). "Influence of ocean heat transport on the climate of the last glacial maximum." *Nature* **385**: 695-699.

Weinelt, M., M. Sarntheim, U. Pflaumann, H. Schulz, S. Jung and H. Erlenkeuser (1996). "Ice-free Nordic Seas during the last glacial maximum? Potential sites of deepwater formation." *Paleoclimates* **1**: 283-309.

Werner, M., U. Mikolajewicz, M. Heimann and G. Hoffmann (1999). "Borehole versus isotope temperatures on Greenland: Seasonality does matter." *Geophysical Research Letters* in press.

Yang, Q. Z., P. A. Mayewski, M. S. Twickler and S. I. Whitlow (1997). "Major features of glaciochemistry over the last 110,000 years in the Greenland Ice Sheet Project 2 ice core." *Journal of Geophysical Research* **102**(D19): 23289-23299.

Chapter 5

Possible Changes of $\delta^{18}O$ in Precipitation Caused by a Meltwater Event in the North Atlantic

ABSTRACT. The Hamburg atmosphere general circulation model ECHAM-4 is used to investigate how a meltwater event in the North Atlantic might alter the signal of stable water isotopes ($H_2{}^{18}O$, HDO) in precipitation. Our results show that such a meltwater event will cause significant changes in the isotopic composition of the precipitation over many parts of the northern Hemisphere, but also in the tropical Atlantic region. Model simulations suggest that for such a scenario isotope anomalies are not always related to temperature changes, but also to changes in the seasonality of precipitation or the precipitation amount. A changed isotopic composition of evaporating ocean surface waters (caused by a massive meltwater input into the North Atlantic) causes temperature-independent isotope anomalies, too. Changes of the deuterium excess are even more affected by the imposed oceanic isotope anomaly due to the non-linearity of the evaporation process.

5.1 INTRODUCTION

One of the most puzzling problems of climate research is the question for the cause of the strong and rapid climate changes during the last 70,000 years known as Heinrich events, Dansgaard-Oeschger events and the Younger Dryas. These events can be traced in paleorecords almost from the entire world including the tropics, (e.g. Johnsen et al. 1992, Brook et al. 1996, Curry and Oppo 1997). Two main hypotheses for their origin are currently discussed: One is a reduction of northward Atlantic heat transport due to a shutdown or reduction of North Atlantic Deep Water (NADW) formation triggered by strong meltwater and/or iceberg discharge from the European and/or North American ice shields (Stocker 1998). The other explanation claims that the cause for this variability lies in the tropics (Cane 1998).

Most of our knowledge about these past climate changes is based on proxy records, e.g. ice cores, pollen records and marine sediment cores. From these proxy records changes in, for example, temperature and precipitation are estimated. The required transfer functions are in general derived from present-day spatial variations of proxy (e.g. isotopes in ice cores) and physical quantities (e.g. temperature and precipitation). These transfer functions are often nonunique and there is no guarantee that they are also appropriate for temporal variations.

However, this approach is widely used to compare estimates of past climate changes with the results of model sensitivity studies. In this paper we will use a different approach. Here we will show a simulation study, which explicitly models the cycling of two stable water isotopes ($H_2{}^{18}O$, HDO) in the hydrological cycle. Modelling of both $H_2{}^{18}O$ and HDO enables additional analyses of the deuterium excess *d* (defined as $d = \delta D - 8\delta^{18}O$), a parameter which mainly depends on temperature and humidity at the evaporation site (Merlivat and Jouzel 1979, Johnsen et al. 1989). Focusing on the simulation of a meltwater event into the Labrador Sea we investigate the following questions: (1) In which regions can we detect isotope anomalies in a colder climate forced by a rapid shutdown of the NADW formation? (2) Is a changed isotopic composition in precipitation (usually given as $\delta^{18}O$ or δD) always coupled to changed surface temperatures? (3) A massive fresh water input with a strong depletion in heavy isotopes will alter the isotopic ocean surface water composition $\delta^{18}O_{Ocean}$. How much does this effect the $\delta^{18}O$ signal in precipitation? (4) Will changes of the deuterium excess *d* reveal additional information?

5.2 Model Experiments

Our results are based on three model experiments using the Hamburg atmosphere general circulation model (AGCM) ECHAM-4 in T30 mode (spatial resolution: 3.75 x 3.75 degrees). Each experiment was run for 10 years in equilibrium state after a spin-up time of one year. In the first experiment (further referred to as control run) both sea surface temperatures (SSTs) and $\delta^{18}O_{Ocean}$ were set to present-day values. For the two other experiments we prescribed colder SSTs. But while the $\delta^{18}O_{Ocean}$ values were still set to modern values in the second experiment, we assumed a changed isotopic composition $\delta^{18}O_{Ocean}$ in the third one. A comparison between the second and third experiment will enable us to clearly distinguish between the effects of changed SSTs and additionally changed $\delta^{18}O_{Ocean}$. The prescribed monthly SST fields for all three experiments were derived from simulations with the coupled ocean-atmosphere general circulation model (OAGCM) ECHAM-3/LSG (Voss et al. 1998). The ECHAM-3/LSG OAGCM was forced into a colder state by a meltwater spike input into the Labrador Sea with a 500 year long triangle-shaped time history (maximum: 0.625 Sv) (Schiller et al. 1997). The meltwater input led to a freshening of the North Atlantic surface waters, thus suppressing deep convection and the formation of NADW. As a consequence, the thermohaline circulation of the Atlantic was weakened until the end of the freshwater input. Poleward heat transport in the North Atlantic was strongly reduced, leading to a simulated cooling of almost the entire Northern Hemisphere. We calculated monthly mean SSTs of years 300 to 400 of an OAGCM control run and the OAGCM meltwater experiment, respectively, to use as boundary conditions for the isotope control and cold climate experiments (Fig. 1a). For the cold climate scenario with an additional changed $\delta^{18}O_{Ocean}$ field we used

results of an experiment with an OGCM coupled to an atmospheric energy balance model (Mikolajewicz 1996). This model was forced with a meltwater spike, identical to the one of in the OAGCM experiment mentioned above. Although not identical, mean SST changes between the control and cold climate state of this OGCM experiment were similar to the coupled OAGCM simulations. In this experiment a highly idealised $\delta^{18}O$ of seawater was included. We used the mean of the $\delta^{18}O_{Ocean}$ changes of years 300 to 400 of the OGCM experiment as a prescribed boundary condition for our third isotope experiment (Fig. 1b). The showed pattern is a combination of the $\delta^{18}O$ of meltwater and $\delta^{18}O$ changes of seawater caused by changes of the ocean circulation.

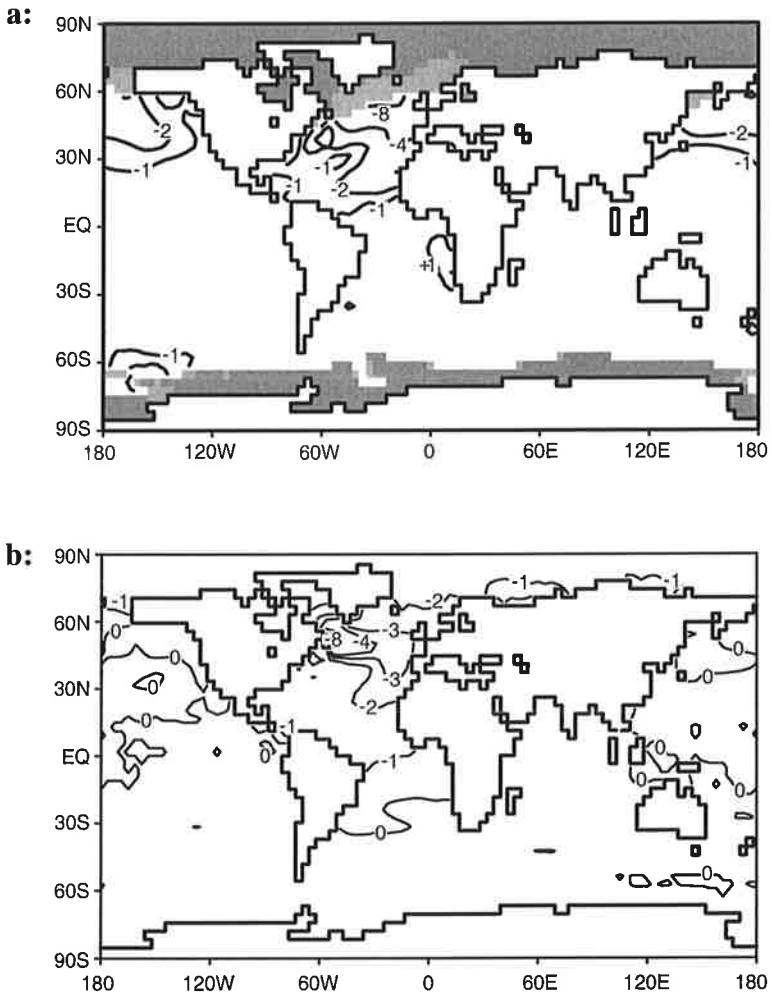

Figure 1: Differences of the boundary conditions between the control and cold climate experiments: (a) mean anomalies of sea surface temperatures SSTs and sea ice (temperature contour lines at -1, -2, -4, -8, -16 °C; dark grey area: sea ice prescribed in both climates at least half of the year, light grey area: additional sea ice prescribed at least half of the year for the cold climate), (b) anomalies of the isotopic composition of the ocean surface water $\delta^{18}O_{Ocean}$ (contour lines at 0, -1, -2, -3, -4, -8‰).

The deuterium excess *d* of ocean surface water was set to zero in all our experiments. Such a *d*-excess value is valid for recent climate conditions but might be slightly higher after a meltwater event. Meltwater from the Laurentian ice shield was probably enriched in the deuterium excess. Measurements on the Dye3 ice core, Greenland, show *d*-excess values between 4‰ and 8‰ for different climate stages (Johnsen et al. 1989). Except SSTs and $\delta^{18}O_{Ocean}$ we did not change any other boundary condition such as topography, ice shield distribution or solar insolation, which were all set to present-day values in the experiments.

We are fully aware that this set-up does not represent a realistic simulation of the conditions occurring during a rapid climate change event. Nevertheless the experiments allow an assessment of the first order effects in the isotopic composition of precipitation after a meltwater induced rapid northern hemisphere cooling event, such as the Younger Dryas. Since most other boundary conditions will probably have remained fairly constant during a rapid climate change, we believe that analysing the anomalies between the different model experiments can reveal important information.

5.3 RESULTS

The mean changes of $\delta^{18}O$ in precipitation between the control climate and the cold climate are shown in Fig. 2a-2c. For further analyses we have split the $\delta^{18}O$ anomalies in two parts: (1) the $\delta^{18}O$ changes caused by colder SSTs alone (Fig. 2a), (2) additional $\delta^{18}O$ changes in precipitation for the colder climate caused by the assumed change in $\delta^{18}O_{Ocean}$ (Fig. 2b). Colder SSTs alone affect the $\delta^{18}O$ signal over the Atlantic region, Scandinavia and the western part of Europe (Fig. 2a). The strongest isotope depletion (-8‰) can be observed over the northern Atlantic in the area of the Norwegian Sea, slightly east of the area of maximum cooling. Another minimum of isotope values is located over the northern Pacific region centred at the Bering Strait area associated with the prescribed cooling and the increased sea ice cover. This Pacific signal is much weaker than the Atlantic one but still shows a decrease of -4‰. A dipole-like pattern of isotope changes is found in the tropical Atlantic region between 30°N and 30°S. The positive branch (+2‰) is found north of the equator. It is mainly located over the ocean but extends into the northern part of South America. The negative branch (-4‰) is seen over the Atlantic south of the equator. The additional anomalies of $\delta^{18}O$ in precipitation induced by changed $\delta^{18}O_{Ocean}$ values of the Atlantic (Fig. 2b) are very similar to the $\delta^{18}O_{Ocean}$ input field (Fig. 1b). Although the extreme ocean water depletion of -8‰ at the coast of Labrador is not reflected in the precipitation signal, the -2‰ and -1‰ contour lines between forcing ($\delta^{18}O_{Ocean}$) and response ($\delta^{18}O$ in precipitation) are almost identical, indicating a strong local control of the response signal. Over land surfaces, strongest depletion of -2‰ is found over Western Europe and the Mediterranean region.

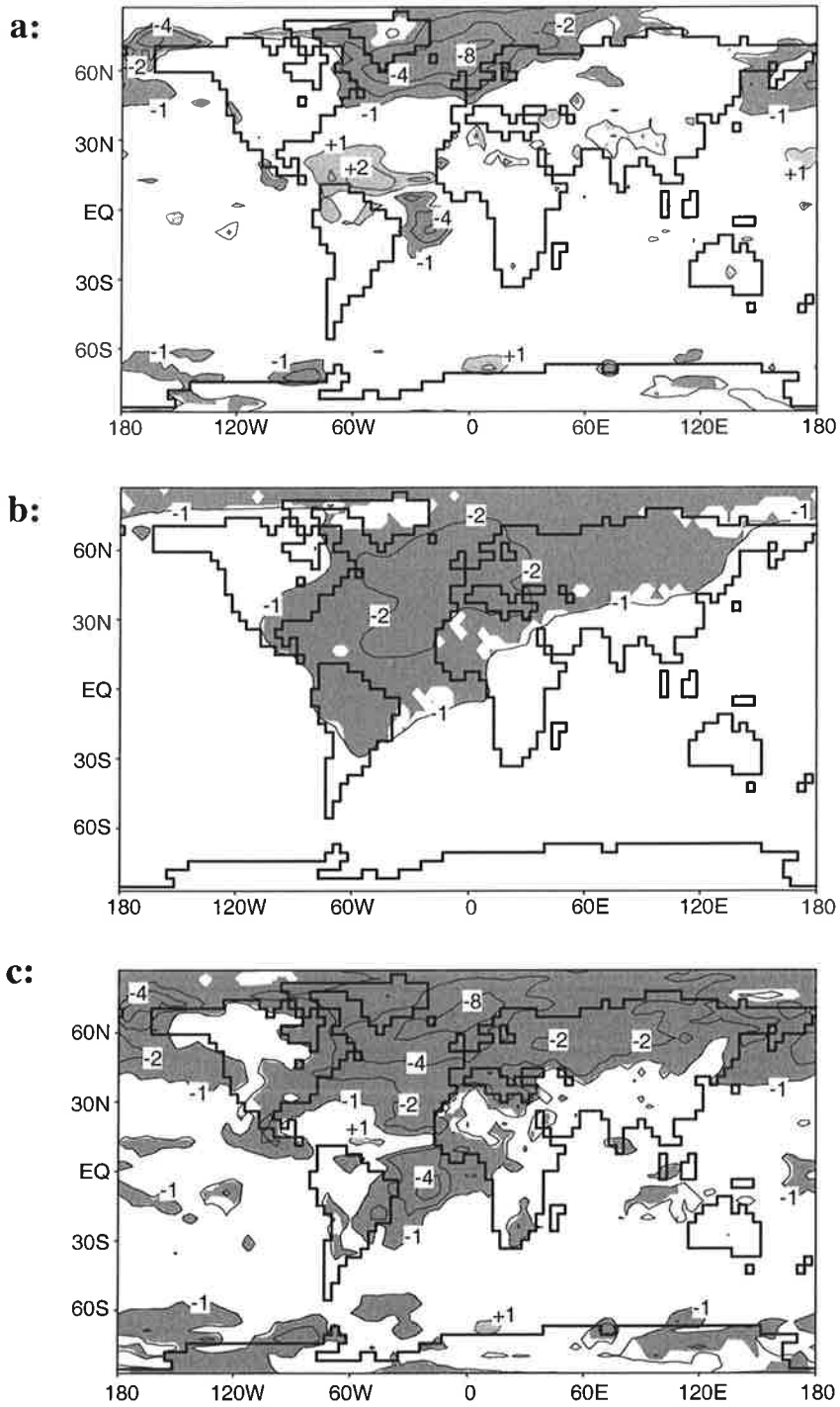

Figure 2: (a) Changes of the $\delta^{18}O$ values in precipitation of the cold climate minus the control climate, if only SSTs are changed for the cold climate. (b) Changes of the $\delta^{18}O$ values in precipitation for the cold climate simulation with both SST and $\delta^{18}O_{Ocean}$ changed, minus the cold climate simulation with only SST changed. (c) Changes of the $\delta^{18}O$ values in precipitation of the cold climate minus the control climate, if both SSTs and $\delta^{18}O_{Ocean}$ are changed for the cold climate. Contour lines in all three plots at ±1, ±2, ±4, ±8‰. Significant $\delta^{18}O$ changes are shaded in light and dark grey (two-sided u-test, 95% level).

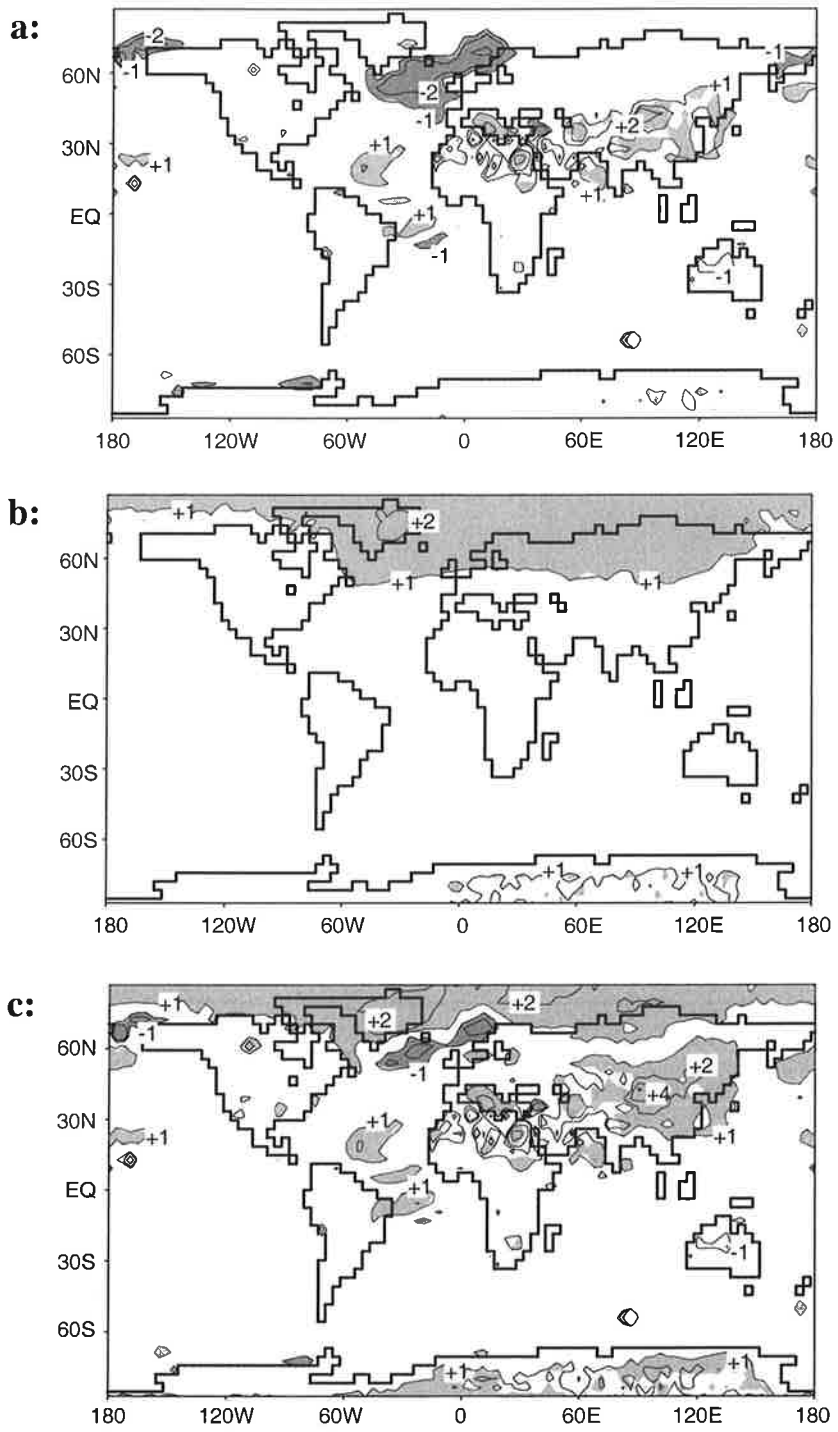

Figure 3: The same as Fig. 2, but for the changes of the deuterium excess *d* (contour lines in all three plots at ±1, ±2, ±4‰, shading of significant changes like in Fig. 2a-2c).

Weaker anomalies of -1‰ to -2‰ are also found above eastern Europe and Siberia, southern Greenland, the east coast of North America, West Africa and almost half of the South American continent. Combining both effects of changed SSTs and changed $\delta^{18}O_{Ocean}$ (Fig. 2c) results in an increased change in $\delta^{18}O$ over central Europe and Siberia. The modelled $\delta^{18}O$ changes over the Summit region of the Greenland ice sheet are also slightly larger. The most striking difference is seen in the tropical Atlantic: While the negative $\delta^{18}O$ anomaly south of the equator increased in size, the positive anomaly of +2‰ north of the equator almost completely vanishes.

Fig. 3a-3c shows the same sequence of anomalies for the deuterium excess. Three clear signals appear in the excess: (1) A local negative signal over the North Atlantic in the order of –1‰ mainly due to the local temperature changes (see Fig. 3a and 3c). (2) A quite strong positive signal over central and southern Asia with a maximum of +4‰ over Tibet due to the long range climate changes caused by the melt water induced lowering of the North Atlantic SSTs (Fig. 3a). (3). A widespread positive anomaly between +1‰ and +2‰ over the high northern latitudes which is produced by the isotopic composition of the meltwater (see Fig. 3b). The scattered excess signal over northern Africa is probably related to model deficits for areas with only a few rainfall events over a period of several years (Hoffmann et al. 1998).

5.4 DISCUSSION

To understand the modelled isotope anomalies one has to consider the main influences of the $\delta^{18}O$ signal in precipitation. In the extra-tropics, for the present-day climate, $\delta^{18}O$ strongly correlates with surface temperatures ("temperature effect", observed mean spatial slope: 0.61 ‰/°C (IAEA 1992)). But in tropical regions surface temperatures are fairly constant over an annual cycle. There, the $\delta^{18}O$ signal shows a weak negative correlation to the amount of precipitation ("amount effect", observed mean slope -1.3‰/100cm/year (IAEA 1992)).

In the cold climate experiments surface temperatures are reduced in many land regions north of 30°N except parts of Asia and Alaska (Fig. 4a). Similar to the cold SST boundary conditions we find the strongest temperature drop (-20°C) in the area of the Greenland and Norwegian Sea over sea ice. Strong cooling is also seen over the Greenland ice sheet (-8°C to -12°C) and the Bering Strait (-8°C). The latter is directly correlated to a minimum in SSTs, too. The cooling in the northern Pacific is caused by an intensified wintertime outflow of cold air from Siberia (Mikolajewicz et al. 1997). Cooling in the range of -2°C to -4°C is observed over most parts of Europe, Siberia and the east coast of North America. Such colder temperatures above the North Atlantic and Europe will reduce the amount of precipitation in southern Greenland, over the Norwegian Sea and some parts of the European continent (Fig. 4b). But additionally, the Intertropical Convergence Zone (ITCZ) over the Atlantic is strongly

shifted to the southeast. We observe a dipole-like change of the precipitation amounts in the tropical Atlantic region: North of the equator precipitation is strongly reduced (down to -80 mm/month) in a band from Middle America to the Sahel zone while south of the equator precipitation amount increases (up to +140 mm/month). A similar, but weaker shift of the ITCZ is observed in the Pacific, too. The dipole-like precipitation anomaly in the tropical Atlantic is the reason for the very similar dipole-like $\delta^{18}O$ anomaly seen in Fig. 2a. In low latitudes the amount effect dominates the isotope signal. Therefore, lower precipitation amounts north of South America cause a relative enrichment of heavy isotopes in precipitation. Conversely, more precipitation south of the equator is responsible for the stronger depletion in $H_2{}^{18}O$. However, the positive branch of this pattern vanishes if we combine cooler SSTs and a changed $\delta^{18}O_{Ocean}$ (Fig. 2c). The additional isotope depletion caused by the changed $\delta^{18}O_{Ocean}$ field counterbalances the enrichment induced by the amount effect. As a result we see in Fig. 2c only a strong $\delta^{18}O$ anomaly between 0° and 30°S but almost no counterpart north of the equator.

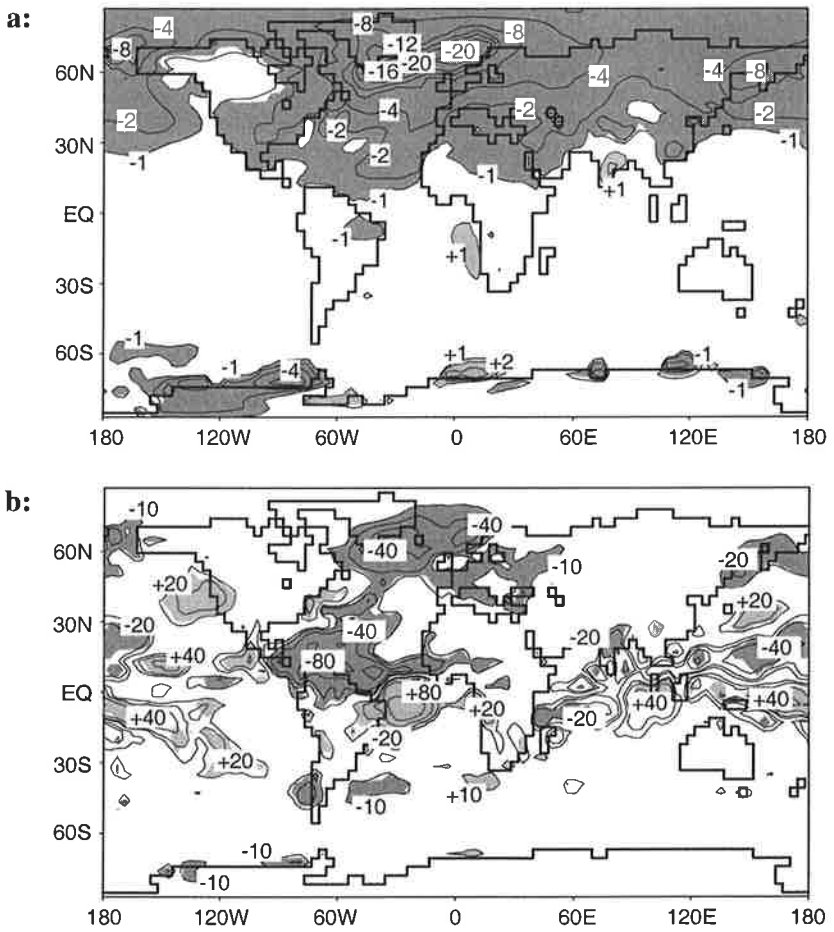

Figure 4: (a): Changes of surface temperature between the control and cold climate experiments. Contour lines are at ±1, ±2, -4, -8, -12, -16, -20°C. Significant temperature changes are shaded in light resp. dark grey (two-sided u-test, 95% level). (b): Same as Fig. 4a, but for the changed amount of precipitation. Contour lines at ±10, ±20, -40, -80 mm/month, shading of significance like in Fig. 4a.

The relatively strong and spatially coherent reaction of the deuterium excess is an astonishing result of our simulation, in particular since the isotopic composition of the meltwater itself was prescribed with an excess of 0‰. As mentioned above, the excess depends not on the temperature gradient between the evaporation and condensation site such as $\delta^{18}O$ and δD but is strongly affected by the isotopic disequilibrium during the evaporation at the sea surface. A slow (rapid) evaporation process, that means low (high) evaporation temperatures and a high (low) relative humidity, produces a small (large) deuterium excess (Merlivat and Jouzel 1979, Johnsen et al. 1989). The direct impact of lower SSTs, therefore, is a lower excess of about -2‰ in the North Atlantic and North Pacific where the imposed temperature anomalies are strongest. The interpretation of the positive signal of up to +4‰ over central and southern Asia, however, is less straightforward. In our control simulation the highest excess values ($d >$ 14‰) were calculated in the very same region. This feature was already reported in a former version of the model (Hoffmann et al. 1998) and is in good agreement with observations. Slight changes in the intensity of the monsoon or local precipitation conditions might have played a role in this very sensitive region, but are not understood yet. The most widespread signal, however, is caused by the isotopic anomaly of the meltwater itself (Fig. 3b). In fact the evaporation process reacts non-linear on the imposed changes of the water isotopes at the sea surface. Using the global evaporation model of Merlivat and Jouzel (1979) we estimated the change of deuterium excess Δd of the vapour formed in the region of the meltwater:

$$\Delta d = \frac{1}{\alpha_D}\frac{(1-k_D)}{(1-k_D \cdot h)}\Delta\delta D_{Ocean} - 8 \cdot \frac{1}{\alpha_{18O}}\frac{(1-k_{18O})}{(1-k_{18O} \cdot h)}\Delta\delta^{18}O_{Ocean}$$

with α_{18O} and α_D as equilibrium fractionation factors (Majoube 1971), k_{18O} and k_D as the kinetic fractionation factors during evaporation from the ocean (Merlivat and Jouzel 1979), h as the relative humidity (estimated 80%) and $\Delta\delta D_{Ocean}=8\Delta\delta^{18}O_{Ocean}$ as the imposed change of the isotopic composition of sea water. In this simple calculation, we assume the average change in the North Atlantic (north of 30°N) to $\Delta\delta^{18}O_{Ocean}$ = -3‰. The resulting change of the deuterium excess yields to about +1.9‰ pretty close to the change of more than +1‰ simulated by the ECHAM in northern high latitudes.

As mentioned above, these model experiments represent a sensitivity study and we do not expect an exact match with any observed isotopic composition changes during rapid cooling events in the past. However, given our simulation captures some of the atmospheric responses on a sudden cooling in the North Atlantic, the modelled isotope anomalies should at least be in the same direction and order of magnitude as available observations. A typical example of a rapid cooling event possibly caused by a meltwater spike in the North Atlantic might be the Younger Dryas climate reversal (about 12 kyrs BP). It has been shown that several aspects of the OAGCM simulation, from which our SSTs were taken, agree well with observations of the Younger Dryas (YD) cooling (Mikolajewicz et al. 1997, Schiller et al. 1997). The timing

of this cold reversal has been studied in detail on several Greenland ice cores (e.g. in Blunier et al. 1997, Taylor et al. 1997, Severinghaus et al. 1998). Observed changes of $\delta^{18}O$, deuterium excess, surface temperature and precipitation amount on Summit, central Greenland, are listed in Table 1. The decrease in $H_2{}^{18}O$ in our model simulation is about half of the observed value. But modelled temperature anomalies are three times greater as expected from simulated $\delta^{18}O$ anomalies if the modern (spatial) isotope-temperature-gradient of 0.67‰/°C (Johnsen et al. 1989) is applied. Apparently, a lower (temporal) gradient has to be assumed for a cooling by a meltwater event. Such lower gradient has been reported by gas diffusion thermometry for the Younger Dryas (Severinghaus et al. 1998) and also by borehole thermometry for the Last Glacial Maximum (LGM) (Cuffey et al. 1995, Johnsen et al. 1995, Dahl-Jensen et al. 1998). Latest ECHAM-4 simulations under full glacial boundary conditions are able to reproduce the changed isotope-temperature-relation. The deviation from modern spatial gradient is explained by an increased seasonality of precipitation over Greenland during the LGM (Werner et al. 1999)[1]. Less snowfall during winter season causes a bias of the mean $\delta^{18}O$ values measured in ice cores towards the higher summer signal. Here, we do find a similar change in the seasonality of precipitation for the cold climate simulations (not shown). This confirms previous findings that decreased winter precipitation over Greenland is mainly influenced by cooler SSTs but not by other glacial boundary conditions.

Location		$\delta^{18}O$ (‰)	*d* (‰)	T_S (°C)	Prec. (cm/y)
Summit, Greenland	GRIP/GISP2 ice cores	-5.3	+3		-10 to -12
	ECHAM-4	-2.7 (-1.3)	+3.2 (+1.0)	-11.4 (-11.4)	-14.7 (-14.7)
Sajama, Bolivia	ice cores C-1, C-2	-5.2			(positive)[1]
	ECHAM-4	-1.6 (-0.6)	-0.2 (-0.5)	-0.6 (-0.6)	+12.5 (+12.5)

[1] Relative higher net accumulation during the cold climate of the DCR was observed.

Table 1: Ice core data from Summit, Greenland, and Sajama, Bolivia, and corresponding model results of the ECHAM-4 simulations. Changes in $\delta^{18}O$ values, deuterium excess *d*, surface temperature T_S and precipitation amount from the Younger Dryas stadial YD (resp. the deglaciation climate reversal DCR in the Sajama record) minus early Holocene values are compared to model anomalies caused by changed SSTs and $\delta^{18}O_{Ocean}$ boundary conditions. Model anomalies caused by changed SSTs alone are given in brackets. Ice core data was compiled from Alley et al. (1993), Taylor et al. (1997), and Thompson et al. (1998).

[1] see Chapter 3

A rapid decrease of about +3‰ in the deuterium excess during the transition from the YD to the Pre-boreal has been reported in the Dye3 core, southern Greenland (Dansgaard et al. 1989) and a similar value is measured on the GISP2 core (Taylor et al. 1997). Dansgaard et al. interpret this change as a redistribution of source areas of Greenland's precipitation towards cold high latitudinal regions. In their interpretation, this redistribution was mainly caused by a dramatic retreat of the sea ice border at the end of the YD. Our results, however, imply that for the interpretation of isotope records (and in particular of the deuterium excess) which stem from a region close to the meltwater input the isotopic composition of the meltwater might play a very important role, too.

The YD transition is also archived in different paleorecords in Europe. For example, isotope measurements in the calcite shells of freshwater ostracods from Lake Ammersee, Germany, allow the quantitative reconstruction of the local $\delta^{18}O$ signal in precipitation. They show a decrease in $\delta^{18}O$ of 3-4‰ between the Pre-boreal and the YD (von Grafenstein et al. 1999). Using the classical ^{18}O/T-interpretation with a gradient of 0.6‰/°C for Europe results in a temperature difference of -5°C to -6.7°C for the YD. Our model simulations, however, show only a minor cooling over Europe (-2°C to -4°C). An additional anomaly of -2‰ over central Europe can be related to the changed $\delta^{18}O_{Ocean}$ input.

A rapid cooling after the beginning of the last deglaciation period is also observed in two ice cores retrieved from the Andes (Thompson et al. 1995, 1998). The well-dated Sajama record shows a deglaciation cold reversal (DCR) comparable to the YD signal observed in Greenland ice cores. However, the beginning of this reversal may have started about 1000 years before the onset of the YD (Thompson et al. 1998). The possible relevance of temperatures shifts in the tropics for a global climate change is therefore one of the most interesting, but still unanswered questions. Although our model simulations agree qualitatively well with the Sajama record (Table 1), our findings in the Andes region are highly uncertain. The orography of the Andes is poorly resolved in the spatial T30 resolution, e.g. the grid box of the Sajama ice cap is only 2300 m above sea level (asl) (the ice cores were drilled on 6542 m asl). The main water vapour transported to the Andes originates from the tropical Atlantic and the Amazon region (Grootes et al. 1989). Therefore the dipole-like changes in the $\delta^{18}O$ signal seen in Fig. 2 will definitely have an imprint on the isotope composition of precipitation over the Andes. But since positive and negative anomalies are located so closely together, it is difficult to determine how the $\delta^{18}O$ signal on Sajama would be altered. However, it seems very likely that changes of the $\delta^{18}O$ signal will be induced by the amount effect, and might not be strongly related to changes of the surface temperature.

5.5 CONCLUSIONS

Clearly, the modelled effects of a meltwater event on the $\delta^{18}O$ signal in precipitation strongly depend on the applied boundary conditions. Especially, the effect of a changed $\delta^{18}O_{Ocean}$ field might be reduced if the isotope depletion of the fresh water input is weaker than assumed in the presented simulations. Therefore, the following list of possible effects seen in our sensitivity study should be taken with some caution. Nevertheless, it might help to lead to a better interpretation of paleorecords of fast climatic changes:

- A rapid cooling of the atmosphere by a meltwater spike in the Labrador Sea causes a clear depletion of $H_2{}^{18}O$ in precipitation in most regions of the Northern Hemisphere polewards of 45°N. In general, the depletion of isotopes is related to a cooling of surface temperatures but enhanced due to the depleted surface ocean ^{18}O isotopic composition.
- Surface temperatures on the Greenland ice sheet are much colder than expected from $\delta^{18}O$ values. A change in seasonality of precipitation over Greenland results in a changed temperature-isotope-relation. The use of the present-day spatial relation to convert isotope data into past temperatures seems questionable for fast climate changes recorded in Greenland ice core records (since temperature changes are underestimated).
- In the tropical Atlantic we observe also significant changes in the isotopic composition of precipitation. These changes are not directly related to surface temperature changes but to changes of precipitation amounts induced by a south-eastward shift of the ITCZ.
- A depletion of the isotopic composition of ocean surface waters by a massive melt water input affects the $\delta^{18}O$ signal in precipitation over most parts of Europe and the Mediterranean Sea, eastern parts of North America and northern parts of South America. This additional decrease will lead to an overestimation of temperature shifts if these are calculated from present spatial $\delta^{18}O$-temperature relations.
- Changes of the deuterium excess are even more affected by the imposed oceanic isotope anomaly due to the non-linearity of the evaporation process. Similar to $H_2{}^{18}O$, an interpretation of deuterium excess anomalies as changes in the surface temperatures and humidity at the evaporation site, solely, might yield erroneous results. But more realistic estimates of the deuterium excess anomalies of ocean surface water caused by a meltwater input are needed to evaluate the importance of the reported non-linearity effect.

REFERENCES

Alley, R. B., D. A. Meese, C. A. Shuman, A. J. Gow, K. C. Taylor, P. M. Grootes, J. W. C. White, M. Ram, E. D. Waddington, P. A. Mayewski and G. A. Zielinski (1993). "Abrupt increase in Greenland snow accumulation at the end of the Younger Dryas event." *Nature* **362**: 527-529.

Blunier, T., J. Schwander, B. Stauffer, T. Stocker, A. Dallenbach, A. Indermuhle, J. Tschumi, J. Chappellaz, D. Raynaud and J. M. Barnola (1997). "Timing of the Antarctic cold reversal and the atmospheric CO_2 increase with respect to the Younger Dryas event." *Geophysical Research Letters* **24**(21): 2683-2686.

Brook, E. J., T. A. Sowers and J. Orchardo (1996). "Rapid variations in atmospheric methane concentration during the past 110,000 years." *Science* **273**: 1087-1091.

Cane, M. A. (1998). "Climate change - a role for the tropical Pacific." *Science* **282**: 59-61.

Cuffey, K. M., G. D. Clow, R. B. Alley, M. Stuiver, E. D. Waddington and R. W. Saltus (1995). "Large Arctic temperature change at the Wisconsin-Holocene glacial transition." *Science* **270**: 455-458.

Curry, W. B. and D. W. Oppo (1997). "Synchronous, high-frequency oscillations in tropical sea surface temperatures and North Atlantic Deep Water production during the last glacial cycle." *Paleoceanography* **12**: 1-14.

Dahl-Jensen, D., K. Mosegaard, N. S. Gundestrup, G. D. Clow, S. J. Johnsen, A. W. Hansen and N. Balling (1998). "Past temperatures directly from the Greenland ice sheet." *Science* **282**: 268-271.

Dansgaard, W., J. W. C. White and S. J. Johnsen (1989). "The abrupt termination of the Younger Dryas climate event." *Nature* **339**: 532-534.

Grootes, P. M., M. Stuiver, L. G. Thompson and E. Mosley-Thompson (1989). "Oxygen isotope changes in tropical ice, Quelccaya, Peru." *Journal of Geophysical Research* **94**(D1): 1187-1194.

Hoffmann, G., M. Werner and M. Heimann (1998). "The water isotope module of the ECHAM atmospheric general circulation model - a study on time scales from days to several years." *Journal of Geophysical Research* **103**(D14): 16871-16896.

IAEA (1992). "Statistical treatment of data on environmental isotopes in precipitation." *Technical Report,* I.A.E.A., Vienna.

Johnsen, S. J., H. B. Clausen, W. Dansgaard, K. Fuhrer, N. S. Gundestrup, C. U. Hammer, P. Iversen, J. Jouzel, B. Stauffer and J. P. Steffensen (1992). "Irregular glacial interstadials recorded in a new Greenland ice core." *Nature* **359**: 311-313.

Johnsen, S. J., D. Dahl-Jensen, W. Dansgaard and N. S. Gundestrup (1995). "Greenland paleotemperatures derived from GRIP bore hole temperature and ice core isotope profiles." *Tellus* **47B**: 624-629.

Johnsen, S. J., W. Dansgaard and J. W. C. White (1989). "The origin of Arctic precipitation under present and glacial conditions." *Tellus* **41B**: 452-468.

Majoube, M. (1971). "Fractionnement en oxygen 18 et en deuterium entre l'eau et sa vapeur." *J.Chem.Phys.* **10**: 1423-1436.

Merlivat, L. and J. Jouzel (1979). "Global climatic interpretation of the deuterium-oxygen 18 relationship for precipitation." *Journal of Geophysical Research* **84**(C8): 5029-5033.

Mikolajewicz, U. (1996). "A meltwater induced collapse of the 'conveyor belt' thermohaline circulation and its influence on the distribution of delta-^{14}C and delta-^{18}O in the oceans." *MPI-Report 189*. Max-Planck-Institute for Meteorology, Hamburg.

Mikolajewicz, U., T. J. Crowley, A. Schiller and R. Voss (1997). "Modelling teleconnections between the North Atlantic and North Pacific during the Younger Dryas." *Nature* **387**: 384-387.

Schiller, A., U. Mikolajewicz and R. Voss (1997). "The stability of the North Atlantic thermohaline circulation in a coupled ocean-atmosphere general circulation model." *Climate Dynamics* **13**(5): 325-347.

Severinghaus, J. P., T. A. Sowers, E. J. Brook, R. B. Alley and M. L. Bender (1998). "Timing of abrupt climate change at the end of the Younger Dryas interval from thermally fractionated gases in polar ice." *Nature* **391**: 141-146.

Stocker, T. F. (1998). "Climate change - the seesaw effect." *Science* **282**: 61-62.

Taylor, K. C., P. A. Mayewski, R. B. Alley, E. J. Brook, A. J. Gow, P. M. Grootes, D. A. Meese, E. S. Saltzman, J. P. Severinghaus, M. S. Twickler, J. W. C. White, S. I. Whitlow and G. A. Zielinski (1997). "The Holocene Younger Dryas transition recorded at Summit, Greenland." *Science* **278**: 825-827.

Thompson, L. G., M. E. Davis, E. Mosley-Thompson, T. A. Sowers, K. A. Henderson, V. S. Zagorodnov, P. N. Lin, V. N. Mikhalenko, R. K. Campen, J. F. Bolzan, J. Cole-Dai and B. Francou (1998). "A 25,000-year tropical climate history from Bolivian ice cores." *Science* **282**: 1858-1864.

Thompson, L. G., E. Mosley-Thompson, M. E. Davis, P. N. Lin, K. A. Henderson, J. Coledai, J. F. Bolzan and K. B. Liu (1995). "Late glacial stage and Holocene tropical ice core records from Huascaran, Peru." *Science* **269**: 46-50.

von Grafenstein, U., H. Erlenkeuser, A. Brauer, J. Jouzel and S. J. Johnsen (1999). "A mid-European decadal isotope-climate record from 15,500 to 5000 years B.P." *Science* **284**: 1654-1657.

Voss, R., R. Sausen and U. Cubasch (1998). "Periodically synchronously coupled integrations with the atmosphere-ocean general circulation model Echam-3/LSG." *Climate Dynamics* **14**(4): 249-266.

Werner, M., U. Mikolajewicz, M. Heimann and G. Hoffmann (1999). "Borehole versus isotope temperatures on Greenland: Seasonality does matter." *Geophysical Research Letters* in press.

Chapter 6

Modelling Interannual Variability of Water Isotopes in Greenland and Antarctica

ABSTRACT. An ECHAM-4 simulation with both stable water isotopes $H_2{}^{18}O$ and HDO explicitly included in the water cycle was performed for the period 1950-1994 to examine the interannual to decadal variations of the isotopic composition of precipitation falling on Greenland and Antarctica. The analyses focus on the Summit region, central Greenland, and the Law Dome region, East Antarctica, respectively, and reveal that about one-third of the simulated variability in $H_2{}^{18}O$ can be explained by simultaneous changes of the surface temperature at the precipitation sites. Other climate variables influencing the isotope signal are identified by multiple linear regression and the results show clearly that the isotopic composition of polar precipitation integrates the climatic history of a broader region. Additional correlation analyses between the isotope record and indices of the North Atlantic Oscillation (NAO) and the El Niño / Southern Oscillation phenomenon (ENSO) enable the detection of several regions in Greenland and Antarctica, where these climate oscillations are imprinted in the simulated record of isotopic composition of precipitation.

6.1 INTRODUCTION

For more than three decades measurements of stable water isotopes $H_2{}^{18}O$ and HDO have been used as proxy data for surface temperatures in paleoclimatological studies. Based on the strong spatial correlation between the isotopic composition of precipitation (in general expressed as $\delta^{18}O$ and δD) and surface temperatures, as first described by Dansgaard (1964), past temporal changes of $\delta^{18}O$, e.g. measured in ice cores, are interpreted as changes of temperatures at the precipitation site. For different climatic stages, like the Younger Dryas period or the Last Glacial Maximum (LGM), new isotope-independent temperature estimates from both Greenland and Antarctica (Cuffey et al. 1995, Dahl-Jensen et al. 1998, Salamatin et al. 1998, Severinghaus et al. 1998) challenge the (spatial) calibration of the isotope thermometer, but not the close temporal relation between the isotopic signal and surface temperatures in general. On a much shorter monthly to seasonal time scale, a close temporal relation between the isotopic composition of precipitation and surface temperatures has also been observed for both polar regions (e.g. in Shuman et al. 1995, van Ommen and Morgan 1996). However,

little is known about the cause of the year-to-year variability of $\delta^{18}O$ and δD in precipitation for the present climate. So far, any attempt to interpret the observed variability of $\delta^{18}O$ measured in ice cores from both Greenland and Antarctica has been inhibited by the lack of long-term observational records of climate variables which are possibly related to the isotope signal, e.g. the temperature at the precipitation site. In addition, post-depositional effects (wind drift, re-layering of snow, diffusion of the isotope signal) might add some noise to the δ-values in the firn and hence complicate the interpretation of the observed isotope variability.

In this study we will apply a different approach by using an atmospheric general circulation model (AGCM) with both water isotopes $H_2{}^{18}O$ and HDO explicitly built into the hydrological cycle of the model. Isotope modelling with AGCMs has been shown to be a helpful tool to study the important mechanisms influencing the δ-signals of precipitation for various climatic boundary conditions (e.g. in Joussaume et al. 1984, Jouzel et al. 1987, Charles et al. 1994, Hoffmann et al. 1998). In contrast to field measurements, all climate variables of an AGCM simulation which affect the isotopic fractionation processes are known. This enables a rigorous test of potential variables influencing the isotope signal to determine the variables most strongly related to the isotope anomalies. For example, Cole et al. (1999) reported a weak correlation between isotopes in precipitation and temperatures for only certain continental regions of the extratropics in a 12-year AGCM simulation.

Here, we present results of an AGCM isotope experiment covering the period 1950-1994 and our analyses focus on the following questions: (1) Is the isotopic composition of precipitation of Greenland and Antarctica a reliable proxy for surface temperatures on interannual to decadal time scales? (2) Which other climate variables are of importance to explain the simulated variability in the $\delta^{18}O$ signal? (3) Are climate phenomena like the El Niño / Southern Oscillation (ENSO) phenomenon or the North Atlantic Oscillation (NAO) imprinted in the $\delta^{18}O$ signal of polar precipitation?

6.2 Model Description and Boundary Conditions

The applied model was the Hamburg AGCM ECHAM-4 (Roeckner et al. 1996) with both water isotopes $H_2{}^{18}O$ and HDO explicitly cycled through the water cycle of the model (Hoffmann and Heimann 1993). The simulation was performed in T30 resolution (3.75° by 3.75° spatial grid, 19 vertical levels). Monthly observed sea surface temperatures (SST) and sea-ice distribution of the GISST2.2 data set of the British Meteorological Office (UKMO) were prescribed for the period 1950-1994. Atmospheric concentrations of greenhouse gases (CO_2, CH_4, N_2O) were also prescribed according to the observations (IPCC 1992).

6.3 Results & Discussion

6.3.1 The Simulated Isotope Record of Summit, Central Greenland

For Greenland, our analyses will focus on the central region of this ice sheet, which encloses the Summit region. During the years 1989-1993 several seasons of fieldwork were performed in this region within the framework of the European Greenland Ice Core Program (GRIP) and the U.S. Greenland Ice Sheet Project 2 (GISP2). The observations of numerous glaciological studies enable a detailed comparison of observational data to simulation results for this area of the Greenland ice sheet. The simulated $\delta^{18}O$ record of the grid box enclosing the Summit region in central Greenland is compared to a stacked isotopic record of 6 individual ice cores of the GRIP and GISP2 drilling sites for the period 1950-1986 (White et al. 1997). The mean simulated isotope value between 1950-1986 ($\delta^{18}O$ = -29.1‰) is lower than the stacked observations ($\delta^{18}O$ = -35.1‰), which can be explained by the coarse model resolution: The grid box enclosing the Summit region is ~500m lower than the true Summit location. The deviation between the mean simulated surface temperature (-27.7°C) and the observations (-32°C) can also be related to the coarse model resolution. Mean modelled precipitation values (27.1cm/a) are comparable to the measurements (23cm/a). Analysing the year-to-year variations, the 1σ standard deviation of the modelled $\delta^{18}O$ record ($\Delta\delta^{18}O$ = ±0.7‰) is found to be in agreement with the observations ($\Delta\delta^{18}O$ = ±0.8‰) for the period 1950-1986. Time-series of both the observed and simulated $\delta^{18}O$ records are shown in Fig. 1. It is noticed that the modelled isotope anomaly of any arbitrary calendar year (i.e. the deviation from the long-time mean value) does not match the observations. However, one should not expect such an agreement since the internal noise level of the atmosphere in these latitudes is relatively large.

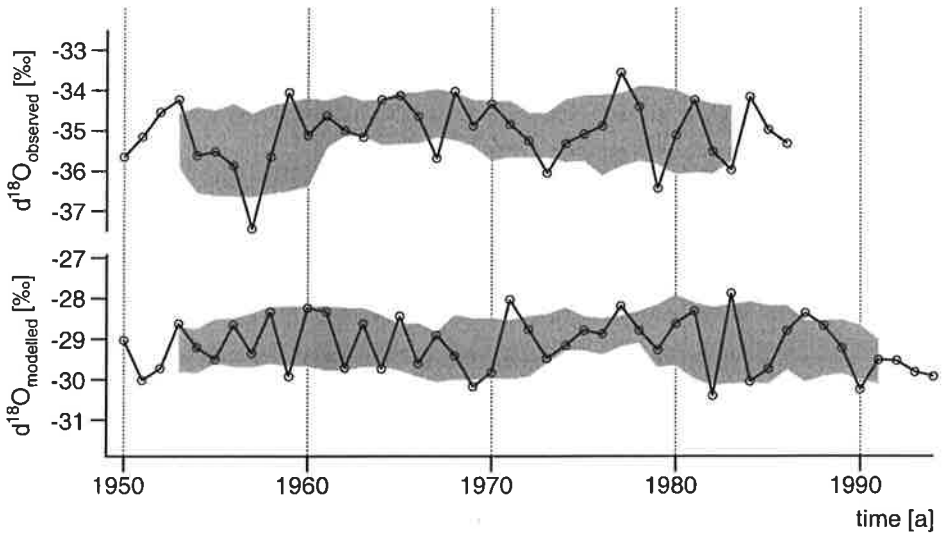

Figure 1: Comparison of the observed stacked annual GRIP/GISP2 isotope record (White et al. 1997) and the modelled annual ECHAM-4 isotope record of the grid box enclosing Summit, Greenland (solid lines). The grey area represents the calculated 1σ standard deviation of a 7-year running mean.

6.3.2 Interannual Variations of $\delta^{18}O$ in Central Greenland

In a previous study of White et al. (1997), about 50% of the variability of the stacked GRIP/GISP2 $\delta^{18}O$ record was explained by a multiple linear regression of average coastal Greenland temperature, winter NAO, the annual temperature seesaw between Jakobshavn and Oslo, insolation changes and SST (20°-30°N). However, due to the lack of temperature observations in the Summit region it remained open, how much of the $\delta^{18}O$ variability reflects the climatic history of a broader region, and how much is related to variability in surface temperatures at the precipitation site. To calculate the latter, we compared the simulated $\delta^{18}O$ record of central Greenland (averaged over 4 grid boxes in the region 70.5°-78.0°N, 35.6-43.1°W) with the surface temperature T_S in the same area (Fig. 2a) for the period 1950-1994. The regression between $\delta^{18}O$ and T_S has a slope of m = 0.15‰/°C and a correlation coefficient of r=0.28, indicating only a weak correspondence between the two time series. To take into consideration that the $\delta^{18}O$ signal is only archived during precipitation events, a record of precipitation-weighted annual temperatures $T_{S,pr}$

$$T_{S,pr} = \Sigma_i (T_{S,i} \cdot prec_i) / \Sigma_i (prec_i)$$

with $T_{S,i}$ and $prec_i$ as monthly temperatures (i=1..12) of an individual year, was also evaluated. This results in a larger correlation between $\delta^{18}O$ and temperature (r = 0.52, m = 0.20‰/°C) and about 26% of the annual variance of $\delta^{18}O$ can be explained by simultaneous changes of $T_{S,pr}$ (Fig. 2b). It is interesting to note that the interannual slope derived from the simulation is not equal but close to the simulated seasonal slope (m = 0.33‰/°C, r = 0.84), and that both temporal slopes are smaller than the modelled spatial slope of the Greenland ice sheet

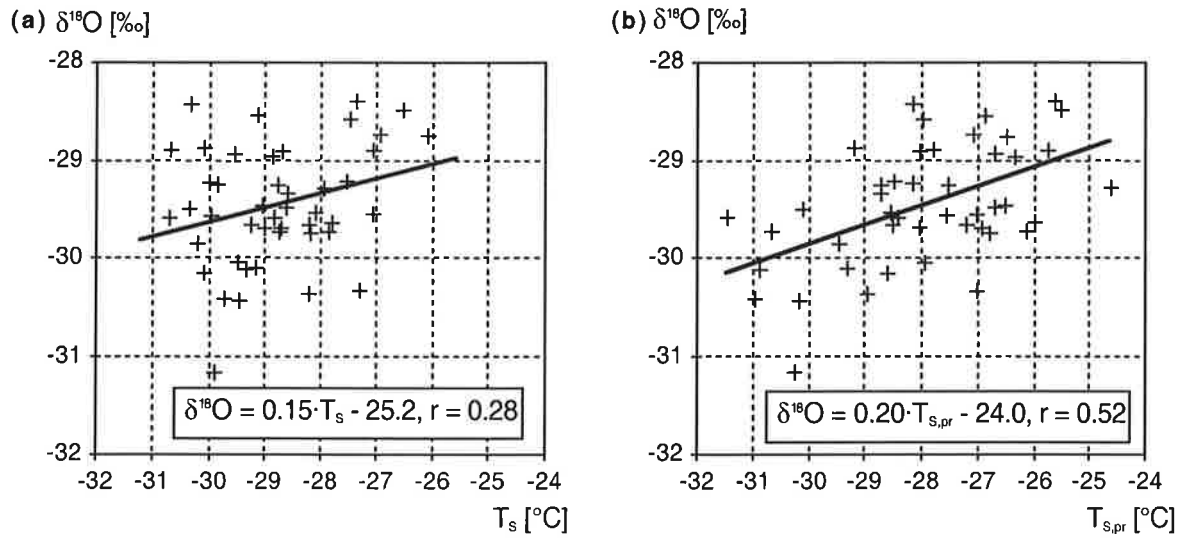

Figure 2: (a) Simulated annual mean $\delta^{18}O$ values versus arithmetic mean surface temperatures T_S in central Greenland, for the period 1950-1994. Correlation equation and coefficient of a linear regression (solid line) are given in the text box. (b) The same as (a) but for precipitation-weighted surface temperatures $T_{S,Pr}$.

(m = 0.55‰/°C, r = 0.90). However, in contrast to ECHAM-4 simulations for the climate of the last glacial maximum (Werner et al. 1999)[1] the present-day deviations between the interannual temporal and the spatial $\delta^{18}O$-T_S-gradient can not be explained by a change of the seasonality of precipitation.

It is evident from the preceding analysis that the simulated variability of $\delta^{18}O$ must be influenced by additional climate variables, which are not strongly correlated to surface temperatures on the ice sheet themselves. To identify some of them, the relationships between the $\delta^{18}O$ signal and a set of 21 climate variables were analysed. This set included three records describing the climate at the precipitation site: surface temperature, temperature of the warmest tropospheric model level (further referred to as inversion temperature) and precipitation amount. The simulated annual NAO index, the seesaw record of surface temperatures from Oslo, Norway, minus Jakobshavn, West Greenland, and the Niño-3 index were also added to the set of variables. Furthermore, we included SST records averaged over four regions (0-20°N, 20-40°N, 40-60°N, 60-90°N) of the Atlantic and the Pacific, respectively, and the simulated annual surface temperatures of North America. Previous ECHAM-4 simulations indicated that these source areas of water vapour contribute a significant amount to the precipitation of central Greenland (Werner et al. 1999)[1]. Correlation maps of $\delta^{18}O$ and several variables (surface temperature, evaporation flux, sea level pressure, 500hPa geopotential height, relative humidity of the lowest model level above surface) were used to identify additional regions of strong correlation ($|r| > 0.4$). Averaged annual records of 6 regions were included in the correlation analysis (Fig. 3).

Parameter	correlation coefficient r	explained variance	probability of chance correl.
SST (Atlantic,0-20N)	-0.22	4.7%	14.7%
SST (Pacific,60-90N)	0.10	1.1%	48.9%
ΔT Seesaw	-0.45	20.7%	0.2%
NAO-index	-0.45	19.8%	0.3%
SLP (Spain)	-0.53	28.3%	0.0%
T (West Greenland)	0.62	38.2%	0.0%
T (West Greenland), prec.w.	0.68	46.7%	0.0%
Geopotential Height (Greenland)	0.59	34.6%	0.0%
T Inversion	0.34	11.3%	2.4%
Niño-3-index	-0.18	3.4%	21.9%

Table 1: Linear correlation coefficients, explained variance and the probability of chance correlation between several climate variables and the simulated mean $\delta^{18}O$ signal in central Greenland.

[1] see Chapter 3 & 4

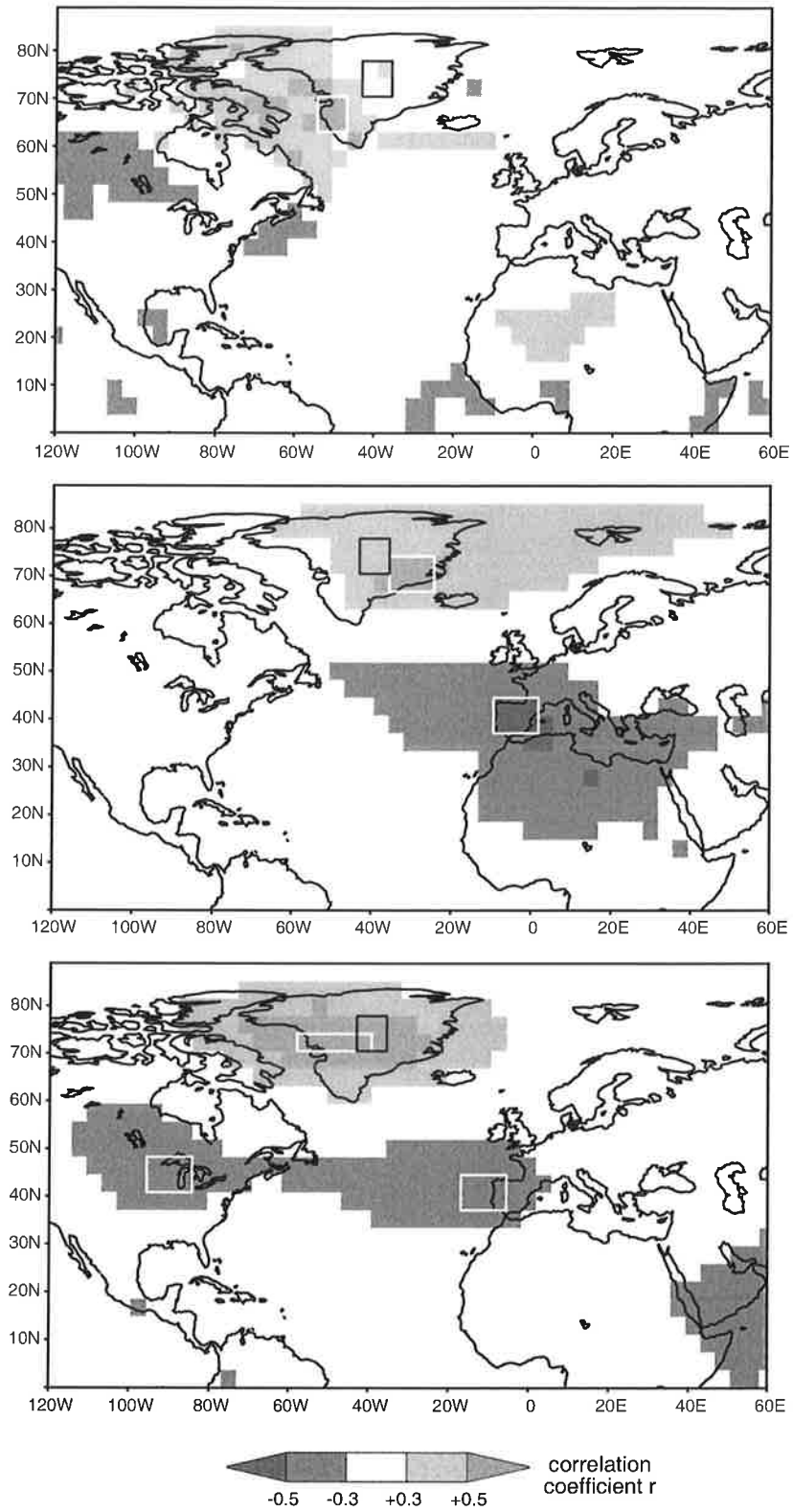

Figure 3: Correlation maps of $\delta^{18}O$ in precipitation in central Greenland (average of area in the black rectangle) and simulated surface temperature (top), sea level pressure (middle) and geopotential height at 500hPa (bottom). The white rectangles define several areas of strongest correlation.

It is noteworthy that the correlation map between $\delta^{18}O$ and sea level pressure results in a NAO-like pattern with highly positive correlation centred north-west of Iceland.

For this set of 21 variables, a selection of the best subset (as defined by Mallows' C_p statistic) of all possible combinations of a multiple linear regression yields 10 climate variables explaining together about 78% ($r = 0.89$) of the total variance of the modelled $\delta^{18}O$ record (Table 1). Seven variables are highly correlated (probability of chance correlation < 5%) with the $\delta^{18}O$ record themselves. However they are not totally independent as shown by a cross-correlation analysis (Table 2). Excluding both SST records listed in Table 1, the Niño-3 index and the arithmetic mean temperature record at the west coast of Greenland (strong cross-correlation with the seesaw temperature pattern) leaves a set of 6 climate variables, which still explains 60% of the simulated $\delta^{18}O$ variability. The multiple regression equation is

$$\delta^{18}O = -3.9 + 0.03 \cdot \Delta T(\text{Seesaw}) + 0.09 \cdot \text{NAO} - 0.13 \cdot \text{SLP(Spain)} + 0.32 \cdot T_{s,pr}(\text{West Greenland}) + 0.02 \cdot \text{Geopotential(Greenland)} - 0.18 \cdot T(\text{Inversion})$$

and the overall evolution of the $\delta^{18}O$ record is fitted well by the combination of these 6 variables[2] (Fig. 4). It is not surprising that the inversion temperature at the precipitation site rather than the surface temperature is explicitly included in the regression model since the former is closer related to the temperatures during formation of precipitation (Krinner et al. 1997). The (precipitation-weighted) surface temperature changes at the west coast, however, are strongly correlated to the $\delta^{18}O$ anomalies of central Greenland (Table 1). One might interpret those temperatures at the west coast as a proxy for the history of air masses transported from the south-west to the Greenland ice sheet, which obviously have a significant impact on the variability of the $\delta^{18}O$ signal in central Greenland.

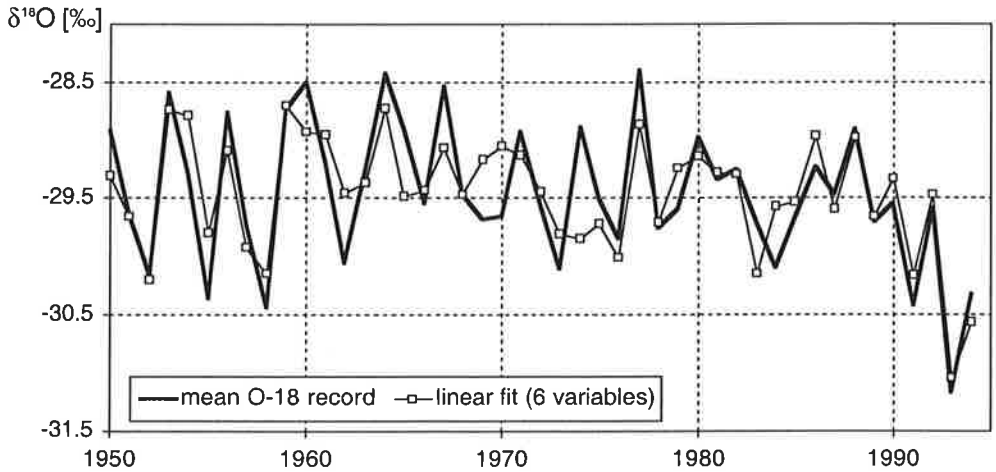

Figure 4: Simulated annual $\delta^{18}O$ record of central Greenland and the fit of a multiple linear regression (6 climate variables) for the period 1950-1994.

[2] Units of the climate variables are °C (all temperatures), hPa (sea level pressure) and gpm (geopotential height). The units of the preceding factors are ‰/°C, ‰/hPa and ‰/gpm, respectively.

	ΔT Seesaw	NAO	SLP (Spain)	T (West G.)	T (West G.) prec. w.	Geopot. H. (Greenland)	T Inversion
ΔT Seesaw	1.00						
NAO	0.46	1.00					
SLP (Spain)	0.40	0.65	1.00				
T (West Greenland)	-0.89	-0.58	-0.49	1.00			
T (West Greenland) prec.w.	-0.65	-0.37	-0.53	0.71	1.00		
Geopotential Height (Greenland)	-0.60	-0.72	-0.45	0.62	0.50	1.00	
T Inversion	-0.59	-0.13	-0.21	0.53	0.46	0.60	1.00

Table 2: Linear cross-correlation between different climate variables related to the $\delta^{18}O$ signal in central Greenland.

6.3.3 The Imprint of the NAO

To reconstruct a paleo-NAO record by ice core data the found correlation of the NAO and the $\delta^{18}O$ signal in the regression model is of special interest. Recently, Appenzeller et al. (1998) reported a strongly negative correlation between the NAO record of Hurrel (1995) and the annual snow amount derived from the NASA-U core drilled in West Greenland, whereas only a weak correlation was observed for central Greenland. About one-third of the total variability could be explained by a linear correlation between the annual NAO record and the net snow accumulation at the NASA-U drill site for the past 130 years. Our model results are in good agreement with the observations of Appenzeller et al. (Fig. 5). Correlation coefficients between the NAO and precipitation amounts are strongly negative west of Summit ($r < -0.5$) and positive at the east coast near Scoresbysund. At the most, about 33% of the interannual variance in modelled precipitation can be related to the NAO. A corresponding correlation of the NAO and the annual mean $\delta^{18}O$ values of precipitation results in a slightly different correlation map. Positive correlation coefficients are still found at the east coast of Greenland, but the pattern of negative correlation is shifted to the region south-west of the Summit drill site. About 35% of the simulated changes of $\delta^{18}O$ in the latter region can be related to variability in the NAO. Especially, the increasing trend of the simulated NAO index between 1980-1994 is also found in the $\delta^{18}O$ record. On the contrary, the short-term anomalies of the NAO between 1950-1970 can not be identified in the $\delta^{18}O$ series (bottom part of Fig. 5). These results indicate that decadal variations of the NAO might be identified by $\delta^{18}O$ anomalies while shorter year-to-year NAO variations are masked by the "noise" in the $\delta^{18}O$ record. However, in order to confirm these results, large ensembles of isotope simulations should be conducted.

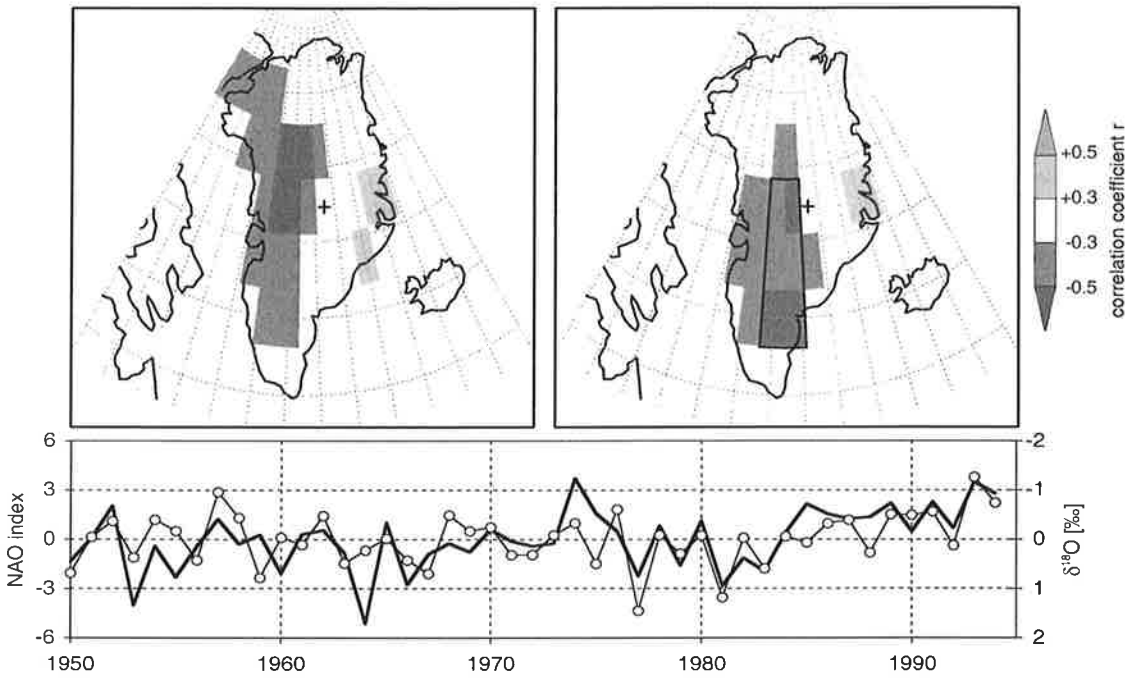

Figure 5: Correlation maps of the simulated annual NAO index and the modelled amount of precipitation in Greenland (left) and of the NAO index and the $\delta^{18}O$ values of precipitation (right). The cross marks the location of the Summit drill site. Bottom part: Time series of the simulated NAO index (black line) and mean $\delta^{18}O$ anomalies (open circles) of the region south-west of Summit (area of the black rectangle in upper right map). For clarity reasons, the $\delta^{18}O$ axis is reversed.

6.3.4 The Simulated Isotope Record of Law Dome, East Antarctica

Annual mean precipitation over most parts of Antarctica is less then 10cm/a (Bromwich 1988). The dryness of this remote area makes observations of interannual $\delta^{18}O$ variations in Antarctica more difficult than in Greenland, since seasonal cycles of $\delta^{18}O$ with wavelengths shorter than 20cm are obliterated during the firnification process (Johnsen 1977). Thus, for most Antarctic regions, annual variations of the isotopic composition of precipitation can only be measured for a few years to decades in the uppermost firn layers. Only ice cores from coastal regions with much higher precipitation amounts offer the opportunity to study interannual changes of $\delta^{18}O$ in precipitation for longer time periods. One of such drilling sites is the region around Law Dome (66.8 °S, 112.8°E) in coastal East Antarctica where preserved isotopic seasonality has been measured for the last 700 years (van Ommen and Morgan 1997). The following analyses of our model simulation will exemplary focus on this region. Mean annual model values of surface temperature (T_S = -26.2°C) and isotopic composition of precipitation ($\delta^{18}O$ = -22.1‰) of the grid box enclosing the Law Dome drilling site are in fair agreement with the observations (T_S = -22°C, $\delta^{18}O$ = -21.8‰) for the period 1980-1992

(Delmotte et al. 1999). The mean simulated seasonals amplitude of T_S (~20°C) and $\delta^{18}O$ (~9‰) are also comparable to measurements (16°C and 8‰, Delmotte et al. 1999). Due to the coarse spatial model resolution the precipitation amounts at several coastal sites in Antarctica are underestimated in the ECHAM-4 simulation, e.g. at Law Dome (observed: 64.4cm/a, simulated: 33.5cm/a).

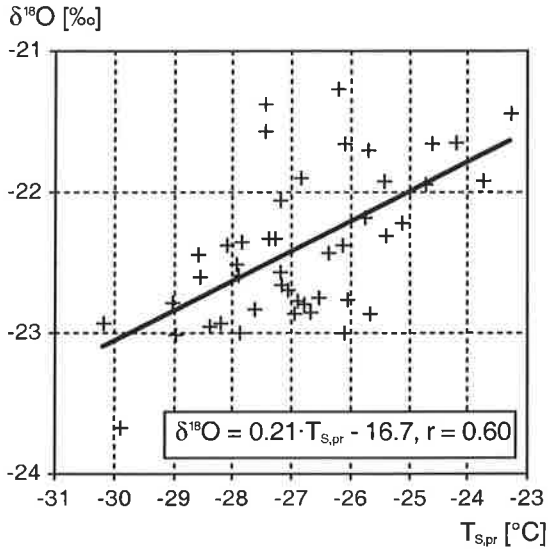

Figure 6: Simulated annual mean $\delta^{18}O$ values versus precipitation-weighted surface temperatures $T_{S,pr}$ near Law Dome, Antarctica, for the period 1950-1994. Correlation equation and coefficient of a linear regression (solid line) are given in the text box.

6.3.5 Interannual Variations of $\delta^{18}O$ near Law Dome

Like for central Greenland, the relation between simulated interannual variations of $\delta^{18}O$ and surface temperature is analysed first. A linear correlation of annual values (averages of three coastal grid boxes between 66.8-70.5°S, 106.9-118.1°W) of surface temperatures T_S and $\delta^{18}O$ values indicates a weak correspondence between both variables (r = 0.34, m = 0.17‰/°C). Using precipitation-weighted annual mean surface temperatures $T_{S,pr}$ instead of T_S results in an improved correlation (r = 0.60, m = 0.21‰/°C), shown in Fig. 6. Similar to the results for central Greenland, there is some correspondence between the interannual and the seasonal $\delta^{18}O$-T_S-gradient (m = 0.25‰/°C, r= 0.61) and both simulated temporal gradients strongly deviate from the modelled spatial $\delta^{18}O$-T_S-slope (m = 0.72‰/°C, r=0.95) of East Antarctica. In addition, this analysis between $\delta^{18}O$ and $T_{S,pr}$ reveals that no more than 36% of the simulated interannual $\delta^{18}O$ variability around Law Dome can be related to simultaneous changes in surface temperatures.

A multiple linear regression analysis is performed for identifying other climate variables influencing the $\delta^{18}O$ signal near Law Dome. The investigated set of climate variables includes again three records at the precipitation site (surface temperature, precipitation amount, inver-

sion temperature), plus the Niño-3 index and the modelled NAO index. SST records averaged over four different ocean regions (0-20°S, 20-40°S, 40-60°S, 60-90°S) of the Atlantic, the Pacific and the Indian Ocean, respectively, were also included in further analyses. Half of the modelled precipitation at Law Dome stems from the tropical and subtropical Indopacific, but some water masses also origin from the Atlantic and the Antarctic Current (Werner et al. 1999)[3]. In contrast to Greenland, no specific regions with high correlation coefficients ($|r| > 0.4$) were detected in correlation maps of the $\delta^{18}O$ record of the Law Dome region and several other climate variables (surface temperatures, evaporation flux, sea level pressure, 500hPa geopotential height, relative humidity of the lowest model level above surface). In total, 19 climate records were included in the multiple regression analysis. Defining again the best subset of climate variables by Mallows' C_p statistic results in a linear combination of 4 climate variables explaining together 50% ($r = 0.71$) of the simulated interannual $\delta^{18}O$ variability for the period 1950-1994:

$$\delta^{18}O = -19.3 + 0.03 \cdot \text{precipitation} + 0.37 \cdot \text{SST(Pacific,60-90°N)} - 0.39 \cdot \text{T(Inversion)} + 0.49 \cdot \text{T(Inversion, prec. weighted)}$$

The inversion temperature of the Law Dome region enters twice in this model equation: As the arithmetic mean record and as the precipitation-weighted record. However, only the latter and the record of annual precipitation amount are strongly correlated (probability of chance correlation < 5%) to $\delta^{18}O$ itself (Table 3). A linear regression model with these two variables explains only 36% of the variability in $\delta^{18}O$ ($r = 0.61$) and is not superior to the simple linear correlation between $\delta^{18}O$ and T_S. A comparison of the time series of the $\delta^{18}O$ record and of the multivariable fit reveals that the regression fails to reproduce some strong $\delta^{18}O$ anomalies between 1981 and 1989 (Fig. 7). The cause for these strong $\delta^{18}O$ anomalies remains unclear. A direct correlation with exceptional strong ENSO events (e.g. 1982/83) is not found.

Parameter	correlation coefficient r	explained variance	probability of chance correl.
precipitation amount	0.40	16.2%	0.7%
SST (Pacific,60-90S)	0.21	4.5%	15.6%
T Inversion	0.26	6.6%	8.5%
T Inversion, prec. weighted	0.58	34.0%	0.0%

Table 3: Linear correlation coefficients, explained variance and the probability of chance correlation between several climate variables and the simulated mean $\delta^{18}O$ signal of the Law Dome region.

[3] see Chapter 4

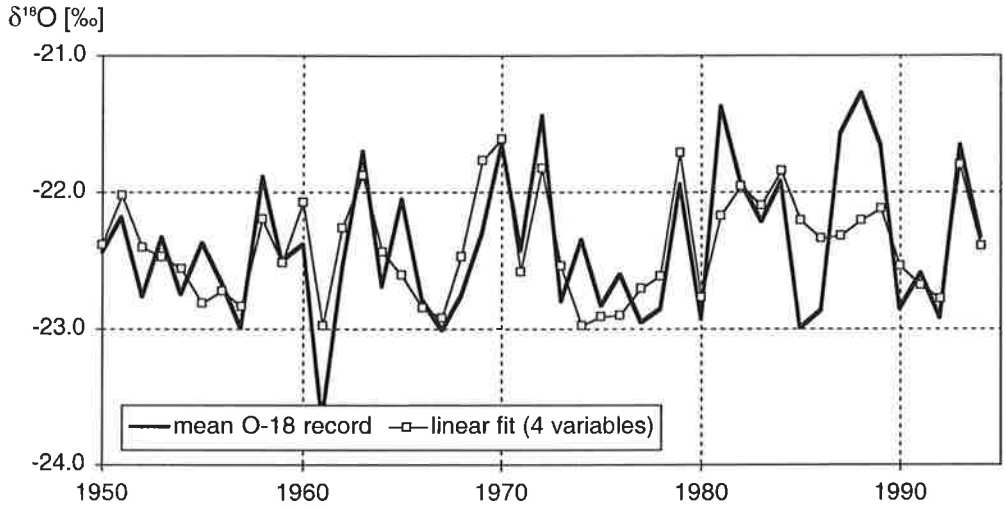

Figure 7: Simulated annual $\delta^{18}O$ record of the region near Law Dome, East Antarctica, and the fit of a multiple linear regression (4 climate variables) for the period 1950-1994.

6.3.6 The Imprint of ENSO

A correlation map between the modelled $\delta^{18}O$ record and the Niño-3 index enables the identification of Antarctic regions potentially influenced by the El Niño / Southern Oscillation (ENSO) phenomenon (Fig. 8). Significant correlations are found for several coastal regions with highest correlations south-east of the Vostok drill site where 28% of the interannual $\delta^{18}O$ variability can be related to ENSO. However the dryness of this area (annual precipitation amount less than 5cm/a) probably inhibits a reconstruction of past ENSO extremes. A better region might be the area south-east of the Law Dome drilling site where precipitation amounts are much higher. About 21% of the modelled $\delta^{18}O$ variability in this region can be related to the Niño-3 index ($r = 0.46$). To check the robustness of our model findings, we repeated the analysis for the shorter period 1970-1994, when the prescribed sea-ice coverage around Antarctica is more accurate. As seen in Fig. 8, a similar pattern of positive correlation between $\delta^{18}O$ and the Niño-3 index is simulated for this shorter time period, and to some extent additional regions of negative correlations are found west of the Antarctic Peninsula and in Dronning Maud Land. The latter may be related to coherent variations between ENSO and sea-ice coverage around Antarctica, as reported by several authors (e.g. Gloersen 1995). However, due to the shorter time period, the probability of chance correlation has also increased.

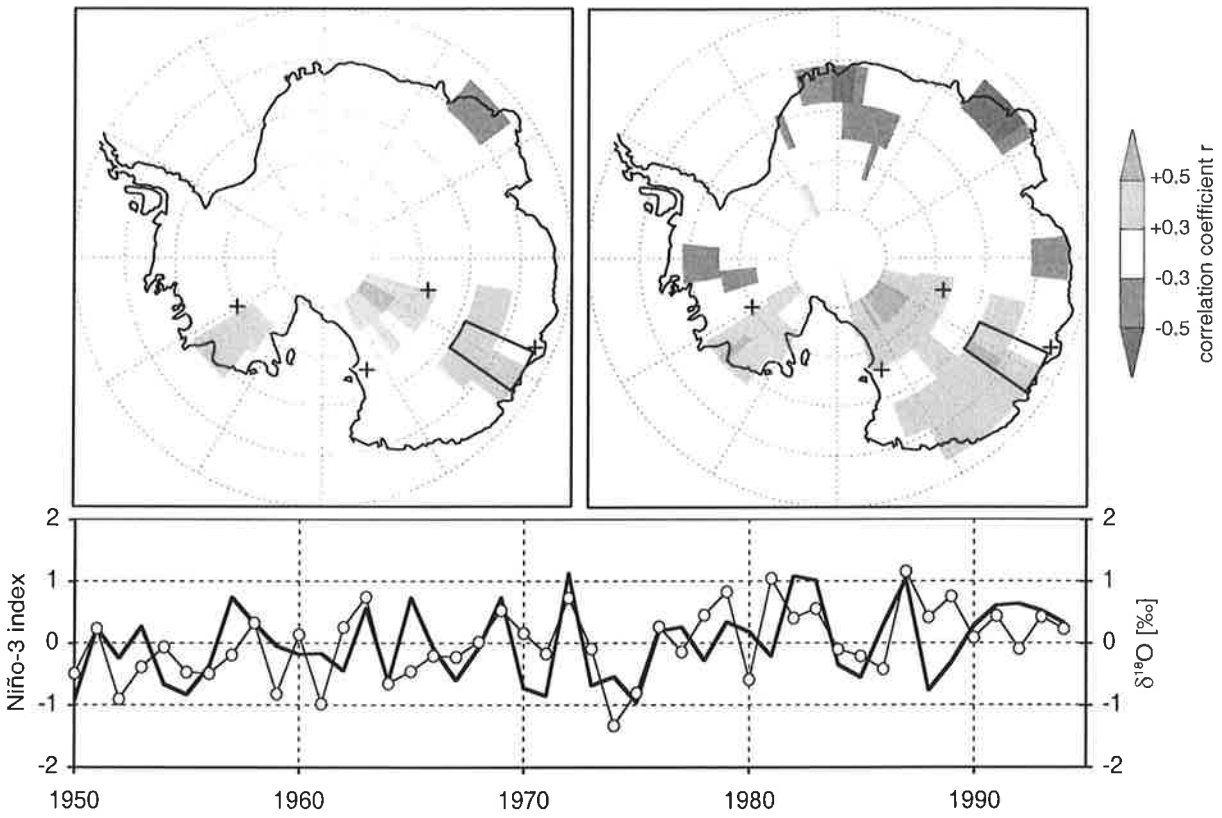

Figure 8: Correlation maps of the Niño-3 index and the modelled $\delta^{18}O$ values of precipitation in Antarctica for the period 1950-1994 (left) and for the period 1970-1994 (right). The crosses mark the location of four Antarctic drill sites: Vostok, Law Dome, Taylor Dome, Byrd ice core (from east to west). Bottom part: Time series of the Niño-3 index (black line) and the mean $\delta^{18}O$ anomalies (open circles) of the region south-east of Law Dome (area of the black rectangle in the upper maps).

6.4. Conclusions

The analyses of the simulated isotopic composition of polar precipitation showed clearly that the ECHAM-4 model is able to reproduce the interannual variability of $\delta^{18}O$ in agreement with measurements of several ice cores from Greenland and Antarctica. About one-third of the modelled $\delta^{18}O$ variability can be related to simultaneous surface temperature anomalies at the precipitation sites in central Greenland and near Law Dome, Antarctica, respectively. On interannual to decadal time scales, the $\delta^{18}O$ signal is a more reliable proxy for precipitation-weighted temperatures than for arithmetic mean temperature values, and the temporal isotope-temperature-relation is significantly lower than the modelled spatial relation, both in Greenland and Antarctica.

The analyses of this AGCM simulation also demonstrated that the isotopic composition of precipitation integrates the history of several climate variables, which can be identified by a

multiple linear regression technique. Interannual to decadal $\delta^{18}O$ variability is a complex signal and not easy to decipher, since variability in the long-range transport and mixing of air masses from different source regions contribute additional "noise" to the $\delta^{18}O$ signal in precipitation, which is not linked to the climate at the precipitation site. However, the $\delta^{18}O$ records of ice cores may be used to reconstruct past climate indices, like NAO or ENSO, since those climate phenomena are imprinted in the isotopic composition of precipitation. Our ECHAM-4 simulation showed the potential usefulness of isotope AGCMs for identifying regions where the $\delta^{18}O$ variability is strongly correlated to NAO (Greenland) or ENSO (Antarctica).

REFERENCES

Appenzeller, C., T. F. Stocker and M. Anklin (1998). "North Atlantic oscillation dynamics recorded in Greenland ice cores." *Science* **282**: 446-449.

Bromwich, D. H. (1988). "Snowfall in high southern latitudes." *Reviews of Geophysics* **26**: 149-168.

Charles, C. D., D. H. Rind, J. Jouzel, R. D. Koster and R. G. Fairbanks (1994). "Glacial-interglacial changes in moisture sources for Greenland: Influences on the ice core record of climate." *Science* **263**: 508-511.

Cole, J. E., D. Rind, R. S. Webb, J. Jouzel and R. Healy (1999). "Climatic controls on interannual variability of precipitation delta O-18: Simulated influence of temperature, precipitation amount, and vapor source region." *Journal of Geophysical Research-Atmospheres* **104**(D12): 14223-14235.

Cuffey, K. M., G. D. Clow, R. B. Alley, M. Stuiver, E. D. Waddington and R. W. Saltus (1995). "Large Arctic temperature change at the Wisconsin-Holocene glacial transition." *Science* **270**: 455-458.

Dahl-Jensen, D., K. Mosegaard, N. S. Gundestrup, G. D. Clow, S. J. Johnsen, A. W. Hansen and N. Balling (1998). "Past temperatures directly from the Greenland ice sheet." *Science* **282**: 268-271.

Dansgaard, W. (1964). "Stable isotopes in precipitation." *Tellus* **16**(4): 436-468.

Delmotte, M., V. Masson, J. Jouzel and V. Morgan (1999). "A seasonal deuterium excess signal at Law Dome, coastal eastern Antarctica: a southern ocean signature." *Journal of Climate* submitted.

Gloersen, P. (1995). "Modulation of hemispheric sea-ice cover by ENSO events." *Nature* **373**: 503-506.

Hoffmann, G. and M. Heimann (1993). "Water tracers in the ECHAM general circulation model." *Isotope Techniques in the Study of Past and Current Environmental Changes in the Hydrosphere and the Atmosphere*, International Atomic Energy Agency, Vienna.

Hoffmann, G., M. Werner and M. Heimann (1998). "The water isotope module of the ECHAM atmospheric general circulation model - a study on time scales from days to several years." *Journal of Geophysical Research* **103**(D14): 16871-16896.

Hurrell, J. W. (1995). "Decadal trends in the North Atlantic oscillation - regional temperatures and precipitation." *Science* **269**: 676-679.

IPCC (1992). "Climate Change 1992." *The Supplementary Report to the IPCC Scientific Assessment*. ed. by: T. Houghton, B. A. Callander and K. V. Varney, Cambridge University Press, Cambridge.

Johnsen, S. J. (1977). "Stable isotope homogenization of polar firn and ice." *Symposium on Isotopes and impurities in snow and ice*, Internat. Union of Geodesy and Geophysics, Internat. Assc. Sci. Hydrol., Commision of Snow and Ice, Grenoble.

Joussaume, J., R. Sadourny and J. Jouzel (1984). "A general circulation model of water isotope cycles in the atmosphere." *Nature* **311**: 24-29.

Jouzel, J., G. L. Russell, R. J. Suozzo, R. D. Koster, J. W. C. White and W. S. Broecker (1987). "Simulations of the HDO and $H_2{}^{18}O$ atmospheric cycles using the NASA GISS general circulation model: The seasonal cycle for present-day conditions." *Journal of Geophysical Research* **92**(D12): 14739-14760.

Krinner, G., C. Genthon and J. Jouzel (1997). "GCM analysis of local influences on ice core delta signals." *Geophysical Research Letters* **24**: 2825-2828.

Roeckner, E., K. Arpe, L. Bengtsson, M. Christoph, M. Claussen, L. Dümenil, M. Esch, M. Giorgetta, U. Schlese and U. Schulzweida (1996). "The atmospheric general circulation model Echam-4: Model description and simulation of present-day climate." *MPI-Report 218*. Max-Planck-Institute for Meteorology, Hamburg.

Salamatin, A. N., V. Y. Lipenkov, N. I. Barkov, J. Jouzel, J. R. Petit and D. Raynaud (1998). "Ice core age dating and paleothermometer calibration based on isotope and temperature profiles from deep boreholes at Vostok Station (East Antarctica)." *Journal of Geophysical Research* **103**(D8): 8963-8977.

Severinghaus, J. P., T. A. Sowers, E. J. Brook, R. B. Alley and M. L. Bender (1998). "Timing of abrupt climate change at the end of the Younger Dryas interval from thermally fractionated gases in polar ice." *Nature* **391**: 141-146.

Shuman, C. A., R. B. Alley, S. Anandakrishnan, J. W. C. White, P. M. Grootes and C. R. Stearns (1995). "Temperature and accumulation at the Greenland Summit: Comparison of high resolution isotope profiles and satellite passive microwave brightness temperature trends." *Journal of Geophysical Research* **100**(D5): 9165-9177.

van Ommen, T. D. and V. I. Morgan (1997). "Calibrating the ice core paleothermometer using seasonality." *Journal of Geophysical Research* **102**(D8): 9351-9357.

van Ommen, T. D. and V. I. Morgan (1996). "Peroxide concentrations in the Dome Summit South ice core, Law Dome, Antarctica." *Journal of Geophysical Research* **101**(D10): 15147-15152.

Werner, M., M. Heimann and G. Hoffmann (1999). "Isotopic composition and origin of polar precipitation in present and glacial climate simulations." *Tellus* submitted.

Werner, M., U. Mikolajewicz, M. Heimann and G. Hoffmann (1999). "Borehole versus isotope temperatures on Greenland: Seasonality does matter." *Geophysical Research Letters* in press.

White, J. W. C., L. K. Barlow, D. Fisher, P. Grootes, J. Jouzel, S. J. Johnsen, M. Stuiver and H. Clausen (1997). "The climate signal in the stable isotopes of snow from Summit, Greenland - results of comparisons with modern climate observations." *Journal of Geophysical Research* **102**(C12): 26425-26439.

Chapter 7

Conclusive Remarks

7.1 Summary

The aim of this Ph.D. thesis was a better understanding of the observed temporal and spatial variability of the isotopic composition of polar precipitation. Several open questions about the interpretation of the observed isotope values in ice cores were raised in the introduction (Chapter 1). A summary of the different results presented in Chapter 2-6 gives some answers:

1. *How good are isotope ECHAM-4 AGCM simulation results for both polar regions for the present-day climate? Are the main characteristics of present isotope data from ice cores (e.g. geographical distribution, seasonal cycle, temperature dependency) well reproduced in a numerical simulation?*

For Greenland, the detailed comparison of an ECHAM-4 T42 simulation with ice core data in Chapter 2 has shown that the skill of the Hamburg AGCM in simulating the observed spatial variability of water isotopes in precipitation for the present climate is quite satisfactory. The geographical pattern of surface temperature, precipitation amount and $\delta^{18}O$ in precipitation agrees well with the instrumental data. However, the spatial resolution of the ECHAM model is crucial and most deviations between model results and observations can be related to the smoothed topography used in the AGCM simulation. In Chapter 2 and 3 it was also demonstrated that the ECHAM-4 simulations reproduce the correct seasonal cycle of δ-values and the deuterium excess in polar precipitation. This aspect is a clear improvement compared to older ECHAM-3 simulations where the seasonality was less pronounced for Greenland (Hoffmann et al. 1998). It is not based on a different isotope parameterisation but rather on the general model improvements built into ECHAM-4.

For Antarctica, the model also performs well, although not as well as for Greenland, since we found a general trend to higher modelled δ-values than observed. As discussed in Chapter 4, the simultaneous deviations of both simulated $\delta^{18}O$ and deuterium excess values from the

observations exclude the possibility of erroneous source regions of Antarctic precipitation as an explanation. It rather points to a parameterisation problem of the water isotopes in the ECHAM model.

2. *Is $\delta^{18}O$ a reliable temperature proxy for different climate stages like the last glacial maximum (LGM)? Can AGCM simulations help to explain some observed deviations between isotope-based and other (isotope-independent) temperature estimates for this climatic period?*

The results of Chapter 3 and 4 clearly show that $\delta^{18}O$ (or δD) is a reliable proxy for surface temperatures during the LGM. But it is also demonstrated that the isotopic paleothermometer archives temperatures only during precipitation events. Therefore the seasonal timing of the precipitation is a very crucial parameter for the interpretation of mean isotope values measured in ice cores for different climate stages, like the LGM. For the latter the deviations between isotope-based and isotope-independent estimates of glacial surface temperatures can most likely be explained by a substantial decrease of winter precipitation during the LGM. This change in seasonality is related to water masses, which stem from the high- and mid-latitudinal northern Atlantic. For Antarctica, the simulation results presented in Chapter 4 indicate that the isotopic paleothermometer might not be biased by such an effect of changed seasonality during the LGM.

3. *Which mechanisms might effect the isotopic composition of precipitation during a transition between two different climatic stages, e.g. during the transition from the LGM to the Holocene?*

The sensitivity experiments presented in Chapter 5 focus on the isotopic effects of a meltwater event in the North Atlantic, a scenario that is discussed for the understanding of rapid climate changes, like Dansgaard-Oeschger-events, the Heinrich events or the Younger Dryas period. Our AGCM study showed that two temperature-independent effects might alter the mean isotopic composition of precipitation falling in Greenland. Similar to the LGM simulation in Chapter 3, we observe a changed seasonality of precipitation for a climate change induced by a meltwater pulse in the North Atlantic. In addition, the freshwater input alters the isotopic composition of ocean surface waters and thereby the isotopic composition of precipitation in Greenland and many other regions of the Northern Hemisphere. For the tropical Atlantic regions, further changes of the $\delta^{18}O$ values in precipitation can be related to a simulated south-eastward shift of the Intertropical Convergence Zone.

4. *Are the observed present-day $\delta^{18}O$ variations on interannual to decadal time scales also temperature driven or more dominated by (other) atmospheric circulation changes? Is it possible to identify regions in Greenland or Antarctica, where climate oscillations like the NAO or ENSO are imprinted in the $\delta^{18}O$ variations of precipitation?*

Simulated interannual $\delta^{18}O$ variations of an AGCM experiment for the period 1950-1994 agree well with the variations measured in several Greenland ice cores. As shown in Chapter 6, the isotopic variability on such time scales is only weakly related to surface temperature anomalies in Greenland and Antarctica, respectively. Interannual $\delta^{18}O$ variability of the present climate integrates the climate history of a broad region and isotope variations correlate with several climate variables. Both the NAO and ENSO are imprinted in the $\delta^{18}O$ values of precipitation and about one-third of the $\delta^{18}O$ variability in some regions of Greenland and Antarctica might be related to the NAO and ENSO phenomenon, respectively.

In summary, we conclude that the performed ECHAM-4 experiments have clearly shown the usefulness of isotope AGCMs for furthering our understanding of several aspects of the observed variations of $\delta^{18}O$ and δD in polar precipitation on various time scales. Our results have also demonstrated the ability of isotope AGCMs to identify physical processes meaningful to the interpretation of the isotopic composition of polar precipitation. The mechanisms identified by the model and their effect on the isotope records can then be tested by further isotope measurements in ice cores or other water isotope archives.

7.2 Further Research Topics

One of the most interesting problems of the near future will be an accurate temporal calibration of the isotopic paleothermometer for both polar regions. Recently, two more ice core studies revealed the failure of isotope-based surface temperature estimates on Greenland for the beginning of the Bølling period 14,600 years ago (Severinghaus and Brook 1999), and for a Dansgaard-Oeschger-event ~70,000 years ago (Lang et al. 1999). There exist now 6 isotope-independent temperature estimates between 70,000 years BP and present, which all suggest cooler surface temperatures on Greenland than previously assumed (Jouzel 1999). The AGCM results presented in Chapter 3-5 are in agreement with the observations for the LGM as well as for a climate state which represents a Younger Dryas-like period. However two questions remain unanswered: (a) Are the isotope-based LGM temperature estimates for Antarctica (~6-7°C cooler than present) more trustworthy than the estimates for Greenland, as suggested by our AGCM results in Chapter 4? Preliminary borehole temperature estimates at Vostok indicate some agreement (Salamatin et al. 1998) but more isotope-independent temperature estimates are needed for Antarctica. (b) Can all deviations of isotope-based

temperature estimates be explained by a similar change in the seasonality of precipitation? Here, further sensitivity studies and climate simulations for different time periods might help for a detailed understanding. For some rapid climate variations, like the Dansgaard-Oeschger-events, the use of an ocean-atmosphere-coupled isotope model (OAGCM) is needed for an appropriate model approach.

The use of an isotope OAGCM would also be very helpful for further studying the role of the tropics during past climate changes. While ice cores from South America are in remarkably good agreement with the ice cores from Greenland (see Fig. 2 in Chapter 1) it is still an open question whether the tropical regions played a more active or passive role during climate transitions, e.g. discussed in Cane (1998) and Stocker (1998). In addition, the results of the meltwater experiments in Chapter 5 indicate some mechanisms, like a shift of the Intertropical Convergence Zone, which might alter the $\delta^{18}O$ signals in tropical precipitation, but not in the precipitation of high-latitudinal regions like Greenland.

However, the use of isotope GCMs as a tool for the interpretation of tropical ice core data is still limited by the coarse spatial resolution of the performed simulations. A much finer spatial grid size is necessary to evaluate whether isotope AGCMs correctly simulate the observed isotopic composition of precipitation measured in the alpine regions of the Andes or the Tibetan Plateau.

Such high-resolution isotope models would also be very helpful for further studies regarding the correlation of the ENSO or NAO phenomenon and $\delta^{18}O$ variations of precipitation on interannual to decadal time scales. For the task of reconstructing past ENSO events, ice cores from the nearby Andes might be a better archive than ice cores from far-removed cores in Antarctica. For the polar regions further statistical analyses should focus on methods of uniquely identifying ENSO- or NAO-related anomalies in the existing $\delta^{18}O$ ice core data.

From a modeller's perspective, further research is definitely needed for a better understanding of the deuterium excess signal d in precipitation. Although mean values and the seasonal cycle of the ECHAM-4 simulations are in agreement with the observations for Greenland for the present climate, model deficits are reported for Antarctica and for the simulation of the LGM climate. As stated by Hoffmann (1995) the deuterium excess signal is much more dependent on the model parameterisation than the $\delta^{18}O$ (or δD) value itself. Further sensitivity studies with prescribed present or LGM boundary conditions might help to test whether the ECHAM model is able to simulate the observed simultaneous decrease of both $\delta^{18}O$ and d for a glacial climate. It will also be very interesting to evaluate how general improvements of the next model release ECHAM-5 (e.g. a new mass-conservative advection scheme) effect the simulated isotopic composition of polar precipitation.

REFERENCES

Cane, M. A. (1998). "Climate change - a role for the tropical Pacific." *Science* **282**: 59-61.

Hoffmann, G. (1995). "Stabile Wasserisotope im Allgemeinen Zirkulationsmodell ECHAM." *Examensarbeit Nr.27*, Max-Planck-Institut für Meteorologie, Hamburg.

Hoffmann, G., M. Werner and M. Heimann (1998). "The water isotope module of the ECHAM atmospheric general circulation model - a study on time scales from days to several years." *Journal of Geophysical Research* **103**(D14): 16871-16896.

Jouzel, J. (1999). "Calibrating the isotopic paleothermometer." *Science* **286**: 910-911.

Lang, C., M. Leuenberger, J. Schwander and S. J. Johnsen (1999). "16°C rapid temperature variation in central Greenland 70,000 years ago." *Science* **286:** 934-937.

Salamatin, A. N., V. Y. Lipenkov, N. I. Barkov, J. Jouzel, J. R. Petit and D. Raynaud (1998). "Ice core age dating and paleothermometer calibration based on isotope and temperature profiles from deep boreholes at Vostok Station (East Antarctica)." *Journal of Geophysical Research* **103**(D8): 8963-8977.

Severinghaus, J. P. and E. J. Brook (1999). "Abrupt climate change at the end of the last glacial period inferred from trapped air in polar ice." *Science* **286**: 930-934.

Stocker, T. F. (1998). "Climate change - the seesaw effect." *Science* **282**: 61-62.